Influence of dye–titania complex formation on photoelectric conversion properties of the dye-dispersing titania

March 2014

Rudi Agus Setiawan

Contents

Chapter 1

General Introduction

1.1 Introduction

Dye sensitized solar cells (DSSCs) have extensively been studied as potential alternatives to conventional solar cells using inorganic materials since Grätzel et al. reported them in 1991.[1] DSSCs are different from conventional solar cells, and generally contain wide-bandgap nanocrystalline titania sensitized with ruthenium polypyridine complexes[2–6] or metal-free organic dyes[7–11] as photoanodes. Such DSSCs have many benefits; i.e., their material abundance, compatibility with flexible application, design variety, such as transparency and multicolor options.[12–15]

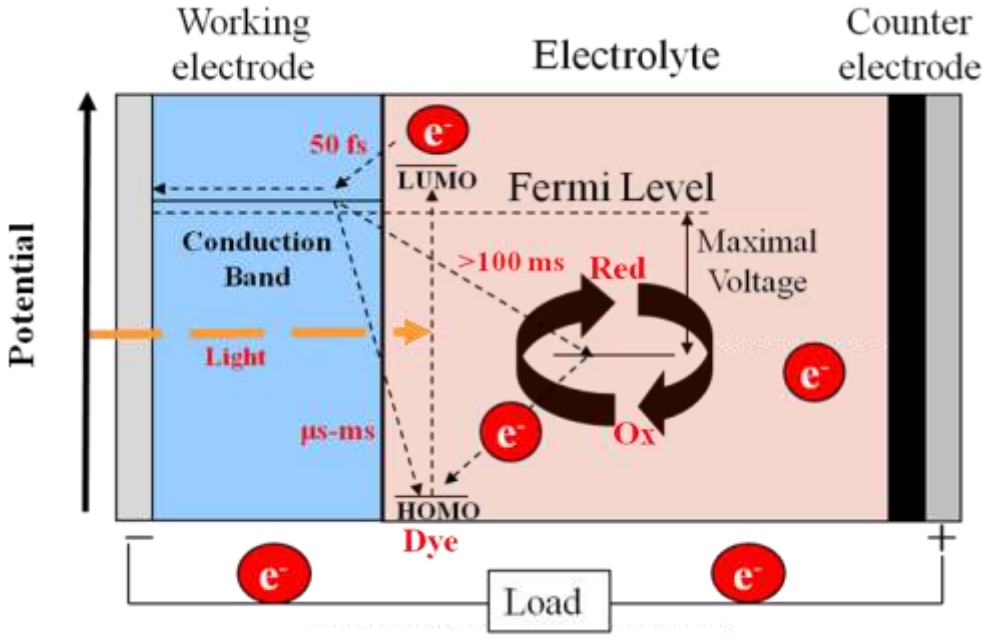

Figure 1–1 Structure and operating principle of dye-sensitized solar cell

The general operating mechanism of the DSSC is shown in Figure 1–1. During irradiation with sunlight, the dye molecule is photo-excited and the excited electron is injected into the conduction band of titania, then the resulting oxidized the dye is subsequently reduced by

electron donation from the electrolyte; usually the solution of an organic solvent or ionic liquid containing the I_3^-/I^- redox couple. The iodide is regenerated, in turn, by reduction of triiodide at the counter electrode. The circuit is completed through the external load.[16–20] The voltage generated during the light irradiation corresponds to the difference between the Fermi level of the semiconductor in the anode and the redox potential of the electrolyte.[21–23] Ideally, electric power is permanently generated without any chemical transformation. Along with these processes, the electrons injected into the conduction band of the semiconductor may be recombined with the oxidized dye sensitizers or electron acceptor species in the electrolyte solution.

At present, various studies have been done in order to optimize the photoelectric conversion properties of DSSCs. Numerous dyes have been investigated, as well as electrolytes and types of mesoporous films with different morphologies and compositions. Many parameters affect the photoelectric conversion properties, which are mainly determined by short-circuit current density (J_{sc}), open-circuit voltage (V_{oc}), and fill factor. The J_{sc} depends on the incident photon to current conversion efficiency (IPCE). IPCE is the most important factor, which is determined by (1) light harvesting efficiency of sensitizer dye molecules, (2) charge injection efficiency, and (3) charge transport efficiency in titania conduction band, with respect to the photoanode performance.[24] As described above, the V_{oc} is derived from the difference between the Fermi level of the titania and redox potential of the electrolyte. The shift in the conduction band edge and charge recombination at the device interfaces significantly affect the V_{oc}. The fill factor is almost determined by shunt resistance of the conduction substrate and series resistance at the device interfaces.[24]

Many sensitizer dyes are adsorbed on TiO_2 surface through the carboxylate group.[23,25] The enhancement of interaction between the dye and titania contributes to the improvement of IPCE

due to enhancing the light absorption and electron injection. Therefore, basic knowledge for enhancing the electronic interaction between the titania and dye is very important for development of the dye-sensitized titania electrodes.

In order to improve the absorption efficiency of the organic dyes and the interaction between dye and titania, Nishikiori et al. systematically investigated a new preparation method of the working electrodes containing the dye-dispersing titania by a sol–gel process.[26–30] The sol–gel method is a simple technology and is widely used to synthesis a novel glass or ceramics. The reaction starts from a solution of organic or inorganic compounds of metals. The sol–gel transition of the system occurs due to hydrolysis and polycondensation reaction of such compounds. The object materials can be obtained by heating the gels. One of the advantages of the sol–gel method is, in general, high homogeneity of the prepared materials. The dye molecules are expected to be homogenously dispersed in the gel matrix by mixing the dye and titania precursor in advance.

In a conventional method for preparing the working electrodes of the DSSCs, the dyes are adsorbed onto the titania thin films. This method allows the dye to be adsorbed onto only the surface of the relatively large aggregates of the titania particles. Unlike the conventional method, the dye-dispersing titania prepared by the sol–gel method is expected to allow the dye molecules to be dispersed onto the surface of the individual nanosized titania particles at a molecular level. This is important for improving the light absorption efficiency. The concentration of the dye incorporated in the dye-dispersing titania film was about five times higher than that of the dye adsorbed on the conventional film. The other advantage is the high contact area between the dye and titania. This can improve the dye–titania interaction and electron injection from the individual dye molecules into the titania.

The gel of the dye-dispersing titania was presumed to consist of amorphous, nanosized, and

particle-like units, which have a semiconductor-like quasiconduction band structure with a low density of states. The dye molecules exist in the nanopores of the gel. Furthermore, the effect of the hydrothermal treatment on their photoelectric conversion properties has also been investigated because it is an effective method to crystallize the amorphous phase and improve the photoelectric conversion performance.[26–29] It was reported that the crystallization of amorphous titania to anatase was achieved by a hydrothermal treatment at a low temperature because water molecules catalyzed the hydrolysis and sequential polymerization of the titanium compounds, and they led to the rearrangement of the TiO_6 octahedra.[31]

Nishikiori et al. reported that the dye molecules probably formed complex with titanium species on the titania particle surface in dye-dispersing titania systems.[28] Such complex species played a significant role on the electron transfer process that affected photoelectric conversion properties in such systems. The steam treatment was conducted in order to promote the crystal growth of the titania particles and enhance their photoelectric conversion efficiency. Water was heated at 100℃ and the dye-dispersing titania gel samples were exposed to its steam. The pressure of the steam was about 100 kPa. Based on the spectroscopic and photoelectric measurements of the dye–titania systems, the influence of the steam treatment on the dye–titania chemical interaction and complex formation is discussed in detailed in this dissertation. Furthermore, the influence of the dye–titania complex formation on the conduction band edge of the titania is also discussed based on the potential photocurrent onset measurement. At the end, the photoelectric conversion properties of compositionally-graded dye–titania electrodes, which are prepared with two types of the dye-dispersing titania layers with different concentration of the dye, will be also shown in order to confirm the function of the conduction band-controlled electrodes.

1.2 Scope of Chapter

In this study, xanthenes dyes were used as sensitizers. Xanthene dye molecules are known to form a chelate complex with the titanium species on the titania surface.[25] The influence of steam treatment on the dye–titania complex formation, their influence on the electron transfer process and photoelectric conversion properties in dye-dispersing titania electrodes were discussed in chapter 2, 3, and 4.

In chapter 2, simple spectroscopic and photocurrent measurements of the xanthene dye-dispersing titania gels prepared by the sol–gel method were conducted in order to clarify the influence of a steam treatment on the dye–titania interaction and electron transfer. The simple spectroscopic measurements such as UV–vis and FTIR spectra of the fluorescein- and eosin Y-dispersing titania were mainly observed as a function of the steam treatment time in order to discuss the mechanism of the complex formation between each dye and titania. Based on the I-V curves and IPCE spectra, the influence of the dye–titania complexes containing various xanthenes dyes on the electron transport and photoelectric conversion efficiency was also discussed.

In chapter 3, the influence of the dye–titania complex on the photoinduced electron transfer process in the dye-dispersing titania gel films was discussed based on steady state and time-resolved fluorescence spectroscopy. Transient absorption spectroscopy is generally used to study the photoinduced electron transfer process in the dye–titania systems. Time-resolved fluorescence spectroscopy is more sensitive than transient absorption spectroscopy.[32] The influence of the dye–titania interaction on the very fast fluorescence quenching process was discussed in connection with the photoinduced electron injection process from the dye to the titania.

In chapter 4, the subject is the influence of dye–titania complex formation on the shift in the

conduction band edge of titania. The shift in the conduction band edge of titania was observed by the measurement of the potential dependence of the photocurrent called the "photocurrent onset measurement".[33,34] This was determined by cyclic voltammetry (CV) during light irradiation for the band-gap excitation of the titania (Photo-CV) in order to estimate the shift in the conduction band edge of the titania in each electrode. The correlation between the shifts in conduction band edge and the change in the V_{oc} value was also discussed in this chapter.

In chapter 5, the electrodes using a new material "compositionally-graded dye–titania", were investigated. The compositionally-graded dye–titania electrode was prepared by combining the dye-dispersing titania thin films having different compositions of dye and titania through a sol–gel process. Based on measurements of the spectroscopic and photoelectric properties of such electrode, the electron transfer efficiency in the compositionally-graded dye–titania working electrode was discussed compared to that of the conventional electrode in this chapter.

Finally, in chapter 6, all the investigations in this dissertation were summarized.

References

(1) B. O'Regan, M. Grätzel

Nature, 353 (1991), pp. 737-740

(2) H. S. Jung, J. K. Lee

Journal of Physical Chemistry Letters, 4 (2013), pp. 1682-1693

(3) I. Shin, H, Seo, M. K. Son, J. K. Kim, K. Prabakar, H. J. Kim

Current Applied Physics, 10 (2010), pp. S422-S424

(4) S. Ito, T. N. Murakami, P. Comte, P. Liska, C. Grätzel, M. K. Nazeeruddin, M. Grätzel

Thin Solid Films, 516 (2008), pp. 4613-4619

(5) Y. G. Lee, S. Park, W. Cho, T. Son, P. Sudhagar, J. H Jung, S. Wooh, K. Char, Y. S. Kang

Journal of Physical Chemistry C, 116 (2012), pp. 6770-6777

(6) C. Y. Li, C. Su, H. H. Wang, P. Kumaresan, C. H. Hsu, I.T. Lee, W. C. Chang, Y. S. Tingare, T. Y. Li, C. F. Lin, W. R. Li

Dyes and Pigments, 100 (2014), pp. 57-65

(7) T. Funaki, M. Yanagida, N. O. Komatsuzaki, Y. Kawanishi, K. Kasuga, H. Sugihara

Solar Energy Materials and Solar Cells, 93 (2009), pp. 729–732

(8) G. C. Vougioukalakis, T. Stergiopoulos, G. Kantonis, A. G. Kontos, K. Papadopoulos, A. Stublla, P. G. Potvin, P. Falaras

Journal of Photochemistry and Photobiology A: Chemistry, 214 (2010), pp. 22–32

(9) J. J. Kim, J. Yoon

Inorganica Chimica Acta, 394 (2013), pp. 506–511

(10) T. Funaki, M. Yanagida, N. O. Komatsuzaki, K. Kasuga, Y. Kawanishi, M. Kurashige, K. Sayama, H. Sugihara

Inorganic Chemistry Communications, 12 (2009), pp. 842–845

(11) P. Chen, J. H. Yun, F. D. Angelis, E. Mosconi, S. Fantacci, S. J. Moon, R. H. Baker, J. Ko, M. K. Nazeeruddin, M. Grätzel

Nano Letters, 9 (2009), pp. 2487-2492

(12) X. Cheng, S. Sun, M. Liang, Y. Shi, Z. Sun, S. Xue

Dyes and Pigments, 92 (2012), pp. 1292-1299

(13) J. K. Lee, S. M. Lee, S. B. Lee, K. H. Kim, S. E. Cho, S. I. Jang, S. H. Park, W. P. Hwanga, M. H. Seo, M. R. Kim

Current Applied Physics, 11 (2011), pp. S140-S146

(14) M. Liang, Z. Y. Wang, L. Zhang, H. Y. Han, Z. Sun, S. Xue

Renewable Energy, 36 (2011), pp. 2711-2716

(15) Z. Wan, C. Jia, L. Zhoua, W. Huo, X. Yao, Y. Shi

Dyes and Pigments, 95 (2012), pp. 41-46

(16) H. S. Uam, Y. S. Jung, Y. Jun, K. J. Kim

Journal of Photochemistry and Photobiology A: Chemistry, 212 (2010), pp. 122−128

(17) V. Thavasi, V. Renugopalakrishnan, R. Jose, S. Ramakrishna

Material Science and Engineering R, 63 (2009), pp. 81-99

(18) S. J. Thompson, N. W. Duffy, U. Bach, Y. B. Cheng

Journal of Physical Chemistry C, 114 (2010), pp. 2365-2369

(19) A. Y. Anderson, P. R. F. Barnes, J. R. Durrant, B. C. O'Regan

Journal of Physical Chemistry C, 115 (2011), pp. 2439-2447

(20) B. K. An, W. Hu, P. L. Burn, P. Meredith

Journal of Physical Chemistry C, 114 (2010), pp. 17964-17974

(21) T. Marinado, K. Nonomura, J. Nissfolk, M. K. Karlsson, D. P. Hagberg, L. Sun, S. Mori, A. Hagfeldt

Langmuir, 26 (2010), pp. 2592-2598

(22) Y. Liang, B. Peng, J. Chen

Journal of Physical Chemistry C, 114 (2010), pp. 10992-10998

(23) Z. S. Wang, H. Sugihara

Langmuir, 22 (2006), pp. 9718-9722

(24) J. Xia, S. Yanagida

Solar Energy, 85 (2011), pp. 3143-3159

(25) J. N. O'Shea, J. B. Taylor, E. F. Smith

Surface Science, 548 (2004), pp. 317-323

(26) H. Nishikiori, W. Qian, M. A. El-Sayed, N. Tanaka,; T. Fujii

Journal of Physical Chemistry Letters, 111 (2007), pp. 9008-9011

(27) H. Nishikiori, N. Tanaka, T. Kitsui, T. Fujii

Journal of Photochemistry and Photobiology A: Chemistry, 179 (2006), pp. 125-129

(28) H. Nishikiori, Y. Uesugi, N. Tanaka, T. Fujii

Journal of Photochemistry and Photobiology A: Chemistry, 207 (2009), pp. 204-208

(29) H. Nishikiori, R. A. Setiawan, K. Miyamoto, G. Sukomono, Y. Uesugi, K. Teshima, T. Fujii

RSC advances, 2 (2012), pp. 4258-4267

(30) H. Nishikiori, K. Todoroki, D. Natori, R. A. Setiawan, K. Miyashita, T. Fujii

Chemistry Letters, 42 (2013), pp. 556-558

(31) K. Yanagisawa, J. Ovenstone

Journal of Physical Chemistry B, 103 (1999), pp, 7781−7787

(32) L. Du, A. Furube, K. Hara, R. Katoh, M. Tachiya

Journal of Physical Chemistry C, 114 (2010), pp, 8135−8143

(33) J. M. Bolts, M. S. Wrighton

Journal of Physical Chemistry, 80 (1976), pp. 2641-2645

(34) M. Radecka, M. Rekas, A. Trenczek-Zajac, K. Zakrzewska

Journal of Power Sources, 181 (2008), pp. 46-55

Chapter 2

Influence of steam treatment on dye–titania complex formation and photoelectric conversion property of dye-dispersing titania gel

2.1 Introduction

Electron transfer is an important process to understand the mechanism of the fundamental reaction in electronic devices and further develop their functions and performances. Solar cells have attracted considerable attention as a sustainable device to solve the energy and environmental problems. In the photochemistry field, the electron transfer in photo-functional materials consisting of an organic-inorganic composite, such as the working electrodes of dye-sensitized solar cells, have been studied all over the world.[1–3] Many scientists have investigated the electron donor–acceptor interaction between the dye molecules and the titania in the dye–titania systems used for the dye-sensitized solar cells.[4–15] It was reported that xanthene dye molecules formed a chelate complex with the titanium species on the titania surface in the dye-titania systems. The complex formation induces an interaction between their orbitals and the red-shift in their absorption spectrum. This interaction caused the ligand to metal charge transfer (LMCT) interaction and a fast electron injection into the titania conduction band.[8,9,14]

Nishikiori et al. showed that the hydrothermal treatment of a dye-dispersing amorphous titania film remarkably improved the photoelectric conversion efficiency due to not only its crystallization, but also the dye–titanium complex formation.[16] The electron injection process from the dye excitation states to the titania conduction band is important for the photoelectric

conversion. This process depends on the reduction potential of the excited dye and the conduction band potential of the titania, which are changed by the complex formation. In this chapter, the spectroscopic and photoelectric measurements of the dye–titania system were conducted in order to clarify the influence of the steam treatment on the dye–titania complex formation and the electron injection mechanism. Especially, the potentials of the complex and the conduction band of the titania are discussed.

2. 2. Experimental section

2.2.1. Materials

Titanium tetraisopropoxide, ethanol, fluorescein, sodium fluorescein, eosin Y, rose bengal, hydrochloric acid, nitric acid, diethylene glycol, iodine, lithium iodide, and sodium hydroxide (Wako Pure Chemicals, S or reagent grade), 4-aminofluorescein (Tokyo Kasei, reagent grade), and 5(6)-carboxyfluorescein (LAMBDA, reagent grade) were used without further purification. Water was ion-exchanged and distilled. Glass plates coated with the ITO transparent electrode (AGC Fabritech) were soaked in hydrochloric acid (1.0 mol dm^{-3}) for 2 h and then rinsed with water. The electrolyte used for the electrical measurements consisted of an diethylene glycol solution of iodine (5.0×10^{-2} mol dm^{-3}) and lithium iodide (0.50 mol dm^{-3}).

2.2.2 Preparation of electrodes

The sol–gel reaction system was prepared by mixing 5.0 cm^3 of titanium tetraisopropoxide, 25.0 cm^3 of ethanol, 0.21 cm^3 of water, and 0.21 cm^3 of concentrated nitric acid as the catalyst of the sol–gel reaction and labeled SG-0. Fluorescein (F), sodium fluorescein (SF), 4-aminofluorescein (AF), 5(6)-carboxyfluorescein (CF), eosin Y (EY), and rose bengal (RB), were individually dissolved into SG-0 in which their concentrations were 1.0×10^{-2} mol dm^{-3}

and these systems were labeled SG-F, SG-SF, SG-AF, SG-CF, SG-EY, and SG-RB, respectively. The dip-coated thin films were prepared from the systems in which the sol−gel reaction proceeded for 1 day to prepare the electrodes.

In order to prepare the electrode samples coated with the crystalline titania, the glass plates with the ITO transparent electrode were dip-coated in the dye-free system (SG-0) and then heated at 500 ºC for 30 min. These electrodes were labeled E-0. Furthermore, the working electrodes were prepared in the way in which the E-0 was dip-coated with SG-F, SG-SF, SG-AF, SG-CF, SG-EY, and SG-RB. These working electrodes were labeled WE-F, WE-SF, WE-AF, WE-CF, WE-EY, and WE-RB, respectively. The glass plates without ITO were also coated with SG-F and SG-EY in order to measure their XRD patterns.

The steam-treatment effects on the UV-vis absorption and photocurrent spectra of the electrode samples and on the XRD patterns of the samples were investigated. Water was heated at 110 ºC and the electrode and XRD samples were exposed to its steam for 0–120 min. The pressure of the steam was about 140 kPa.

The conventional dye-sensitized electrodes were also prepared in order to compare them with our original samples. The SG-0 was spread on the glass plates with the ITO transparent electrode and heated at 500 ºC for 30 min. These electrodes were immersed in 1.0×10^{-2} mol dm^{-3} fluorescein and eosin Y ethanol solutions for 24 h, and labeled WE-F-c and WE-EY-c, respectively.

2.2.3. Measurements

The crystalline phase of the film samples was determined using an X-ray diffractometer (Rigaku RINT-2200V). The layer thickness of the electrode samples was estimated from their cross section using a field emission scanning electron microscope (Hitachi S-4100). The

UV-visible absorption spectra of the prepared electrode samples were observed using a spectrophotometer (Shimadzu UV-2500). The amounts of the dyes existing in the electrode samples were estimated from the absorption spectra of the dyes eluted by the 0.1 mol dm^{-3} sodium hydroxide aqueous solution.

The iodine-based electrolyte was allowed to soak into the space between the electrode sample and the counter Pt electrode. Monochromatic lights obtained from a fluorescence spectrophotometer (Shimazdu RF-5300) with a 150 W Xe short arc lamp (Ushio UXL-155) were irradiated on the electrodes for the spectroscopic measurements. Under light irradiation, the short circuit currents of the electrodes were measured by an electrometer (Keithley model 617). The *I*−*V* curves of the electrodes were measured by a potentiostat (Hokuto Denko HSV-100) during irradiation by visible light with a wavelength longer than 400 nm emitted by the 150 W Xe short arc lamp using a sharp cut filter. The intensity at each wavelength of the light source was obtained using a power meter (Molectron PM500A) in order to estimate the incident photon to current conversion efficiency (IPCE) and quantum efficiency for the photocurrent from the excited dye in the electrode samples. The light intensity was confirmed to correlate with the results of the potassium ferrioxalate actinometry. The visible absorbance of the present electrode samples was lower than 1.0 which was sufficient to measure the number of absorbed photons in order to calculate the quantum efficiency.

The dye powders and the flakes of the dye-dispersing film samples were pressed in the KBr pellets and their IR spectra were taken using an FTIR spectrophotometer (Shimadzu FTIR-8300).

2.3. Results and discussion

2.3.1. Crystallinity of titania

The XRD patterns of the fluorescein- and eosin Y-dispersing titania gels were obtained as a function of the treatment time as shown in Figure 2–1. No peak is found in the XRD pattern of both of the untreated amorphous gel films. The peak at around 25° was observed and an anatase type crystal was produced in the film steam-treated for 20 min. The peak looks sharper after the longer steam-treatment time. There was a slight difference between the fluorescein- and eosin Y-dispersing samples. The size of the crystallites of these electrodes was estimated from their full-width at half-maximum of the 25° peak using Sherrer's equation, $D=0.9\lambda/\beta\cdot\cos\theta$. They were 4–6 nm for the fluorescein-dispersing samples and 3–5 nm for the eosin Y-dispersing samples after the steam treatment for 20–120 min. Compared to the heated titania sample, the crystallite size of the film was small and not significantly changed by the steam treatment for more than 20 min based on the XRD analysis.

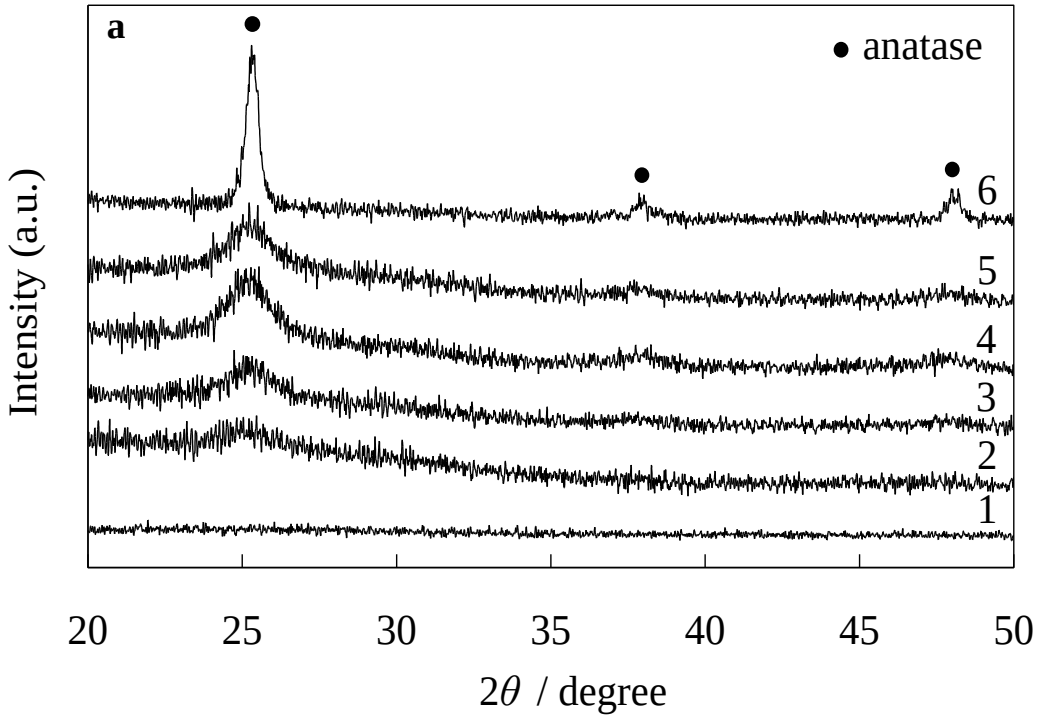

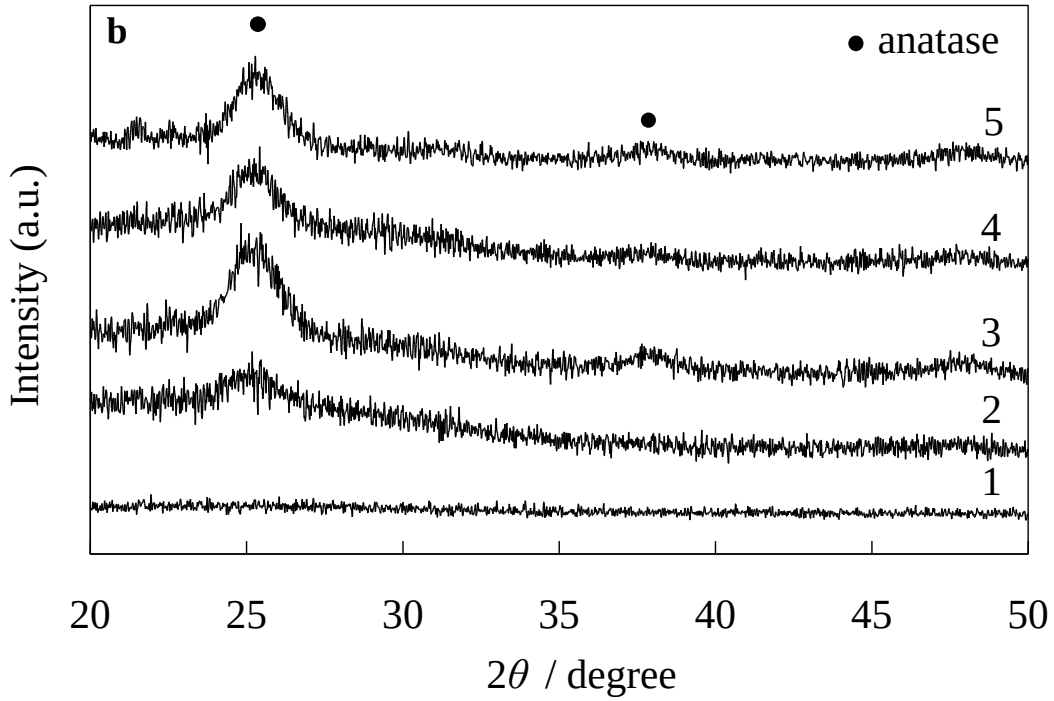

Figure 2–1 XRD patterns of the (a) fluorescein- and (b) eosin Y-dispersing titania gels steam-treated for (1) 0, (2) 20, (3) 40, (4) 60, and (5) 120 min and (6) heated at 500 °C for 30 min.

It is suggested that the untreated dye-dispersing titania gel film consists of the amorphous, nanosized, and particle-like units having a semiconductor-like quasi-conduction band structure with low density of states. The steam treatment promoted the hydrolysis and sequential polycondensation of the titania gel, and the resulting reorientation led to the formation of anatase-type titania nanocrystals.

2.3.2. UV–vis absorption and photocurrent properties of WE-F and WE-EY

Figure 2–2 shows the UV–vis absorption spectra of WE-F and WE-EY observed as a function of the steam treatment time compared to those of WE-F-c and WE-EY-c. The thickness of the dye-containing layer of WE-F and WE-EY was ca. 350 nm and that slightly changed by the steam treatment. The thickness of the titania layer of WE-F-c and WE-EY-c was ca. 2.1 μm.

The absorbance in the UV range due to titania increased during the 20-min steam treatment of WE-F and WE-EY, and then decreased after further steam treatment. The accurate band gaps cannot be estimated due to the gradual absorption rises around the band edges. This is caused by the low crystallinity of the titania layer compared to normal heated titania. The spectra could not be obtained in the wavelength region shorter than 350 nm due to their excessively high absorption. The band gap of the conventional titania electrode, having high crystallinity, was estimated to be around 3.3 eV from the UV absorption spectra of WE-EY-c.

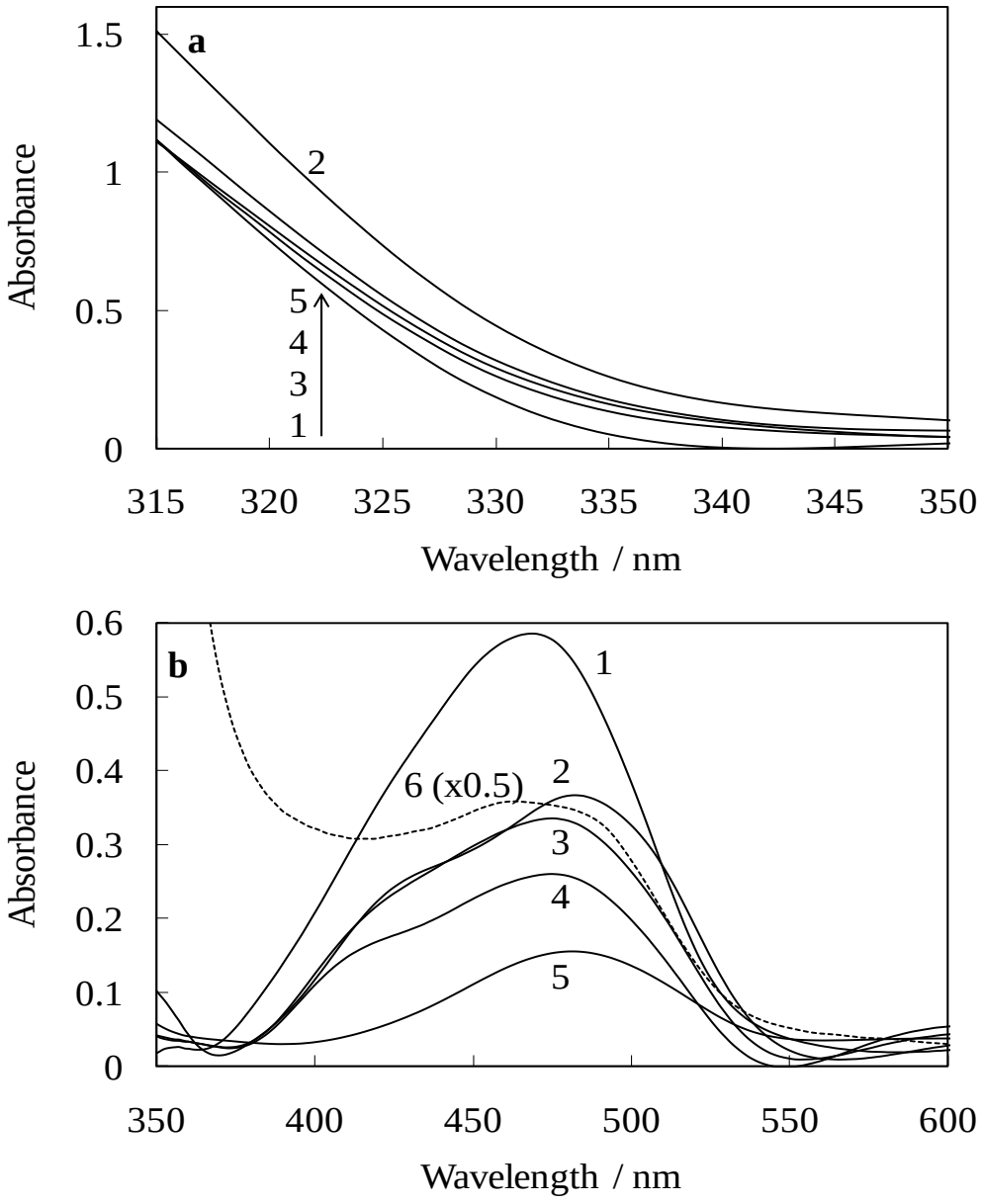

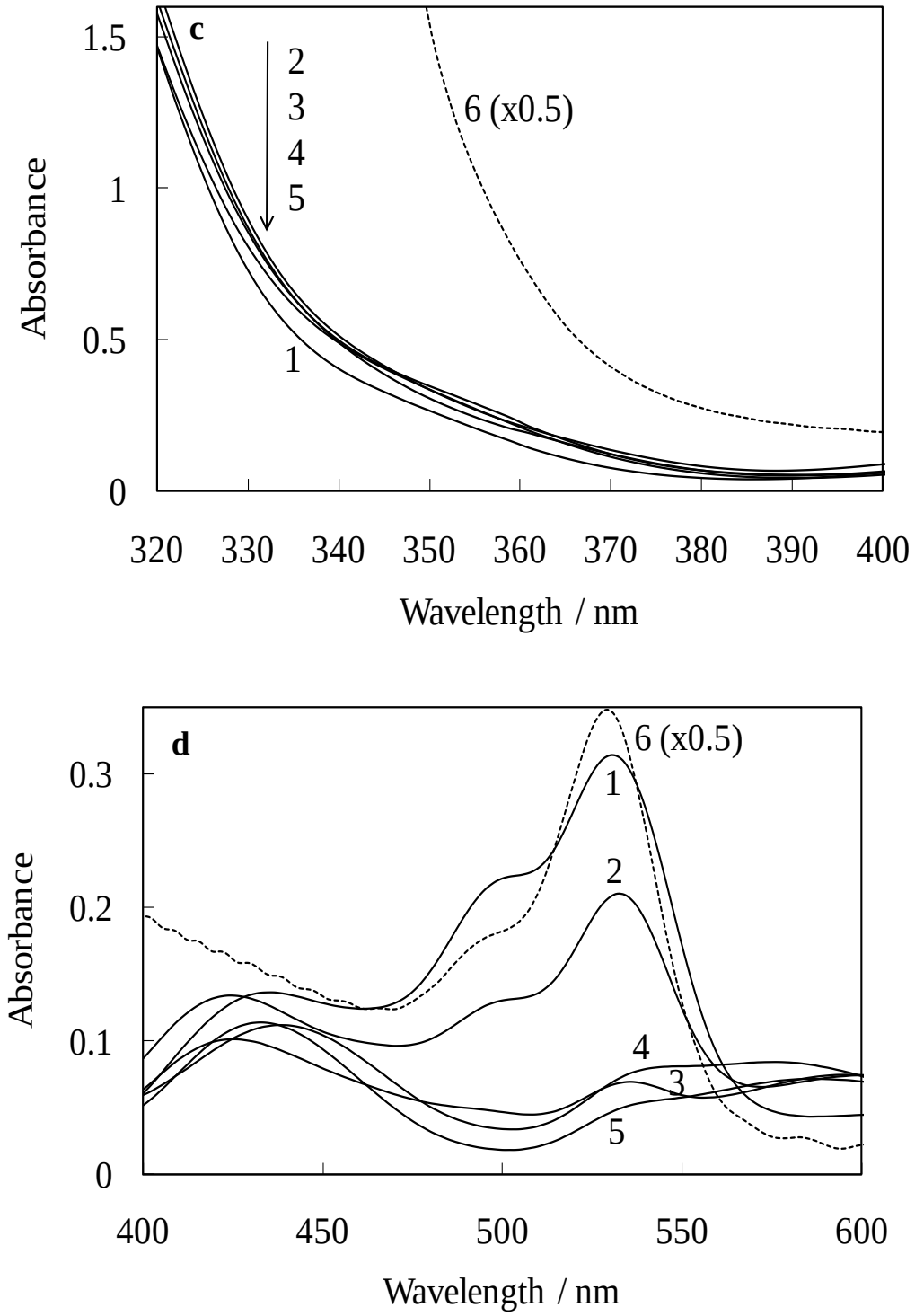

Figure 2–2 UV–vis absorption spectra of (a,b) WE-F and (c,d) WE-EY observed (1) before and after (2) 20-, (3) 40-, (4) 60-, and (5) 120-min steam treatments. These spectra are compared to those of (b-6) WE-F-c and (c,d-6) WE-EY-c, respectively.

In the visible range, the spectrum of the untreated WE-F is located around 470 nm, ranging over a wavelength wider than that observed in solvents. This result indicates that the main fluorescein species were the neutral or anion form (at 450–480 nm) and some fluorescein molecules existed as the dianion form (at around 490 nm).[17] In addition, the longer wavelength band indicates that a small number of fluorescein molecules formed the dianion-like species resulting from the strong interaction and a chelating linkage between the carboxyl group of the dye and the titanium species.[4,5,8–10,14,18] The absorbance decreased to one-third because some amount of water vapor was condensed into liquid on the titania film during the steam treatment, and then some of the fluorescein molecules adsorbed on the titania pore surface were desorbed into the liquid water phase. In addition, the spectral peak of the film was red-shifted from around 470 to 480 nm by the steam treatment.[14, 16,19–21]

The spectral shape became broader to the longer wavelength side. These results indicate that the neutral and anion species were preferentially desorbed from the inside of the titania gel film into the water phase because the species was weakly trapped in the pores of the gel. The stream treatment probably increased the number of fluorescein molecules interacting with the titanium species. The spectrum of WE-F-c is similar to the untreated WE-F, indicating that the fluorescein molecules are weakly adsorbed on the crystalline titania particle surface.

The absorbance of WE-EY decreased with the steam treatment time and its peak at 530 nm did not significantly change. The peak was located at the wavelength longer than that of the dianion species in water [22] due to the ionic interaction with the titania surface. The absorbance was less than one-tenth of the initial value after the 120-min treatment due to the dye desorption. It is expected that the interaction of eosin Y with titania is weaker than that of fluorescein. The spectrum of WE-EY-c is sharper than that of the untreated WE-EY, indicating that the eosin Y molecules weakly interact with the crystalline titania particle surface. The decreases in the

absorbance values of fluorescein and eosin Y in the steam-treated samples correspond to the values obtained from their elution as shown in Figure 2–3. This result indicates that the dye molecules did not change into the colorless form in the titania after the steam treatment.

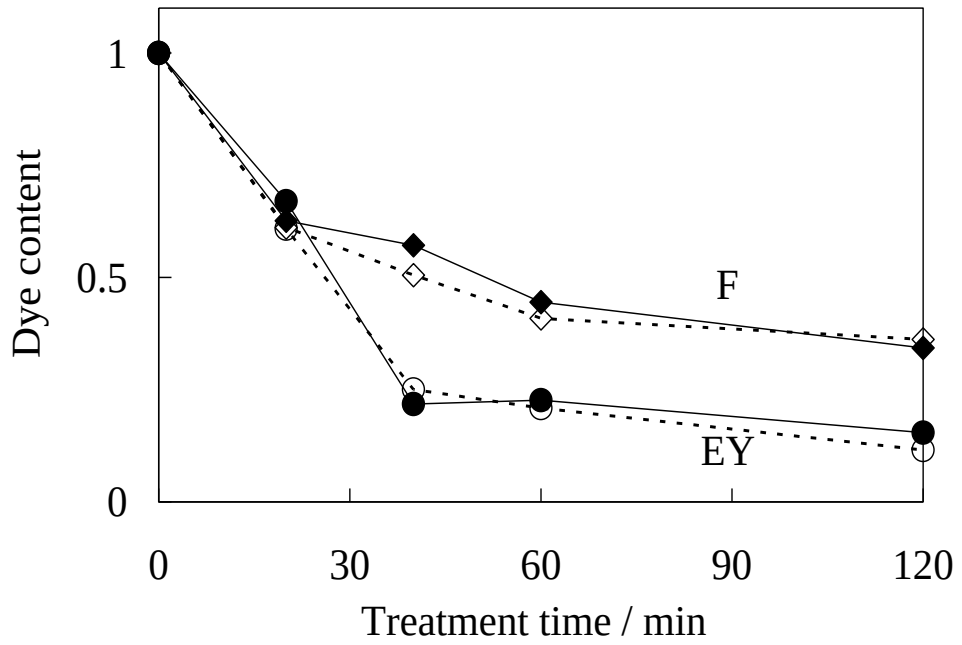

Figure 2–3. Dye content in WE-F (square) and WE-EY (circle) steam-treated for 0–120 min estimated by the UV–vis absorption spectra (solid) of the electrodes and their elusion (open). The values are normalized at 0 min.

The changes in the IPCE spectra of WE-F and WE-EY with the stream treatment are shown in Figure 2–4 compared to those of WE-F-c and WE-EY-c. The IPCE values in the UV range increased during the 20-min treatment similar to the UV absorption of WE-F and WE-EY. The values decreased after the 20-min treatment with their UV absorption even though the crystal growth proceeded during the 60 or 120-min treatment based on the XRD analysis. The decrease in the photocurrent is suggested to be caused by decreasing the electron transport efficiency in the titania because the bonds between the titania particles are weakened by hydrolysis. On the other hand, in

spite of the visible absorbance decrease, the photocurrent of WE-F in the visible range increased during the 120-min treatment, while the peak at 490 nm was shifted to 500 nm. These results suggest that the increase in the IPCE values is due to improvement of the chelate complex formation between the fluorescein and the titanium species (the around 500 nm species) rather than the electric conductivity of the titania gel. The growth and crystallization of the particles and the decrease in the defect density by the 20-min steam treatment improved the electric conductivity.[16–18] The steam treatment enhanced not only the electric conductivity of the titania, but also the dye–titania interaction that plays an important role in generating the photocurrent in this system.

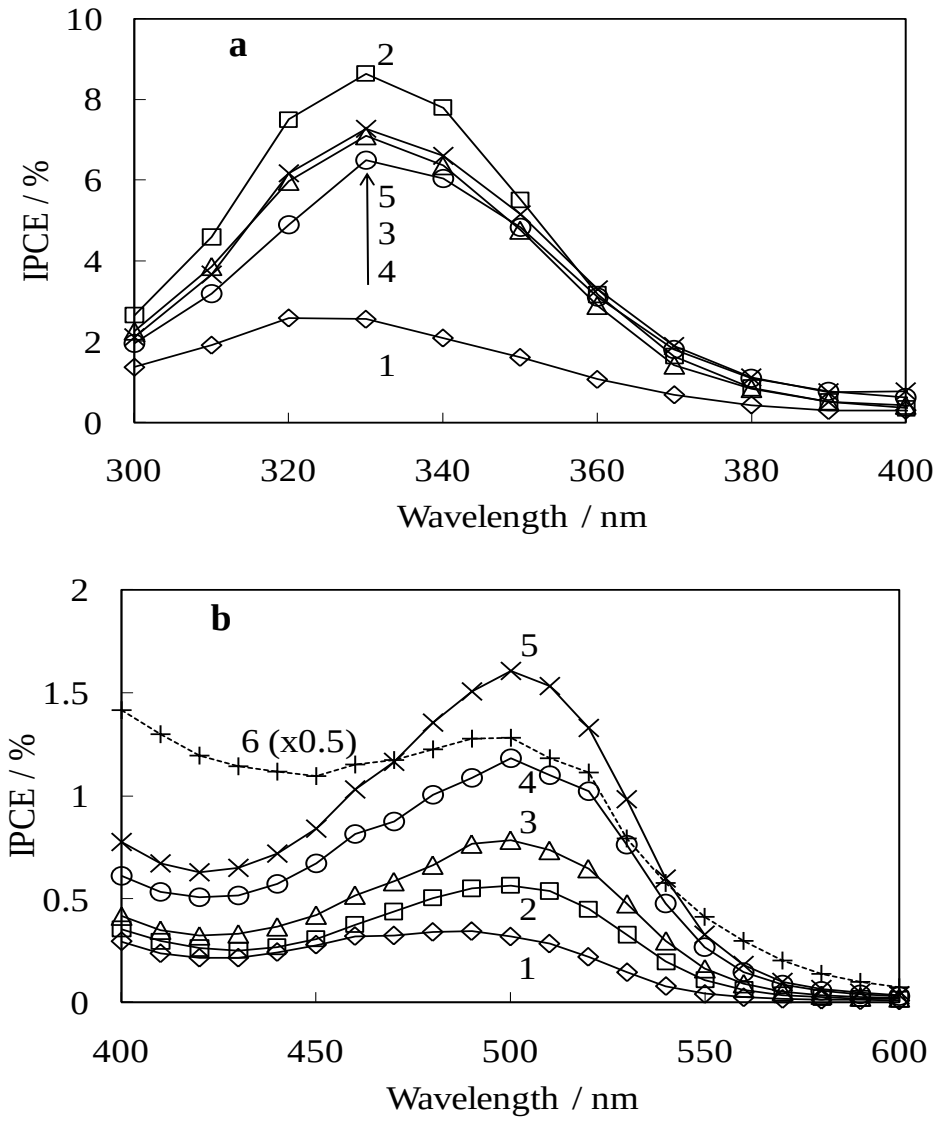

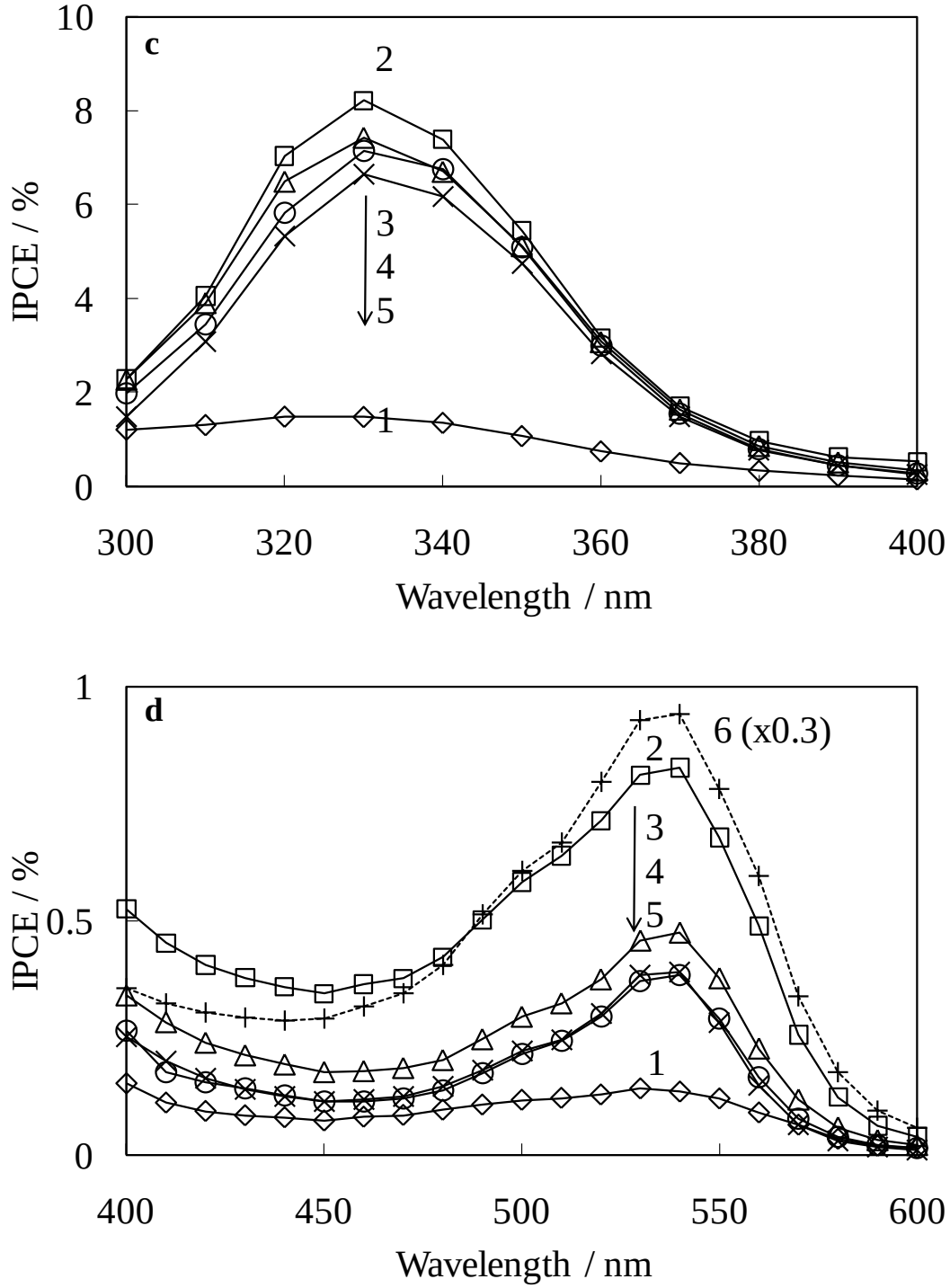

Figure 2–4 IPCE spectra of (a,b) WE-F and (c,d) WE-EY observed (1) before and after (2) 20-, (3) 40-, (4) 60-, and (5) 120-min steam treatments. These spectra are compared to those of (b-6) WE-F-c and (d-6) WE-EY-c, respectively.

On the other hand, the photocurrent of WE-EY in the visible range increased during the 20-min treatment and then decreased with the treatment time. This decrease is mainly due to the desorption of a large number of dye molecules. The spectral peak position was not significantly changed during the treatment. This is because the interaction of eosin Y with titania is weaker than that of fluorescein, and its complex formation is harder. The LUMO level of the dye is an important factor for the rate of injection into the titania conduction band. The IPCE values of the fluorescein-dispersing electrode was improved by the steam treatment better than that of the eosin Y-dispersing electrode although the LUMO level of eosin Y is more negative than that of fluorescein.[15] The complex formation is expected to be more effective for the electron injection.

WE-F-c and WE-EY-c exhibited similar spectral shapes to those of the untreated WE-F and WE-EY, respectively. The IPCE values of the conventional electrodes were much higher than those of the dye-dispersing electrodes due to the higher crystallinity and electric conductivity of the titania, and the higher dye content and absorbance.

2.3.3. FTIR analysis of fluorescein- and eosin Y-dispersing titania

Figure 2–5 shows the FTIR spectra of fluorescein and eosin Y, and the fluorescein- and eosin Y-dispersing titania gels before and after the steam treatment compared to those of the fluorescein- and eosin Y-adsorbed titania samples. The peaks of the carboxyl C=O stretching and the carboxylate COO^- antisymmetric and symmetric stretching vibrations were observed at 1710, 1597, and 1391 cm^{-1} in fluorescein, respectively. In addition, the band at around 1490 cm^{-1} is assigned to the quinone-like C=O stretching vibration.[23] The untreated fluorescein-dispersing sample exhibited the carboxyl band at around 1710 cm^{-1}, the carboxylate bands at 1580 and 1398 cm^{-1}, the quinone-like band at 1450 cm^{-1}. In addition, the phenoxide ion stretching vibration conjugated with the xanthenes ring vibration was also observed at

around 1300 cm^{-1} in the untreated dye-dispersing titania sample.[23] The significant shifts of the carboxylate and quinone-like bands are due to the interaction between the functional groups and the titanium species of titania. The intensity of the carboxyl band decreased and that of the interacting carboxylate and quinone-like bands increased with the steam treatment.

On the other hand, the carboxyl C=O band was not observed in eosin Y or the eosin Y-dispersing sample before or after the treatment. The FTIR spectrum of eosin Y has the carboxylate bands at 1557 and 1352 cm^{-1}, and the quinone-like band at 1458 cm^{-1}. These bands were somewhat shifted to 1558, 1341, and 1441 cm^{-1}, respectively, in the untreated eosin Y-dispersing sample due to the dye-titania interaction. The 60-min treatment relatively decreased the quinone-like band and increased the carboxylate band. The decrease in the quinone-like band intensity was different from the result observed in the fluorescein-dispersing sample. The spectrum of eosin Y was not obtained after the 120-min treatment due to the dye desorption.

The carboxyl group of fluorescein was transformed into the carboxylate and formed a chelate complex with the titanium species during the steam treatment while eosin Y was only the carboxylate form. The proton dissociation constants, pK_a values, of the carboxyl groups of fluorescein and eosin Y are 4.45 and 3.75, respectively.[22] The carboxylate oxygen of fluorescein is more nucleophilic than that of eosin Y and easier to form the coordination complex with metal species. Additionally, the quinone-like carbonyl group of the xanthene ring also interacted with the titanium species. This type of complex formation strongly depends on pK_a values of the hydroxyl group of the xanthene ring, which are 6.80 for fluorescein and 2.81 for eosin Y.[22]

The FTIR spectra of the fluorescein- and eosin Y-adsorbed titania samples are quite similar to those of the only dyes. It is found that the dye molecules only slightly interacted with the titania in the conventional electrodes because the titania particles have high crystallinity and their

surface is low hydrophilic due to a small amount of hydroxyl groups.

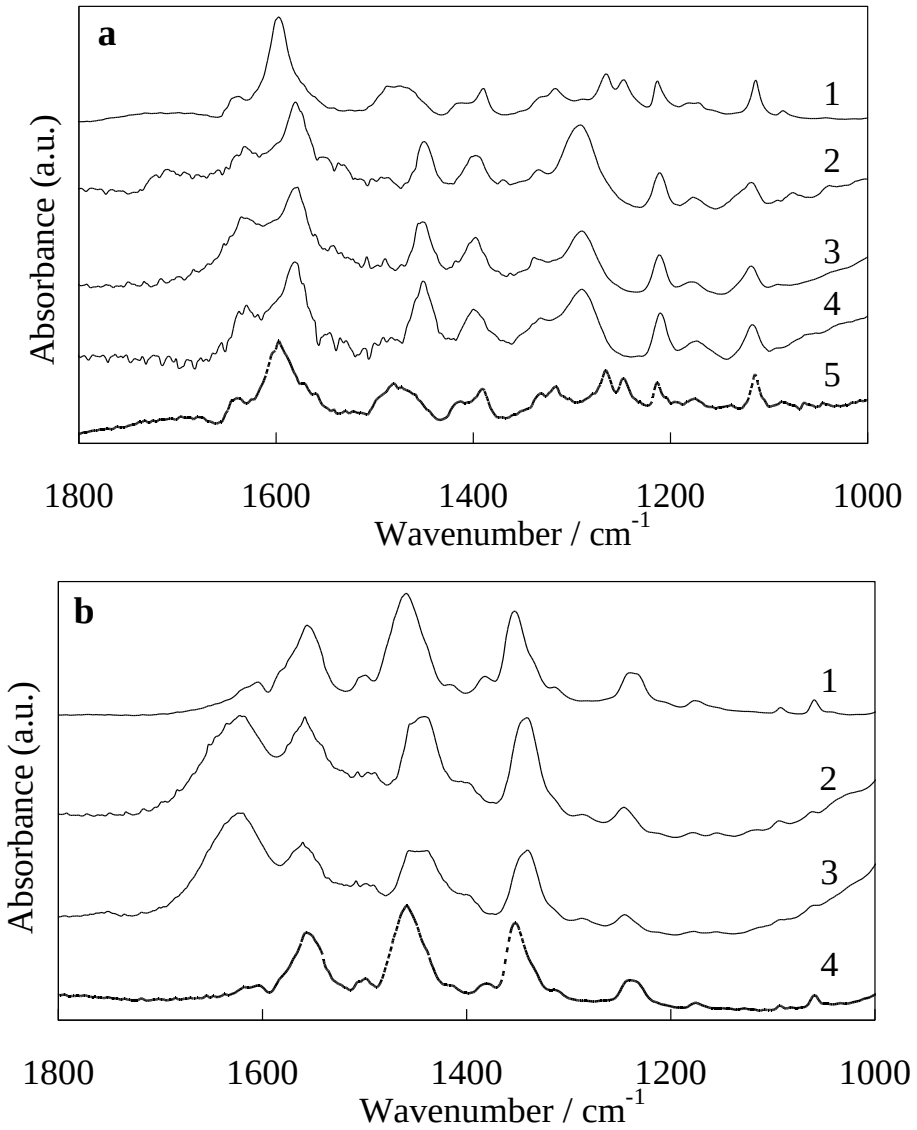

Figure 2–5 FTIR spectra of (a) (1) fluorescein, (2-4) the fluorescein-dispersing titania gel, and (5) the fluorescein-adsorbed titania, and (b) (1) eosin Y, (2,3) the eosin Y-dispersing titania gel, and (4) the eosin Y-adsorbed titania. The spectra of the fluorescein-dispersing titania samples were observed (2) before and after (3) 60- and (4) 120-min steam treatments. The spectra of the eosin Y-dispersing titania samples were observed (2) before and (3) after 60-min steam treatments.

2.3.4. Photocurrent properties of the electrodes containing various xanthene dyes

Figure 2–6 shows the IPCE spectra of the electrode samples containing the other xanthene dyes (SF, AF, CF, RB) before and after the steam treatment. As shown in the fluorescein (F)-dispersing sample, the spectral red-shift due to the treatment was observed in the system containing the dyes, SF of a sodium salt, CF having two carboxyl groups, that promote the interaction with the titanium species, and AF having an electron accepting amino group. On the other hand, for eosin Y (EY), the shift was not observed in the electrode containing RB having electron-accepting groups. The pK_a values for the carboxyl groups of AF and CF are 4.56 (5-aminofluorescein) [24] and 4.3 [14], respectively, and they are close to that of F, i.e., 4.45. The pK_a values for the carboxyl group of RB of 3.51 [25] is close to that of EY, i.e., 3.75. These results support the fact that the nucleophilicity of the carboxylate oxygen in the xanthene dye influences the dye–titania complex formation.

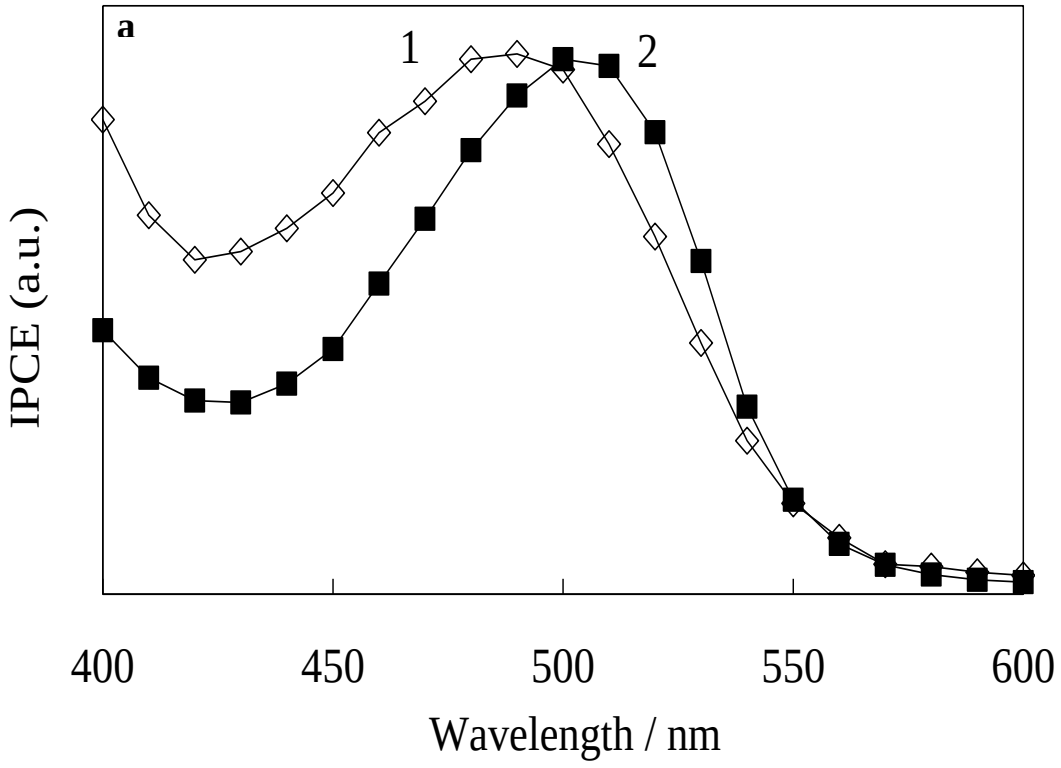

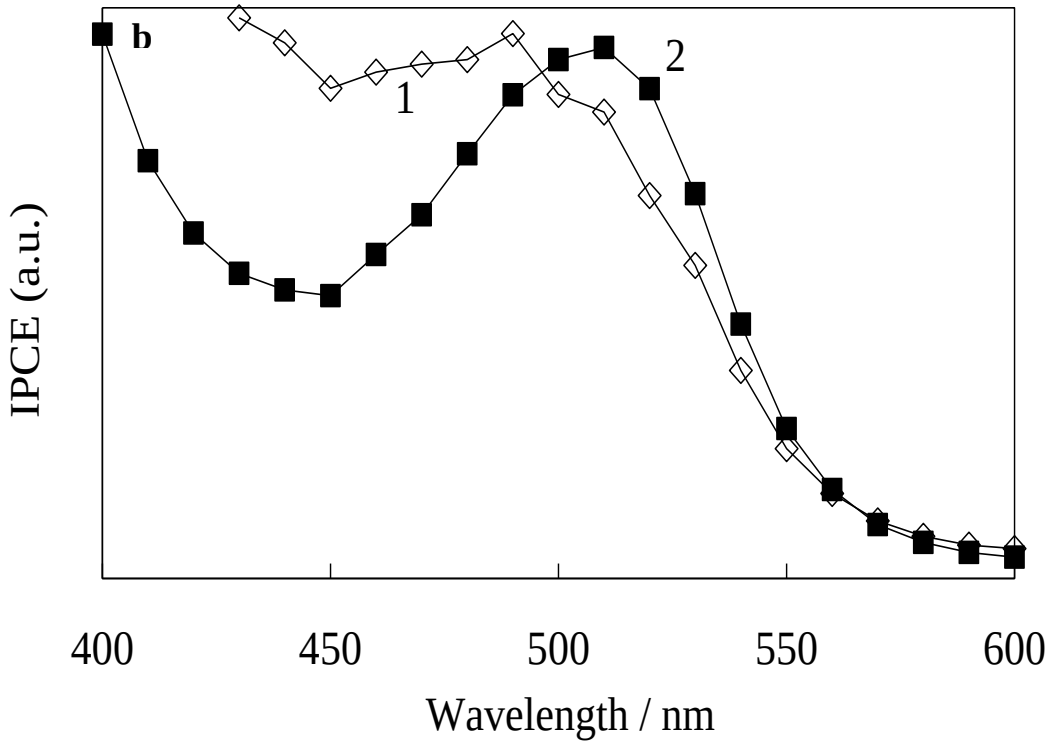
b
1
2
IPCE (a.u.)
400
450
500
550
600
Wavelength / nm

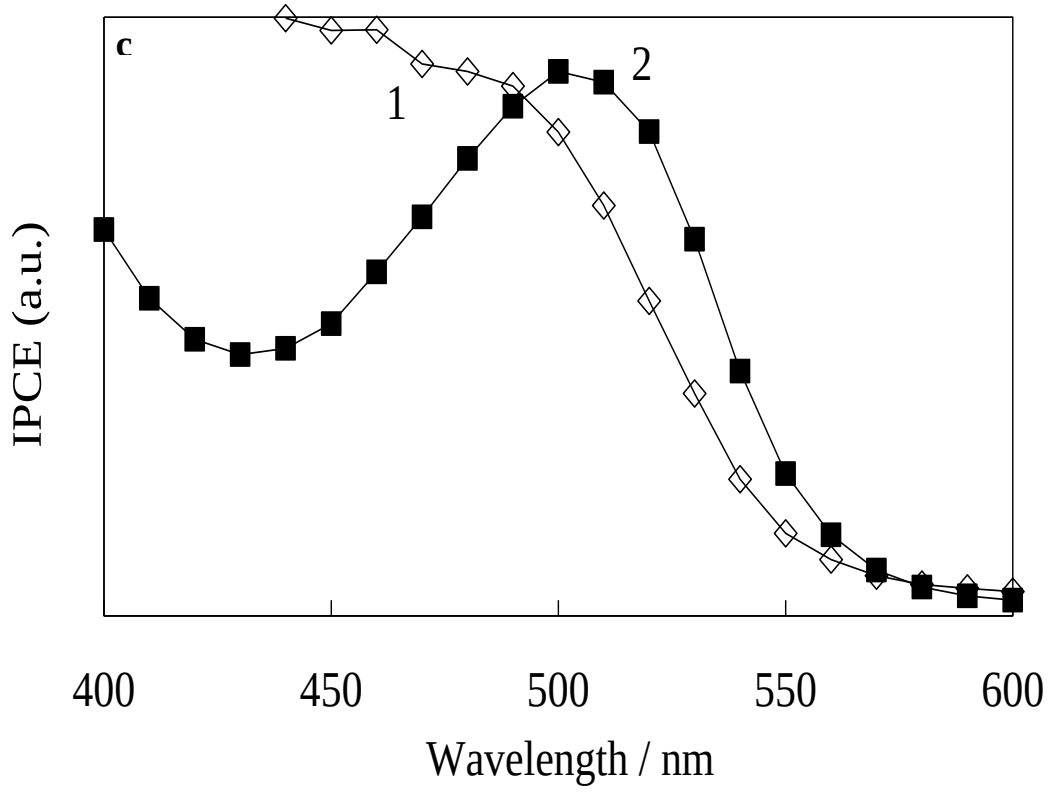
c
1
2
IPCE (a.u.)
400
450
500
550
600
Wavelength / nm

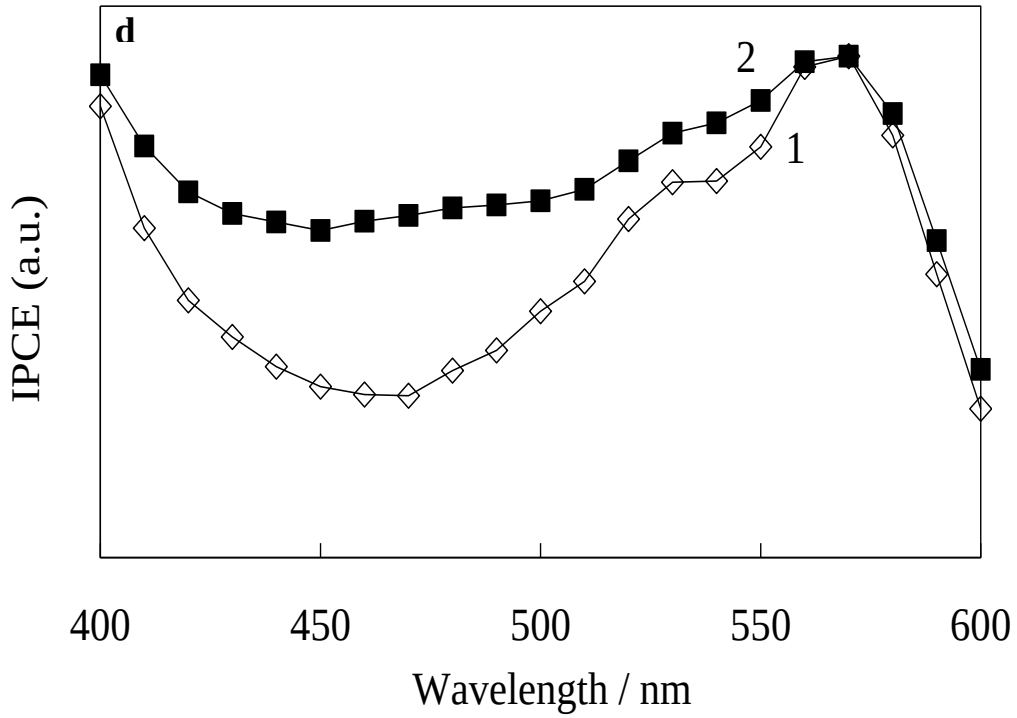

Figure 2–6 Normalized IPCE spectra of (a) WE-SF, (b) WE-AF, (c) WE-CF, and (d) WE-RB observed (1) before and (2) after steam treatments.

2.3.5. Photoelectric conversion properties of the electrodes

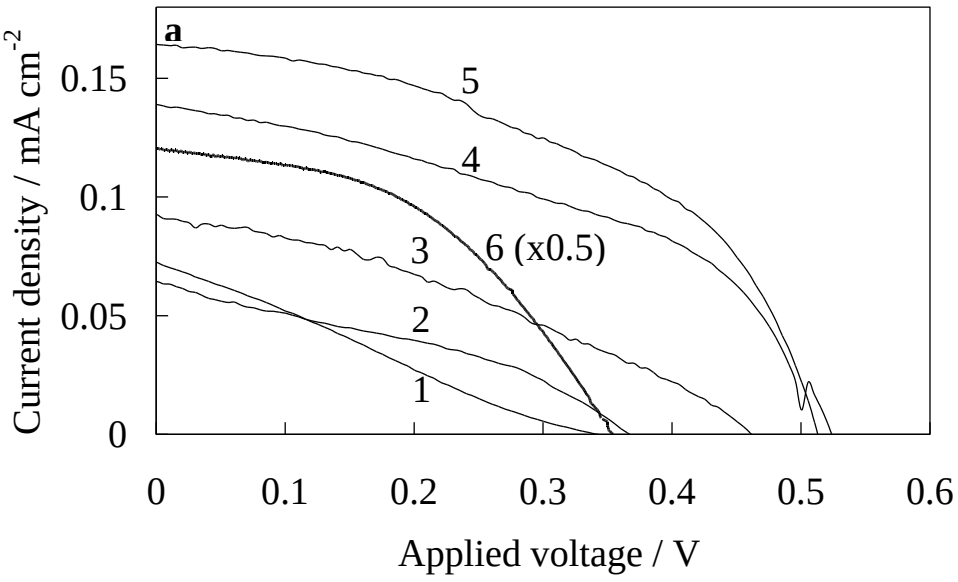

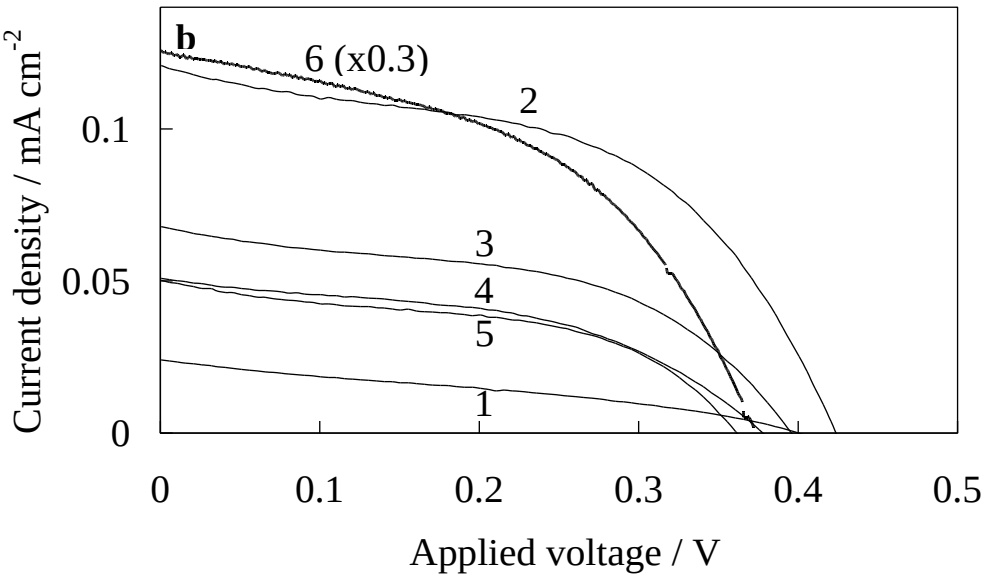

Figure 2–7 *I-V* curves of (a) WE-F and (b) WE-EY observed (1) before and after (2) 20-, (3) 40-, (4) 60-, and (5) 120-min steam treatments. These curves are compared to those of (a-6) WE-F-c and (b-6) WE-EY-c, respectively.

Table 2–1 Photoelectric conversion properties of WE-F and WE-F-c

Treatment time / min	I_{SC} / mA cm^{-2}	V_{OC} / V	*FF*	P_{max} / μW cm^{-2}	^{a}QE / %
WE-F					
0	0.071±0.02	0.34±0.02	0.25±0.02	6.1±1.87	0.71±0.44
20	0.063±0.00	0.37±0.04	0.36±0.18	8.3±3.79	1.6±0.52
40	0.091±0.02	0.46±0.04	0.35±0.08	15±6.08	1.9±0.40
60	0.14±0.02	0.53±0.02	0.45±0.12	33±5.82	5.6±0.31
120	0.16±0.04	0.52±0.00	0.48±0.11	40±9.04	8.4±1.48
WE-F-c	0.24±0.01	0.36±0.00	0.46±0.00	40±2.54	3.9±0.64

Table 2–2 Photoelectric conversion properties of WE-EY and WE-EY-c

Treatment time / min	I_{SC} / mA cm^{-2}	V_{OC} / V	*FF*	P_{max} / μW cm^{-2}	$\boldsymbol{b}_{QE}$ / %
WE-EY					
0	0.024±0.00	0.40±0.01	0.32±0.01	3.1±0.38	0.41±0.11
20	0.12±0.01	0.43±0.02	0.51±0.01	26±4.00	3.5±0.54
40	0.068±0.01	0.40±0.02	0.49±0.00	13±2.76	7.1±1.26
60	0.051±0.02	0.38±0.04	0.48±0.02	9.1±3.00	6.7±0.58
120	0.050±0.02	0.36±0.02	0.48±0.10	8.8±5.44	7.1±1.31
WE-EY-c	0.42±0.02	0.37±0.01	0.48±0.02	75±1.01	4.7±0.12

Key: I_{SC}, short circuit photocurrent density; V_{OC}, open circuit voltage; FF, fill factor; $P_{max,}$ maximum power; QE, quantum efficiency at (a) 500 nm, (b) 540 nm.

Figure 2–7 shows the *I-V* curves of WE-F and WE-EY observed as a function of the treatment time compared to those of WE-F-c and WE-EY-c. Their photoelectric conversion properties of WE-F and WE-F-c, and WE-EY and WE-EY-c are summarized in Tables 1 and 2, respectively. The properties of WE-F indicate an increase in the values of the short circuit current (I_{SC}), open circuit voltage (V_{OC}), fill factor (*FF*), and consequently, the maximum power (P_{MAX}) with the treatment time. The quantum efficiency (QE) of the photoelectric conversion of WE-F at 500 nm also gradually increased as expected. On the other hand, these values of WE-EY, except QE values, increased during the 20-min treatment, and then decreased due to the titania conductivity. The increase in the QE values of WE-EY at 540 nm reflected the improvement in the total electrode performance during the 40-min treatment. The QE values can be regarded as being unchanged after the 60-min treatment even though they are not accurate because the absorbance

is too low. The increase in these values is due to the increase in the titania conductivity based on the results of the XRD analysis. The decrease is mainly due to the dye desorption. Additionally, another reason is also suggested in that the bonds between the crystalline particles were weakened by hydrolysis based on the results of the XRD analysis and UV photocurrent spectroscopy.

The maximum QE values of the stream-treated WE-F and WE-EY are higher than those of the conventional electrodes, WE-F-c and WE-EY-c. The I_{SC} values of WE-F-c and WE-EY-c are significantly higher than those of WE-F and WE-EY because their electric conductivity and dye content are higher. However, the V_{OC} values of the conventional electrodes are close to those of the untreated dye-dispersing electrodes. The QE values are suggested to depend on not only the electric conductivity of the titania, but also the dye–titania interaction and complex formation.

Figure 2–8 shows the changes in the I_{SC} and V_{OC} values with the treatment time for the electrode samples containing each dye. The increase in the I_{SC} and V_{OC} values during the treatment was observed in the electrodes containing the dyes, F, AF, and CF, along with the spectral red-shift. The increase and decrease in these values were observed in the electrodes containing the dyes, EY and RB, without the spectral shift. The I_{SC} and V_{OC} values of the dye-doped electrodes are closely related to the complex formation abilities of the dyes with titanium species.

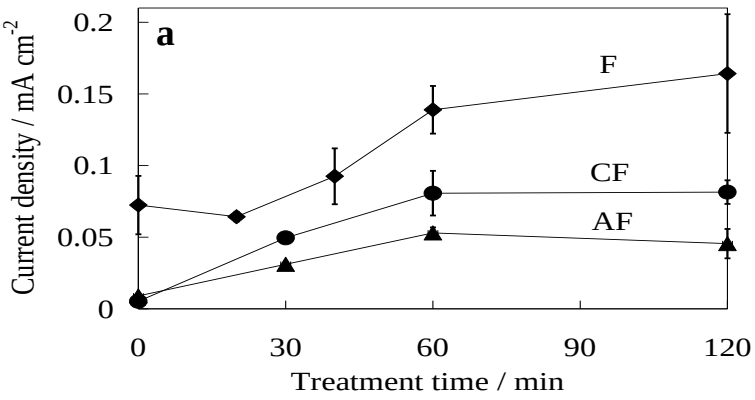

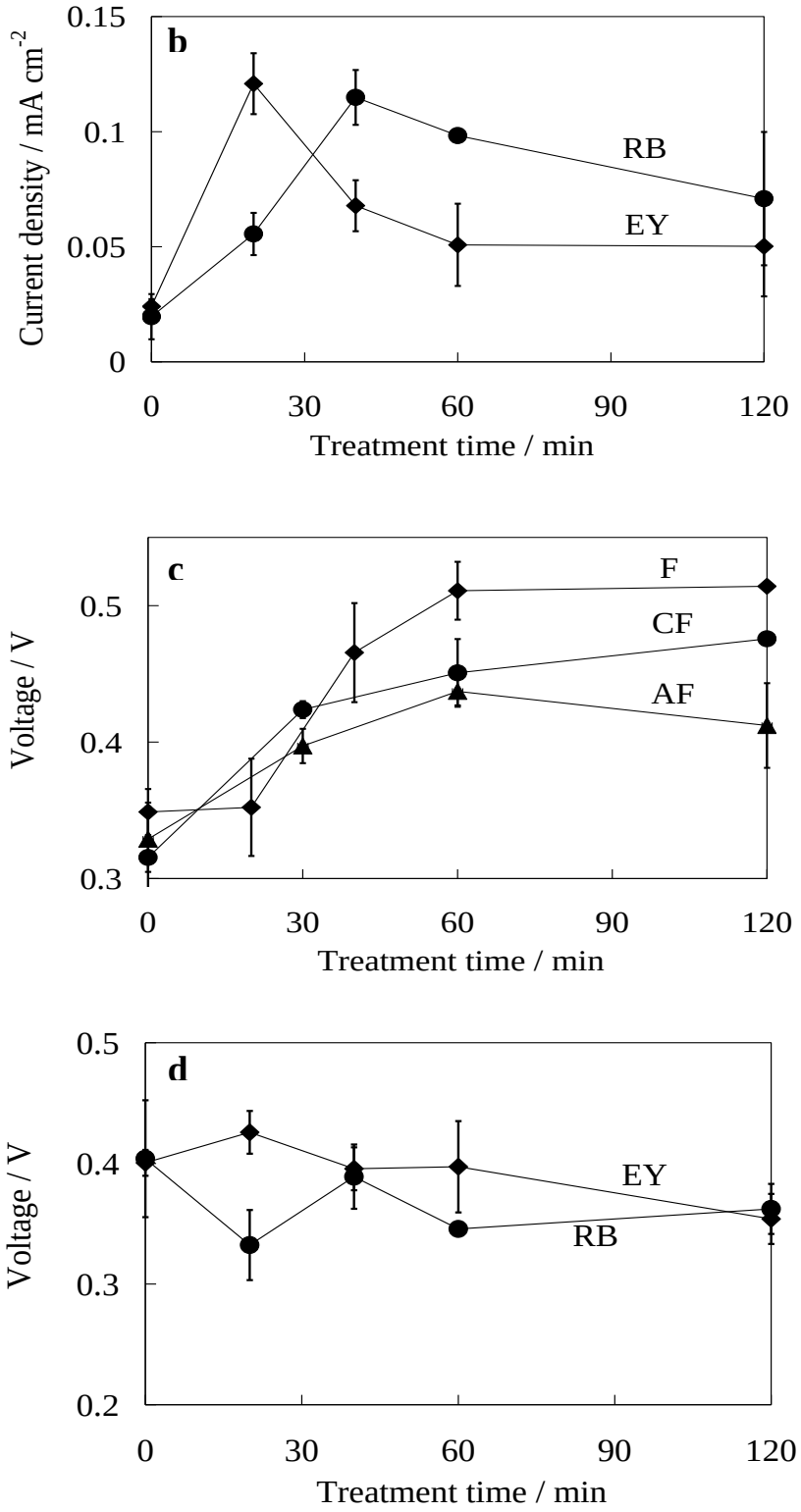

Figure 2–8 Changes in (a,b) I_{SC} and (c,d) V_{OC} values with an increase in the steam treatment time for the electrode samples containing each dye.

2.3.6. Relationship between titania structure and dye–titania complex formation

The photoelectric conversion properties and FTIR spectra of the dye-dispersing titania samples indicate that the chelate complex formation increased the short circuit current and open circuit voltage values. The carboxylate and quinone-like carbonyl of the dyes tend to interact with the titanium species. Fluorescein formed a greater amount of the chelate complex than eosin Y due to its higher reactivity with the titanium species depending on the nucleophilicity of its oxygen atoms of the carboxylate and carbonyl. Active gaseous water promoted the hydrolysis of the titanium species and enhanced their reactivity. Based on the XPS and FTIR analyses, Nishikiori et al. showed that the charge density of the typical Ti^{4+} increased by the formation of anatase-type titania during the steam treatment, which led to the formation of the conduction band with higher density of acceptor states.[26] An increase in the overall crystallinity of titania nanoparticles results in an increase in the surface quality of the nanoparticle, which enhances the dye–titania complex formation.[21] The titanium chelation of the fluorescein species was promoted in the narrow spaces between the titania nanoparticles. This factor appears to play an important role in electron injection from the dye to the titania. The scheme of the changes in the titania structure and the dye–titania interaction by the steam treatment is shown in Figure 2–9.

The V_{OC} is determined from the potential difference between the conduction band edge of the titania and the redox potential of the electrolyte. The change in this value indicates a shift in the conduction band edge. The chelate complex formation on the surface of the titania nanoparticle causes such a potential shift. The dye molecules having a high oxygen nucleophilicity formed a chelate complex with the titanium species on the titania surface to induce an interaction between their orbitals in the steam-treated electrodes based on the spectral red-shift. This interaction caused the ligand to metal charge transfer (LMCT) interaction and the fast electron injection into the titania conduction band.[8,9,14,21] It is suggested that the electrons in the LUMO of the

π–π^*state (S_1) of the xanthene ring are directly injected into the titania conduction band due to the strong interaction between the dye chromophore and titania surface. The V_{OC} values were increased by the steam treatment because the chelate complex formation caused the negative shift in the conduction band potential due to an increase in the negative charge density on the titania surface.[14]

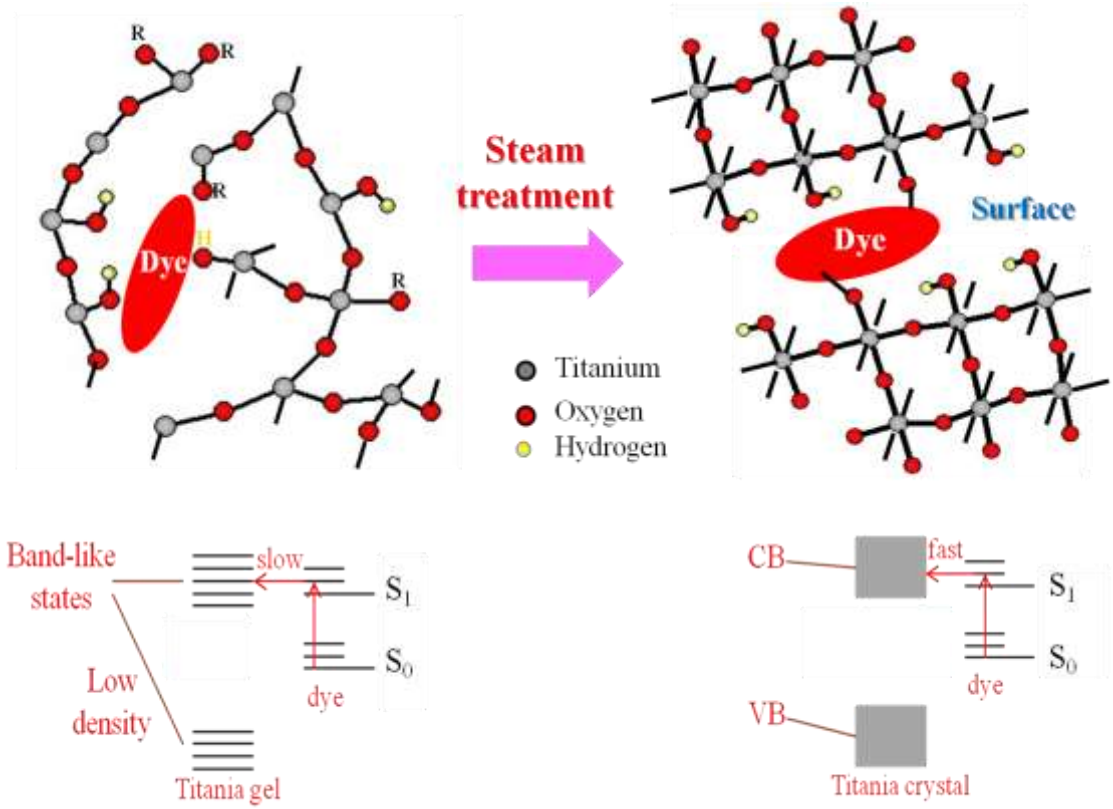

Figure 2–9 Scheme of the changes in the morphological and band structure of the titania and the dye–titania interaction by steam treatment.[21]

2.4. Conclusions

The photocurrent quantum efficiency of the dye-dispersing titania electrode remarkably increased by the steam treatment. The growth and crystallization of the titania particles and the decrease in the defect density by the treatment improved the electric conductivity. In addition to

this, the dye–titania complex formation appears to play an important role in transport of the electron through the electrode. The steam treatment enhanced the dye–titania interaction and promoted the dye–titania chelate complex formation on the titania surface. This is because active gaseous water promoted the hydrolysis of the titanium species and enhanced their reactivity. The titanium chelation of the carboxylate and carbonyl of the dye was promoted in the narrow spaces of the titania networks. The complex formation enhanced the photocurrent due to improvement in the efficiency of the electron injection into the titania conduction. The V_{OC} values were increased by the steam treatment because the chelate complex formation caused the negative shift in the conduction band potential. The dye formed a greater number of chelate complexes with titanium species due to higher nucleophilicity of its oxygen atoms.

References

(1) B. O'Regan, M. Grätzel

Nature, 353 (1991**)**, pp, 737−740

(2) M. K. Nazeeruddin, A. Kay, I. Rodicio, R. Hamphry-Baker, E. Müeller, P. Liska, N. Vlachopoulos, M. Grätzel

Journal of American Chemical Society, 115 (1993**)**, pp, 6382−6390

(3) M. Grätzel

Journal of Photochemistry and Photobiology C: Photochemistry Reviews, 4 (2003), pp, 145−153

(4) K. Murakoshi, G. Kano, Y. Wada, S. Yanagida, H. Miyazaki, M. Matsumoto, S. Murasawa

Journal of Electroanalytical Chemistry, 396 (1995), pp, 27−34

(5) K. Kalyanasundaram, M. Grätzel

Coordination Chemistry Reviews, 177 (1998), pp, 347−414

(6) J. He, F. Chen, J. Zhao, H. Hidaka

Colloids and Surfaces A: Physicochemical and Engineering Aspects, 142 (1998), pp, 49−57

(7) C. Wang, C. Liu, Y. Wang, T. Shen

Journal of Colloid and Interface Science, 197 (1998), pp, 126−132

(8) M. Hilgendorff, V. J. Sundström

Journal of Physical Chemistry.B, 102 (1998), pp, 10505−10514

(9) G. Ramakrishna, H. N. Ghosh

Journal of Physical Chemistry B, 105 (2001), pp, 7000−7008

(10) G. Benkö, M. Hilgendorff, A. P. Yartsev, V. J. Sundström,

Journal of Physical Chemistry B, 105 (2001), pp, 967−974

(11) G. Benkö, B. Skårman, R. Wallenberg, A. Hagfeldt, V. Sundström, A. P. Yartsev

Journal of Physical Chemistry B, 107 (2003), pp, 1370−1375

(12) S. Pelet, M. Grätzel, J. E. Moser

Journal of Physical Chemistry B, 107 (2003), pp, 3215−3224

(13) G. Ramakrishna, A. Das, H. N. Ghosh

Langmuir, 20 (2004), pp, 1430−1435

(14) D. El Mekkawi, M. S. A. Abdel-Mottaleb

International of Journal Photoenergy, 7 (2005), pp, 95−101

(15) G. D. Sharma, P. Balraju, M. Kumar, M. S. Roy

Material and Science and Engineering: B, 162 (2009), pp, 32−39

(16) H. Nishikiori, Y. Uesugi, N. Tanaka, T. Fujii

Journal of Photochemistry and Photobiology A: Chemistry, 207 (2009), pp. 204-208

(17) T. Fujii, A. Ishii, N. Takusagawa, M. Anpo

Research on Chemical Intermediate, 17 (1992), pp, 1−14

(18) J. N. O'Shea, J. B. Taylor, E. F. Smith

Surface Science, 548 (2004), pp, 317−323

(19) H. Nishikiori, N. Tanaka, T. Kitsui, T. Fujii

Journal of Photochemistry and Photobiology A: Chemistry, 179 (2006), pp. 125-129

(20) T. Kitsui, H. Nishikiori, N. Tanaka, T. Fujii

Journal of Photochemical and Photobiology A: Chemistry, 192 (2006), pp, 220−225

(21) H. Nishikiori, W. Qian, M. A. El-Sayed, N. Tanaka,; T. Fujii

Journal of Physical Chemistry Letters, 111 (2007), pp. 9008-9011

(22) N. O. Mchedlov-Petrossyan, V. N. Kleshchevnikova

Journal of Chemical Society, Faraday Transactions, 90 (1994), pp, 629−640

(23) L. Wang, A. Roitberg, C. Meuse, A. K. Gaigalas

Spectrochemica Acta A, 57 (2001), pp, 1781−1791

(24) A. A. Kazarian, E. F. Hilder, M. C. J. Breadmore

Journal of Chromatography A, 1200 (2008), pp, 84–91

(25) M. E. Martínez-Izquierdo, J. S. Durand-Alegría, A. Cabrera-Martín, R. Gallego-Andreu

Analyst, 109 (1984), pp, 377−379

(26) H. Nishikiori, R. A. Setiawan, K. Miyamoto, G. Sukomono, Y. Uesugi, K. Teshima, T. Fujii

RSC advances, 2 (2012), pp. 4258-4267

Chapter 3

Electron transfer in dye-dispersing titania gel films observed by time-resolved fluorescence spectroscopy

3.1 Introduction

Many scientists have investigated the electron donor–acceptor interaction between dye molecules and the titania in the dye–titania systems used for the dye-sensitized solar cells (DSSCs).[1−12] Organic laser dyes are useful materials for utilizing photoenergy due to their high absorption efficiency.[13] It was reported that xanthene dyes, one of the laser dyes, formed a chelate complex with the titanium species on the titania surface in the dye–titania systems. The complex formation induces an interaction between their orbitals and the red-shift in their absorption spectrum. This interaction caused the ligand-to-metal charge transfer (LMCT) interaction and a fast electron injection into the titania conduction band.[5,6,11]

In chapter 2, influence of steam treatment on dye–titania complex formation was discussed. The steam treatment enhanced the photoelectric conversion efficiency of the fluorescein-dispersing titania gel due to not only crystallization of the titania gel, but also the dye–titania surface complex formation.[14−18] The transient absorption spectroscopy indicated that the steam treatment increased the rate of the photoinduced electron transfer from the dispersed fluorescein molecules to the titania.[14] The electron injection process from the dye-excited states to the titania conduction band is important for the photoelectric conversion. Time-resolved fluorescence spectroscopy is more sensitive than transient absorption spectroscopy, and therefore, more suitable to obtain systematic experimental data.[17,19] This is because stronger signal can be obtained in the former than in the latter. In the fluorescence spectroscopy,

fluorescence signal is acquired from the part irradiated by the laser light in the sample, whereas the absorption spectroscopy analyzes the change in the signal at the cross section between pump light and probe light in the sample. In this chapter, fluorescein-dispersing titania gel films were prepared by the nitric acid-catalyzed sol–gel method and steam treatment using a titanium alkoxide solution containing fluorescein. For comparison, fluorescein-dispersing silica–titania binary gel films were also prepared in the same way using silicon and titanium alkoxides. The steady state and time-resolved fluorescence of the fluorescein-dispersing titania gel films were obtained in order to clarify the influence of the dye–titania interaction on the electron transfer from the dye to the titania.

3.2. Experimental section

3.2.1 Sample preparation

Tetraethyl orthosilicate (TEOS), titanium tetraisopropoxide (TTIP), ethanol, fluorescein, hydrochloric acid, nitric acid, and sodium hydroxide (Wako, S or reagent grade) were used without further purification. Water was ion-exchanged and distilled. The glass plates (Matsunami S-1126) were soaked in hydrochloric acid (1.0 mol dm^{-3}) for 2 h and then rinsed with water.

1) The sol–gel reaction system of TEOS was prepared by mixing 3.7 cm^3 of TEOS (= 1.7×10^{-2} mol), 26.0 $cm^3$of ethanol, 0.21 cm^3 of water, and 0.21 cm^3 of nitric acid as the catalyst of the sol–gel reaction. 2) The sol–gel reaction system of TTIP was prepared by mixing 5.0 cm^3 of TTIP (= 1.7×10^{-2} mol), 25.0 cm^3 of ethanol, 0.21 cm^3 of water, and 0.21 cm^3 of nitric acid. 3) The sol–gel reaction systems of the TEOS–TTIP binary were prepared by mixing by alkoxides (TEOS/TTIP = 50/50, 25/75, and 10/90, TEOS + TTIP = 1.7×10^{-2} mol), 25.0 cm^3 of ethanol, 0.21 cm^3 of water, and 0.21 cm^3 of nitric acid. The materials, except for TTIP, stirred

during the addition and then thoroughly for an additional 10 min, were mixed with TTIP under a dry N_2 atmosphere, and stirred for 10 min more.

The concentration of nitric acid was 7.5×10^{-2} mol dm^{-3} in all the sol–gel reaction systems. Fluorescein was dissolved in all the systems at the final concentration of 1.0×10^{-2} mol dm^{-3}. The dip-coated thin films were prepared on the glass plates from these dye-containing systems in which the sol–gel reaction proceeded at 35ºC for 1 day. The steam-treatment effects on the spectroscopic properties of the thin film samples were investigated. Water was heated to 110ºC and the thin film samples were exposed to its steam for 20−120 min. The pressure of the steam was about 140 kPa.

3.2.2. Measurements

The UV-vis absorption and fluorescence spectra of the prepared samples were obtained using a spectrophotometer (Shimadzu UV-3510) and a fluorescence spectrophotometer (Shimadzu RF-5300), respectively. The relative fluorescence quantum yield was obtained by dividing the fluorescence maximum intensity by the absorbance at the excitation wavelength. The flakes of the dye-dispersing film samples were pressed in KBr pellets and their IR spectra were obtained using an FTIR spectrophotometer (Shimadzu FTIR-8300).

A Ti:Sapphire femtosecond pulse laser and streak scope spectroscopic system were used for the time-resolved fluorescence measurements in order to obtain information about the fluorescence quenching due to the electron injection from the dye to the titania.[19,25] The laser system (Clark MXR CPA 2001) generates laser pulses of 150 fs duration (FWHM) with an energy of 750 μJ at 750 nm and a repetition rate of 1 kHz. The second harmonics of the laser pulses (375 nm) was used for the excitation. The fluorescence signal was monitored using a streak scope system (Hamamatsu Photonics C4780). The fluorescence decay curves were

obtained by integrating the fluorescence signals in the 500–550 nm region. The film samples for this measurement were washed with a 0.1 mol dm^{-3} sodium hydroxide aqueous solution and water in order to adjust to the same amount of the dye. The amount of the dye was confirmed by a UV-vis absorption measurement.

3.3. Results and discussion

3.3.1. Steady state spectroscopy

Figure 3–1 shows the visible absorption spectra of the fluorescein-dispersing silica and titania gel films observed as a function of the steam treatment time. The thickness of the dye-dispersing layer of this sample was ca. 350 nm and that slightly changed by the steam treatment.[15–18] For the silica gel film, the absorption peaks were observed at 460 and 485 nm (double maxima), indicating that the main fluorescein species were the anion form.[20] The absorbance decreased by 75%, and the spectral peak and shape of the film were slightly changed during the 120-min steam treatment. The fluorescein molecules were desorbed from the inside of the silica gel film into the water phase because the species was weakly trapped in the pores of the gel by hydrogen-bonding. Steam treatment at 80–100°C was previously found to promote the polymerization of the alkoxide species and the particle growth in the sol–gel systems.[15–18] Hot water promotes the hydrolysis and sequential polymerization of the silicon alkoxide species, resulting in the reorientation of the silica networks. It is suggested that the dye molecules were reoriented by the hot water and the change in the silica networks. During the reorientation, some dye molecules were desorbed into the water phase.

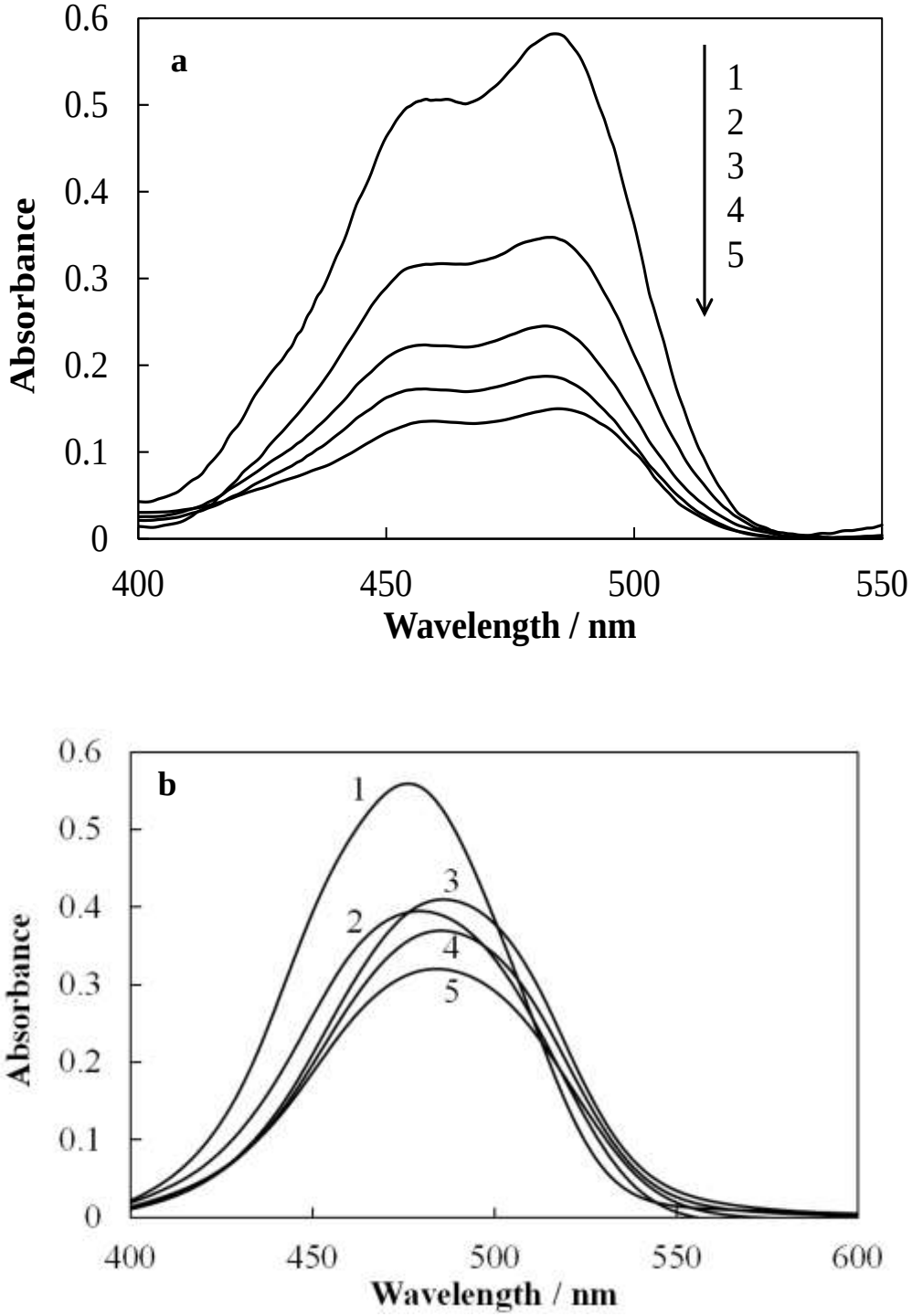

Figure 3–1 UV−vis absorption spectra of the fluorescein-dispersing (a) silica and (b) titania gel films (1) untreated and steam-treated for (2) 20, (3) 40, (4) 60, and (5) 120 min.

The spectrum of the untreated titania gel sample is located around 475 nm, ranging over a

wavelength wider than that observed in solvents. This result indicated that the main fluorescein species were the neutral or anion form (at 450–485 nm) and some fluorescein molecules existed as the dianion form (at around 490 nm).[20] The difference in composition of the species between the silica and titania systems was due to that in their acidity. Acidity of the hydroxyl group is expected to be higher in the silica gels than in the titania gels because electronegativity of silicon is higher than that of titanium. In addition, the longer wavelength band indicated that a small number of fluorescein molecules formed a complex resulting from the strong interaction and chelating linkage between the carboxyl group of the dye and the titanium species.[1,2,5−7,11,21] The absorbance decreased by 40%, and the spectral peak of the film was red-shifted from around 470 to 485 nm by the 120-min steam treatment.[11, 14−16,22,23] The spectral shape became broader on the longer wavelength side. These results indicated that the neutral and anion species were preferentially desorbed from the inside of the titania gel film into the water phase because the species was weakly trapped in the pores of the gel. The increase in the absorbance and the red shift observed during the steam treatment from 20 to 40 min indicated that the anion was transformed into the dianion, having higher molar extinction coefficient, due to desorption of nitric acid added as a catalyst. The sequential decrease in the absorbance was due to the dianion desorption. The stream treatment probably increased the number of fluorescein molecules interacting with the titanium species. This indicated the dye–titania complex formation.

In the other study, the untreated amorphous titania gel was crystallized by the steam treatment.[16] The crystallite size was estimated to be 4–6 nm nm after the steam treatment for 20–120 min by XRD analysis. Compared to the heated titania sample, the crystallite size of the film was small and not significantly changed by the steam treatment for more than 20 min. However, the diffraction peak was sharper after the longer steam-treatment time due to increasing the number of the crystalline particles, which led to increasing the film density.

The fluorescein molecules readily formed the complex with the titania surface because they were encapsulated in the small pores and strongly interacted with the surrounding titania nanoparticles.

Figure 3–2 shows the UV–vis absorption spectra of the fluorescein-dispersing silica–titania gel films steam-treated for 120 min in the different molar ratios of Si/Ti. In the silica gel film (Si/Ti = 100/0), the absorption peaks were observed at 460 and 485 nm, indicating that the main fluorescein species were the anion form. Apparently, the 460-nm band intensity relatively decreased and the 485-nm band broadened with an increase in the titanium content. The longer wavelength band observed in the silica–titania and titania gel films originated from the dianion species and fluorescein–titania complex.

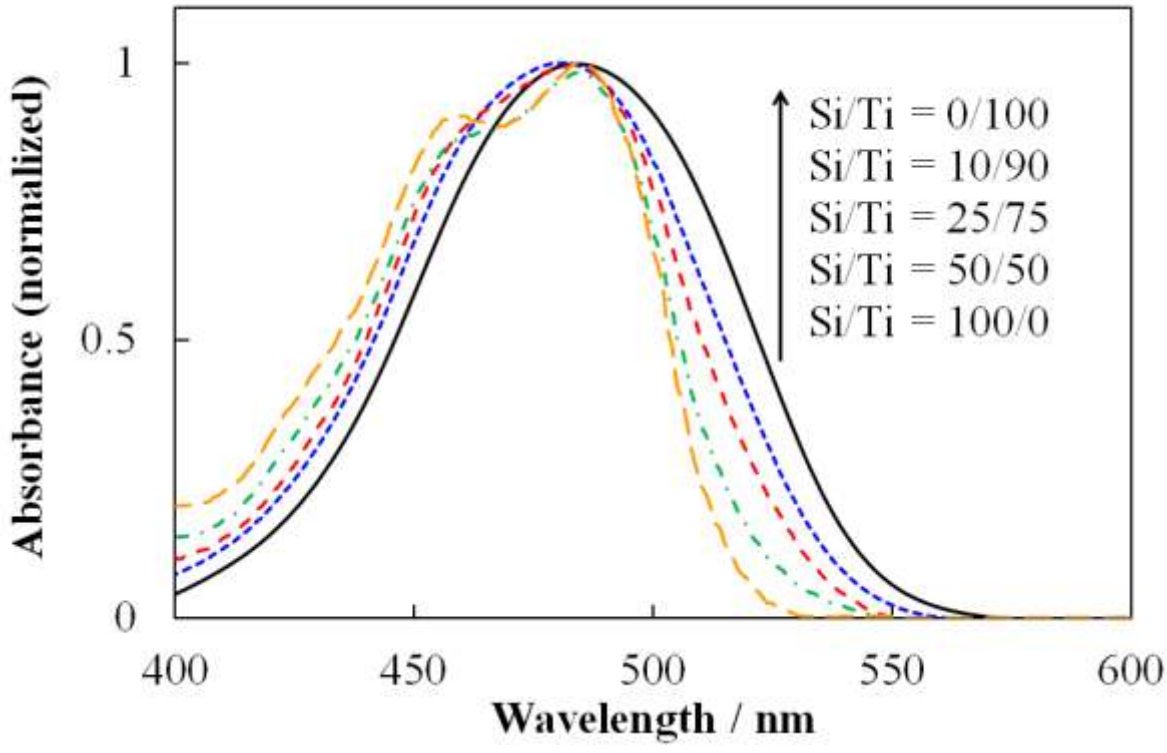

Figure 3–2 UV–vis absorption spectra of the fluorescein-dispersing silica, titania, and silica–titania gel films steam-treated for 120 min.

Figure 3–3 shows the FTIR spectra of fluorescein and the fluorescein-dispersing titania gels before and after the steam treatment. The peaks of the carboxyl C=O stretching and the carboxylate COO^- antisymmetric and symmetric stretching vibrations were observed at 1710, 1597, and 1391 cm^{-1} in fluorescein, respectively. In addition, the band at around 1490 cm^{-1} was assigned to the quinone-like C=O stretching vibration.[24] The untreated fluorescein-dispersing sample exhibited a carboxyl band at around 1710 cm^{-1}, carboxylate bands at 1580 and 1398 cm^{-1}, and a quinone-like band at 1450 cm^{-1}. The significant shifts in the carboxylate and quinone-like bands are due to the interaction between the functional groups and the titanium species of titania. The intensity of the carboxyl band decreased and that of the interacting carboxylate and quinone-like bands relatively increased due to the steam treatment. The peaks of the carboxylate and quinone-like bands were further shifted to a low wavenumber by the steam treatment due to the enhancement of the interaction between the functional groups and the titanium species of titania.

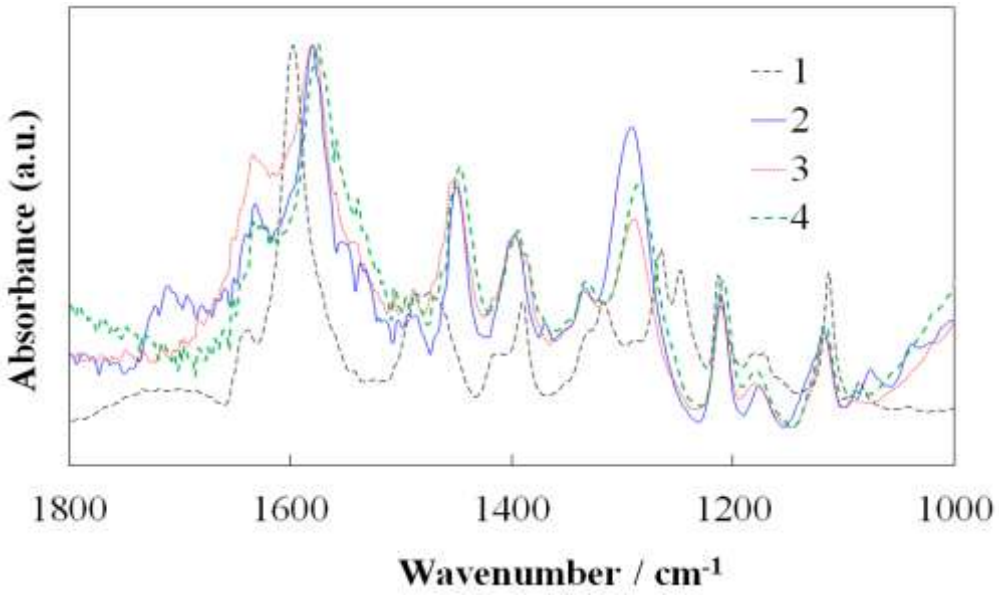

Figure 3–3 FTIR spectra of (1) fluorescein and the fluorescein-dispersing titania gel (2) untreated and steam-treated for (3) 60 and (4) 120 min.

The fluorescence spectra of the silica and titania samples are shown in Figure 3–4. The untreated silica sample exhibited a peak at around 510 nm, which was mainly assigned to the anion of fluorescein.[20,23] The fluorescence intensity remarkably decreased with an increase in the steam treatment time although the spectral peak and shape only slightly changed. This corresponded to the change in the absorption spectrum. The untreated titania sample exhibited a peak at around 535 nm, which was mainly assigned to the dianion species [20,25,26] and its complex with the titania. The fluorescence of the anion species should be much weaker than that of the dianion species based on the peak shape and position, and its lower fluorescence quantum yield.[25] The fluorescence intensities of the titania samples were much lower than those of the silica samples. This value remarkably decreased with the steam treatment time. The spectral peak and shape were only slightly changed, indicating that the relative amounts of the fluorescent species were almost constant.

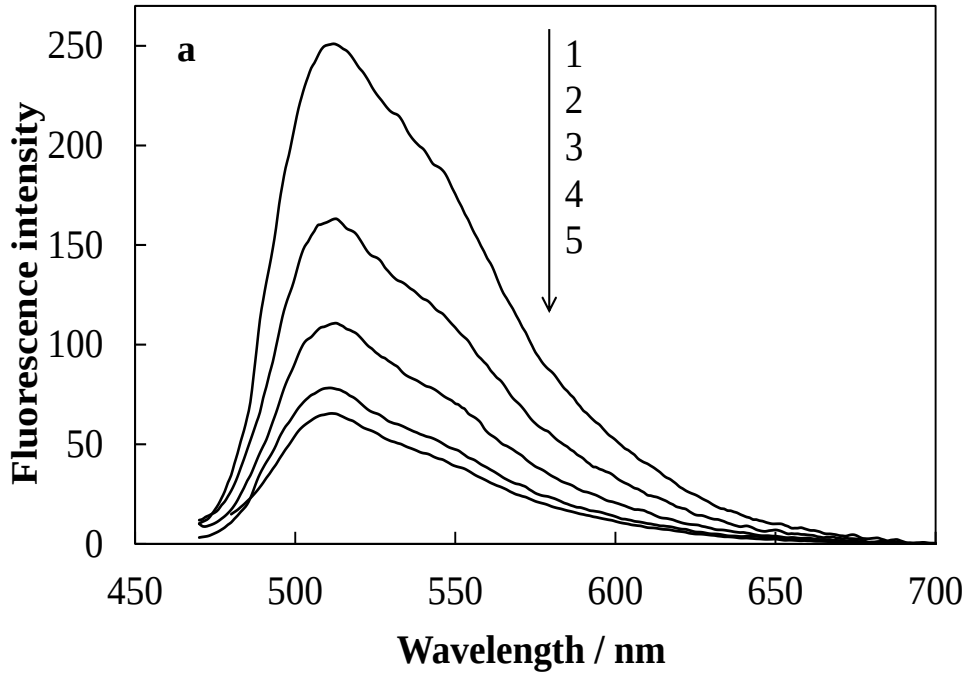

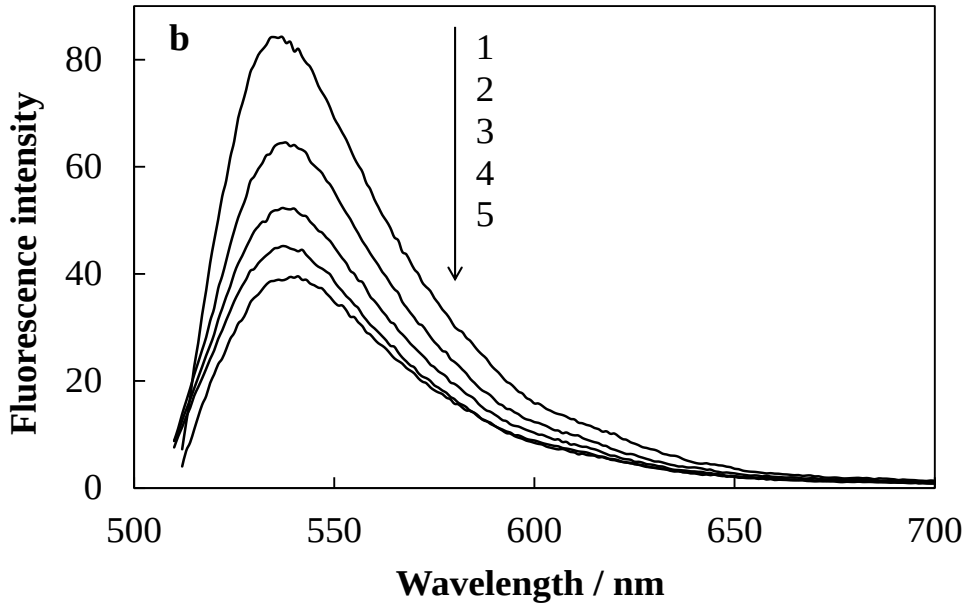

Figure 3–4 Fluorescence spectra of the fluorescein-dispersing (a) silica and (b) titania gel films (1) untreated and steam-treated for (2) 20, (3) 40, (4) 60, and (5) 120 min. These spectra were observed upon excitation at (a) 470 and (b) 500 nm.

The relative fluorescence quantum yields of the silica and titania samples are shown in Figure 3–5. The values were normalized to the fluorescence quantum yield of the untreated silica sample. The value of the silica sample was almost constant, indicating that the species or the environment around the dye molecules was not significantly changed during the steam treatment. The quantum yield of the untreated titania sample was about half that of the silica samples. For the titania samples, the fluorescence quantum yield as well as the intensity decreased with the steam treatment time. This can be due to the dye–titania complex formation. The HOMO and LUMO levels of fluorescein were reported to be 1.65 and −0.58 V vs. SHE, respectively.[27] The LUMO level is more negative than the level of the titania conduction band edge (ca. −0.5 vs. SHE).[28] The fluorescence quenching can be caused by the electron injection from the dye into the titania.[5,6]

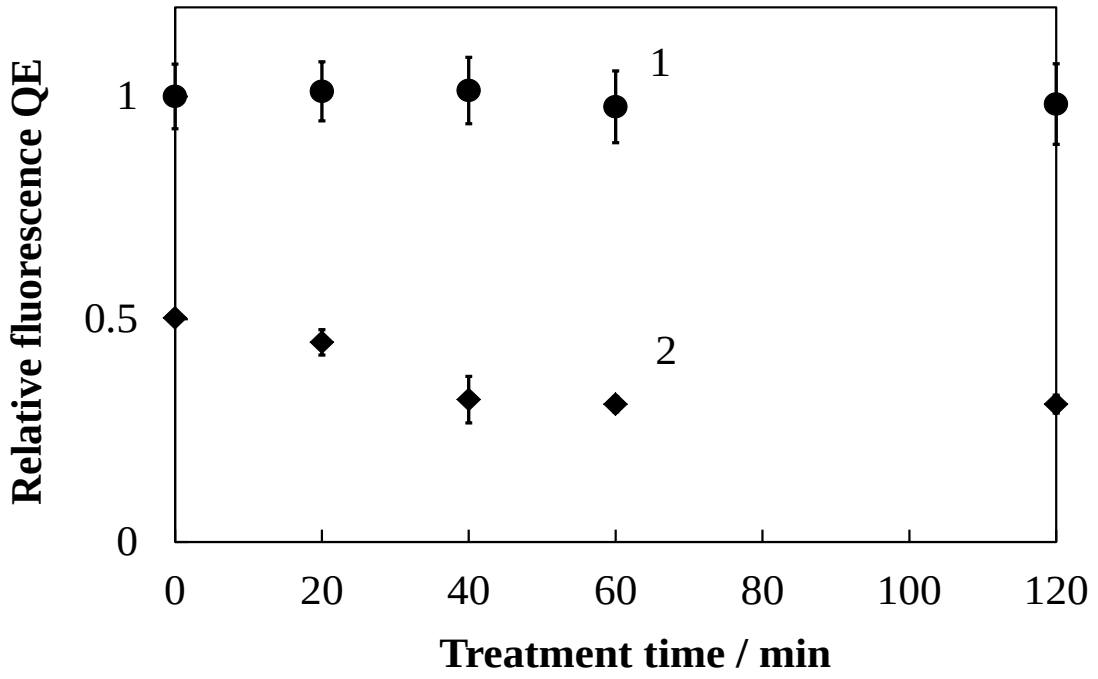

Figure 3–5. Relative fluorescence quantum yield (QE) of the fluorescein-dispersing (1) silica and (2) titania gel films untreated and steam-treated for 20–120 min.

3.3.2. Time-resolved spectroscopy

The fluorescence decay curves were obtained by the time-resolved fluorescence measurement as shown in Figure 3–6. The 375 nm light used for the excitation corresponds to 3.31 eV. In this condition, fluorescein was excited to a highly vibrationally excited state of the S_1.[29] The decay profiles of the dye-dispersing titania gel films were compared to that of the dye-dispersing silica gel film steam-treated for 120 min. All the curves of the titania samples were fitted to a double exponential decay, whereas that of the silica sample was fitted to a single exponential decay with the lifetime of 3.7 ns. The fluorescence intensities just after excitation, i.e., the maximum intensities, and fitting parameters are shown in Table 3–1. The lifetime of the fluorescein anion was reported to be 3.0 and 3.8 ns in water and ethanol,[25,30] respectively, and 4.2 ns in silica.[30] The lifetime observed in the present wet silica gels indicated that the dye molecules were

affected by both the water and dry silica matrix.

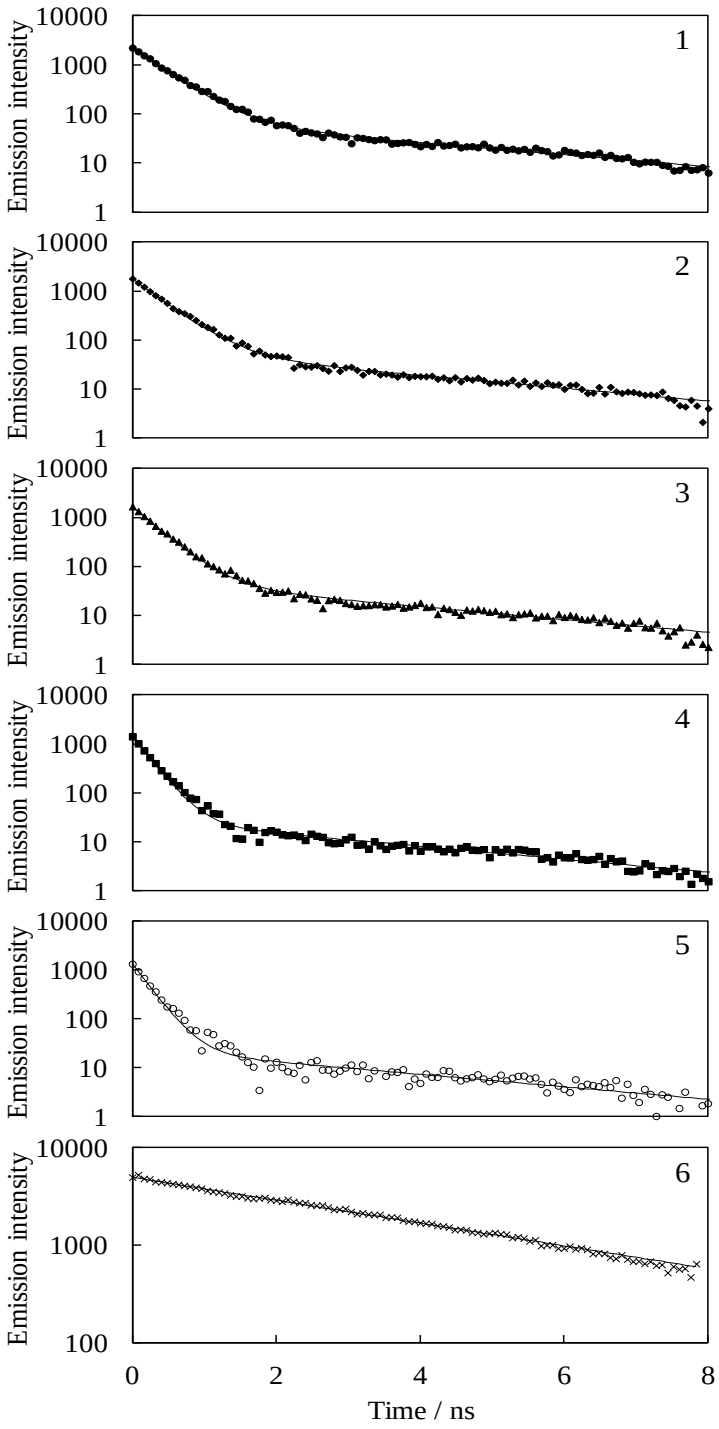

Figure 3–6 Fluorescence decay profiles of the fluorescein-dispersing titania gel films (1) untreated and steam-treated for (2) 20, (3) 40, (4) 60, and (5) 120 min. These profiles are compared to that of (6) the fluorescein-dispersing silica gel films steam-treated for 120 min.

Table 3–1 Emission intensity and fitting parameters of the time-resolved fluorescence of the fluorescein-dispersing titania gel films untreated and steam-treated for 20, 40, 60, and 120 min. These properties are compared to those of the fluorescein-dispersing silica gel films steam-treated for 120 min.

Treatment time / min	Maximum intensity	τ_1 / ns	τ_2 / ns	A_1	A_2
Titania					
0	2230±60	0.41±0.01	3.6±0.1	0.96±0.01	0.04±0.01
20	1800±50	0.39±0.01	3.3±0.1	0.97±0.01	0.03±0.01
40	1680±40	0.34±0.01	3.3±0.1	0.97±0.01	0.03±0.01
60	1410±30	0.23±0.01	3.3±0.1	0.98±0.01	0.02±0.01
120	1340±30	0.22±0.01	3.4±0.1	0.98±0.01	0.02±0.01
Silica					
120	4980±90	-	3.7±0.1	-	1.00

The decay curves of the titania samples consist of two components with the lifetimes of 0.22–0.41 and 3.3–3.6 ns. These values are close to those reported for the dye-adsorbing titania systems.[6] The longer lifetime component is assigned to the original dianion. The fluorescence lifetime of the dianion was reported to be ca. 3−4 ns.[25,26] The shorter lifetime component can be assigned to the fluorescence of the dye interacting with the titania, which is caused by the recombination between the injected electron and the dye.[6] In previous study indicated that the electron injection occurred within a few picoseconds and the recombination between the injected electron and the dye occurred within 20 ps.[14] It is reasonable that the reproduced excited-states of the dye exhibited the fluorescence with the lifetimes of 0.22–0.41 ns in the present systems. In all the films, the exponential function factor for the shorter lifetime

component, A_1, was much higher than that for the longer lifetime one, A_2. The dye somewhat interacted with the titania and exhibited a photoinduced electron transfer to the titania even in the untreated film. The A_1 value slightly increased with the treatment time. On the other hand, a weaker maximum fluorescence intensity was clearly observed in the titania treated for a longer time. The maximum fluorescence intensities of the titania samples were significantly lower than that of the silica sample. The yield of the electron injection from the dye to the titania can have an inverse relation to the fluorescence maximum intensity because the electron injection is reported to occur within 100 ps.[19,31,32] Therefore, the relative electron injection yield in the dye-dispersing titania increased with the steam treatment time as revealed by the transient absorption spectroscopy.[14] This is due to formation of the conduction band with a higher density of acceptor states and the favorable anchoring geometry of the dye after structure transformation from amorphous to crystalline. In this study, the enhancement of the interaction between the dye and titania, which increased the electron injection yield, indicated the dye–titania complex formation.

The steam treatment enhanced not only the electron injection, but also the recombination as previously shown.[14] However, the recombination process was not significant for charge separation in the present systems because it was much slower process than the electron injection. Parts of the injected electrons were trapped by the surface states, and then recombined with the dye. The lifetime of electrons in the conduction band of anatase-type titania was reported to be more than 1 μs due to multiple-trapping electron transport process involving shallow trapping states.[33] The electrons can be transported on the titania particle surface rather than in the bulk in a low crystalline titania such as the present systems.[34] It was also reported that the electrons were transported on the titania nanoparticle surface by such a multiple-electron-trapping process although the rapid free carrier recombination occurred in the bulk crystal.[35]

In previous study concluded that the photocurrent quantum efficiency of the dye-dispersing titania electrode remarkably increased by the steam treatment. [15−18,22,23] The growth and crystallization of the titania particles and the decrease in the defect density by the treatment improved the electric conductivity. In addition to this, the dye–titania complex formation appears to play an important role in transport of the electron through the electrode. The steam treatment promoted the dye–titania chelate complex formation on the titania surface. This is because the active steam promoted the hydrolysis of the titanium species and enhanced their reactivity.[36] The titanium chelation of the carboxylate and carbonyl of the dye was promoted in the narrow spaces of the titania networks. The complex formation enhanced the photocurrent due to the improved efficiency of the electron injection into the titania conduction band. In this study, the absorption and fluorescence properties in the dye-dispersing titania gel samples were continuously changed during the steam treatment for 120 min. The efficiency of the photoelectric conversion due to fluorescein excitation also increased during the steam treatment for 120 min as previously shown.[16] However, the crystal growth proceeded and the efficiency of the photoelectric conversion due to titania excitation increased during the steam treatment for 20 min in the study.[16,18] The steam treatment significantly enhanced the dye–titania interaction that plays an important role in generating the photocurrent in such systems rather than the electric conductivity of the titania.

3.4. Conclusions

Fluorescein-dispersing titania gel films were prepared by the nitric acid-catalyzed sol–gel method and steam treatment using a titanium alkoxide solution containing fluorescein. The steady state and time-resolved fluorescence of the fluorescein-dispersing titania gel films were obtained in order to clarify the influence of the dye–titania interaction on the electron transfer.

A greater degree of fluorescence quenching was observed in the titania steam-treated for a longer time due to the electron injection from the dye into the titania. The fluorescence intensity just after excitation clearly decreased with the treatment time, i.e., the relative electron injection yield increased. Based on FTIR spectroscopy, the titanium species were coordinated to the carboxylate of the fluorescein species, which was enhanced by the steam treatment. The dye–titania complex formation played an important role in the electron injection from the dye to the titania conduction band.

References

(1) K. Murakoshi, G. Kano, Y. Wada, S. Yanagida, H. Miyazaki, M. Matsumoto, S. Murasawa
Journal of Electroanalytical Chemistry, 396 (1995), pp, 27−34

(2) K. Kalyanasundaram, M. Grätzel
Coordination Chemistry Reviews, 177 (1998), pp, 347−414

(3) J. He, F. Chen, J. Zhao, H. Hidaka
Colloids and Surfaces A: Physicochemical and Engineering Aspects, 142 (1998), pp, 49−57

(4) C. Wang, C. Liu, Y. Wang, T. Shen
Journal of Colloid and Interface Science, 197 (1998), pp, 126−132

(5) M. Hilgendorff, V. J. Sundström
Journal of Physical Chemistry.B, 102 (1998), pp, 10505−10514

(6) G. Ramakrishna, H. N. Ghosh
Journal of Physical Chemistry B, 105 (2001), pp, 7000−7008

(7) G. Benkö, M. Hilgendorff, A. P. Yartsev, V. J. Sundström,

Journal of Physical Chemistry B, 105 (2001), pp, 967−974

(8) G. Benkö, B. Skårman, R. Wallenberg, A. Hagfeldt, V. Sundström, A. P. Yartsev

Journal of Physical Chemistry B, 107 (2003), pp, 1370−1375

(9) S. Pelet, M. Grätzel, J. E. Moser

Journal of Physical Chemistry B, 107 (2003), pp, 3215−3224

(10) G. Ramakrishna, A. Das, H. N. Ghosh

Langmuir, 20 (2004), pp, 1430−1435

(11) D. El Mekkawi, M. S. A. Abdel-Mottaleb

International of Journal Photoenergy, 7 (2005), pp, 95−101

(12) G. D. Sharma, P. Balraju, M. Kumar, M. S. Roy

Material and Science and Engineering: B, 162 (2009), pp, 32−39

(13) M. Maeda

Laser Dyes: Properties of Organic Compounds for Dye Lasers; Academic Press: Tokyo, Japan, 1984.

(14) H. Nishikiori, W. Qian, M. A. El-Sayed, N. Tanaka,; T. Fujii

Journal of Physical Chemistry Letters, 111 (2007), pp. 9008-9011

(15) H. Nishikiori, Y. Uesugi, N. Tanaka, T. Fujii

Journal of Photochemistry and Photobiology A: Chemistry, 207 (2009), pp. 204-208

(16) H. Nishikiori, Y. Uesugi, S. Takami, R. A. Setiawan, T. Fujii, W. Qian, M. A. El-Sayed

Journal of Physical Chemistry C, 115 (2011), pp, 2880−2887

(17) H. Nishikiori, Y. Uesugi, R. A. Setiawan, T. Fujii, W. Qian, M. A. El-Sayed

Journal of Physical Chemistry C, 116 (2012), pp, 4848-4854

(18) H. Nishikiori, R. A. Setiawan, K. Miyamoto, G. Sukomono, Y. Uesugi, K. Teshima, T. Fujii

RSC advances, 2 (2012), pp. 4258-4267

(19) L. Du, A. Furube, K. Hara, R. Katoh, M. Tachiya

Journal of Physical Chemistry C, 114 (2010), pp, 8135−8143

(20) T. Fujii, A. Ishii, N. Takusagawa, M. Anpo

Research on Chemical Intermediate, 17 (1992), pp, 1−14

(21) J. N. O'Shea, J. B. Taylor, E. F. Smith

Surface Science, 548 (2004), pp, 317−323

(22) H. Nishikiori, N. Tanaka, T. Kitsui, T. Fujii

Journal of Photochemistry and Photobiology A: Chemistry, 179 (2006), pp. 125-129

(23) T. Kitsui, H. Nishikiori, N. Tanaka, T. Fujii

Journal of Photochemical and Photobiology A: Chemistry, 192 (2006), pp, 220−225

(24) L. Wang, A. Roitberg, C. Meuse, A. K. Gaigalas

Spectrochemica Acta A, 57 (2001), pp, 1781−1791

(25) R. Sjöback, J. Nygren, M. Kubista

Spectrochimica Acta A, 51 (1995), pp, L7–L21

(26) D. Magde, R. Wong, P. G. Seybold

Journal of Photochemical and Photobiology, 75 (2002), pp, 327−334

(27) M. S. Chan, J. R. Bolton

Solar Energy, 24 (1980), pp, 561−574

(28) A. Hagfeldt, M. Grätzel

Chemical Reviews, 95 (1995), pp, 49−68

(29) D.L. Silvaa, R.C. Barreto, E.G. Lacerda Jr., K. Coutinho, S. Canuto

Spectrochimica Acta A, 119 (2014), pp, 63–75

(30) L. Wang, Y. Shao, J. Zhang, M. Anpo

Optical Materials, 28 (2006), pp, 1232−1234

(31) J. B. Asbury, N. A. Anderson, E. Hao, X. Ai, T. Lian

Journal of Physical Chemistry B, 107 (2003), pp, 7376–7386

(32) G. Benkö, J. Kallioinen, J. E. I. Korppi-Tommola, A. P. Yartsev, V. Sundström,

Journal of American Chemical Society, 124 (2002), pp, 489–493

(33) Y. Yamada, Y. Kanemitsu

Applied Physichs Letters, 101 (2012), pp, 133907-1–4

(34) D. Eder, R. Kramer

Physical Chemistry Chemical Physics, 5 (2003), pp, 1314–1319

(35) H. Zhao, Q. Zhang, Y. Weng

Journal of Physical Chemistry C, 111 (2007), pp, 3762–3769

(36) K. Yanagisawa, J. Ovenstone

Journal of Physical Chemistry B, 103 (1999), pp, 7781−7787

Chapter 4

Influence of dye content on the conduction band edge of titania in the dye-dispersing titania electrodes

4.1 Introduction

In recent decades, dye-sensitized solar cells (DSSCs) based on titania have attracted considerable interest as a new potential electric generator due to their low-cost production and simple fabrication process compared to conventional silicon-type solar cells.[1–3] Many efforts have been made in order to achieve a high photoelectric conversion efficiency. In a study, more than an 11% conversion efficiency has been achieved using ruthenium dye complexes as sensitizers.[4] Ruthenium dye complexes are known as superior light harvesting and durable materials, but they are very expensive. Therefore, ruthenium dye complexes are not suitable for the large scale production of such solar cells.

Many studies have been performed for developing new dyes to replace the ruthenium dye complexes, for example, merocyanine dyes,[5] xanthene dyes,[6–10] coumarin dyes,[11,12] etc. Compared to the ruthenium dye complexes, such organic dyes have two advantages for use in DSSCs. One is the high molar extinction coefficient of the organic dyes due to their oscillator being stronger than those of the metal complexes. The other is that no noble metal such as Ru is contained in the dye molecules. This reduces the overall cost of the cell production.[13] However, the narrower optical absorption region and higher volatility of such organic dyes than those of the ruthenium dye complexes are the major problems limiting the efficiency of the DSSCs. A combination of some dyes is able to widen the absorption region and a strong bonding of the dyes to the titania surface inhibits their volatilization. Such techniques require a new technology

to improve the light-harvesting efficiency from the organic dye molecule. The dye-dispersing titania is one of the potential technologies to enhance the light-harvesting from not only the organic dyes[6–10], but also metal-organic dyes such ruthenium complexes dyes.[14]

In chapter 2, it was concluded that the steam treatment of the dye-dispersing titania films remarkably improved the photoelectric conversion efficiency due not only to the crystallization of the titania, but also to the formation of the dye-titanium LMCT complex on the titania surface.[6,9,10] The FTIR spectra of the dye-dispersing titania samples indicated that the chelate complex formation increased the short circuit current and open circuit voltage (V_{oc}).[6,9] Based on the relationship between the increase in the amount of the dye-titania complex and the V_{oc} value, it was concluded that the dye–titania complex formation significantly affected the change in the conduction band edge of the titania.[6,9]

However, the mechanism for the fact that the dye–titania complex formation changes the conduction band edge of the titania and the V_{oc} value of the titania electrode, is still unclear. There are many methods used for the determination of the position of the conduction band edge. The most common method is the Mott-Schottky plot resulting from the measurement of impedance.[15] Cyclic voltammetry (CV) is also one of methods which can determine the band levels of a semiconductor.[16–18] Another common method for the determination of the position of the conduction band edge is the measurement of the potential dependence of the photocurrent called the "photocurrent onset measurement".[19,20]

In this chapter, the measurement of the photocurrent onset determined by CV during light irradiation for the band-gap excitation of the titania (Photo-CV) was conducted in order to estimate the shift in the conduction band edge of the titania in each electrode. The dye–titania complex formation was controlled by changing the dye content in the dye-dispersing titania electrodes in order to discuss influence of such complex species on conduction band edge of the

titania. The photoelectric measurements for the dye–dispersing titania electrodes were also conducted in order to clarify the relationship between the conduction band edge of the titania and the V_{oc} value.

4.2 Experimental

4.2.1 Materials

Titanium tetraisopropoxide, ethanol, fluorescein, hydrochloric acid, nitric acid, diethylene glycol, acetonitrile, tetrabutylammonium perchlorate, iodine, and lithium iodide (Wako, S or reagent grade) were used without further purification. Water was ion-exchanged and distilled. Glass plates coated with the transparent ITO electrode (AGC Fabritech) were soaked in hydrochloric acid (0.10 mol dm^{-3}) for 2h and then rinsed with water. The electrolyte for the Photo-CV consisted of an acetonitrile solution of 0.10 mol dm^{-3} tetrabutylammonium perchlorate. The electrolyte for the photoelectric measurement consisted of a diethylene glycol solution of iodine (5.0×10^{-2} mol dm^{-3}) and lithium iodide (0.50 mol dm^{-3}).

4.2.2 Preparation of Electrodes

The titania sols containing titanium alkoxide, nitric acid, pure water, ethanol, and fluorescein, in which the fluorescein concentrations were 0, 1.0×10^{-3}, 3.0×10^{-3}, and 1.0×10^{-2} mol dm^{-3}, were labeled S0, S1, S2, and S3, respectively. The working electrodes for Photo-CV were prepared by the following steps:(1) The glass plate with the ITO electrode was dip-coated once with S0 and then heated at 500°C for 30 min in order to form the crystalline titania as a substrate layer. This electrodes was dip-coated 10 times with S0, S1, S2, or S3 and then steam-treated for 120 min and labeled WE-S0, WE-S1, WE-S2, and WE-S3, respectively. In addition, the electrode was also dip-coated with S0 and the heat at 500 ℃ for 30 min and labeled WE-HT. In order to

clarify the relationship between the amount of the nitrate ions adsorbed on the titania surface and the shift in the conduction band edge of the titania, the WE-S0 electrodes were treated with sodium hydroxide for 20 and 40 min. These were used as the working electrodes for the Photo-CV. The glass plates without ITO were also coated with the dye-dispersing titania sols in order to obtain the XRD patterns of the titania.

The working electrodes for the photoelectric measurements were prepared by the following steps: (1) The ITO electrode was dip-coated 3 times with S0 and then heated at 500°C for 30 min in order to form the crystalline titania. This layer plays the role as a blocking layer in order to suppress the charge recombination at the interface between the dye-dispersing titania layer and the ITO layer.[21–23] (2) This electrode was dip-coated 5 times with S0, S1, S2, or S3 and then steam-treated for 120 min and labeled PE-S0, PE-S1, PE-S2, and PE-S3, respectively.

4.2.3. Measurements.

The crystalline phase of the film samples was determined using an X-ray diffractometer (Rigaku SmartLab). The UV–vis absorption spectra of the prepared electrode samples were observed using a UV–vis–near IR spectrophotometer (Shimadzu UV-3150). A 340 nm light (4.7 mW cm^{-2}) was obtained from a fluorescence spectrophotometer (Shimadzu RF-5300) with a 150 W Xe short arc lamp (Ushio UXL-155). During the light irradiation, the cyclic voltammogram of each electrode was measured by a potentiostat (Hokuto Denko HSV-100) in a three-electrode cell, assembled with a platinum counter electrode, an Ag/AgCl in saturated KCl (3.4 mol dm^{-3}) electrolyte as the reference electrode, and the working electrode. The applied voltage was swept from −1.5 to 0 V at 10 mV s^{-1} in order to estimate the oxidation potential of the titania conduction band with the excited electrons. The electrolyte was treated with bubbling nitrogen gas for about 30 min before the measurements.

The iodine-based electrolyte was allowed to soak into the space between the electrode sample and the counter Pt electrode. The *I-V* curves of the electrodes were measured by the potentiostat during visible light (0.40 W cm^{-2}) irradiation at a wavelength longer than 400 nm emitted by the 150 W Xe short arc lamp using a sharp cutoff filter. For the *I-V* measurements of WE-S0, no cutoff filter was used due to the absence of dye in the electrode.

The DC electrical resistance of the ITO electrode was measured using a digital multimeter (ADCMT 7461A). The resistivity values for the ITO electrodes unheated and heated at 500ºC for 30 min were 2.0×10^{-4} and 4.9×10^{-4} Ω cm, respectively. The resistivity of the heated ITO was low enough to determine the electric properties of the electrode samples.

The dye powder and the flakes of the dye-dispersing titania film samples were pressed in KBr pellets and their IR spectra were obtained using an FT-IR spectrophotometer (Shimadzu IR Prestige-21). The amounts of the dye and nitrate ions adsorbed on the titania surface were estimated from the UV–vis absorption and IR spectra, respectively.

4.3 Results and Discussion

4.3.1 Influence of the dye content on conduction band edge of titania

The Photo-CV was conducted in order to determine the shift in the conduction band edge of the titania in each electrode. The Photo-CV curves for the dye-dispersing titania electrodes were obtained as a function of the dye content and their oxidation currents are shown in Figure 4–1. The three cycles of the Photo-CV curves of WE-S0 are inserted in Figure 4–1. A shoulder from −0.9 to 1.0 V was observed in the first cycle of the Photo-CV of WE-S0, but the shoulder disappeared after the first cycle. This phenomenon was observed in all the electrode samples. The shoulder can be assigned to the reduction of oxygen adsorbed on the titania surface as shown by Reinhardt et al. [24]

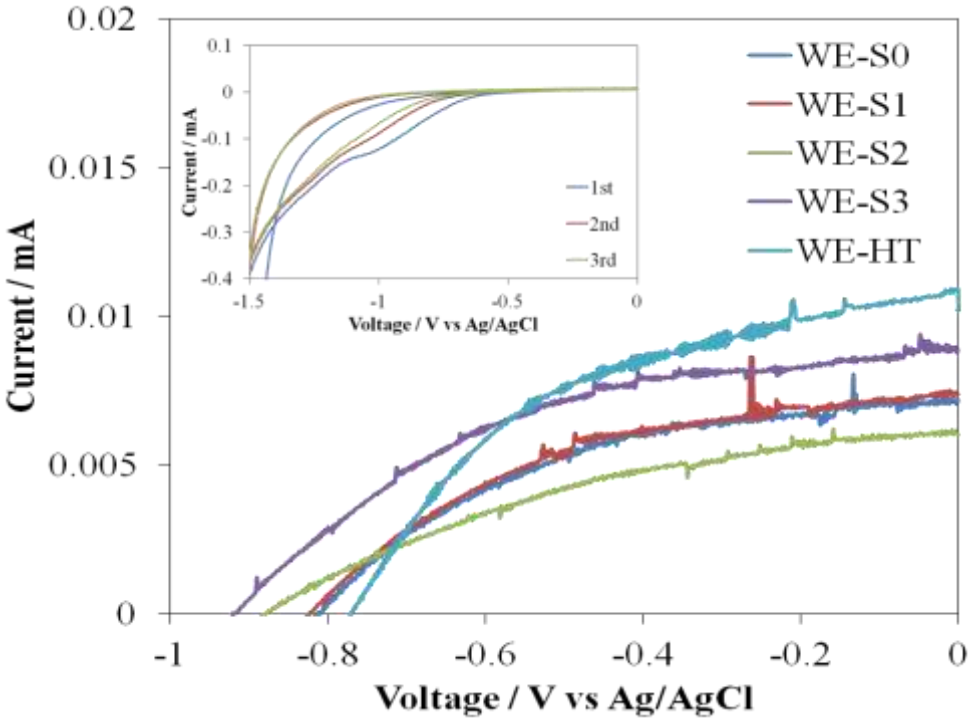

Figure 4–1 Oxidation current of the Photo-CV of the steam treated (WE-S0) and heated (WE-HT) titania electrodes, and the dye-dispersing titania electrodes (WE-S1, WE-S2, and WE-S3).

The conduction band edge of titania was estimated from the onset potential of the oxidation current of the third-cyclic Photo-CV curve of each electrode. As known, the conduction band edge level of anatase-type titania is about -0.50 V (vs SHE),[25] which corresponds to -0.70 V (vs Ag/AgCl). The conduction band edge level of the heated titania electrode (WE-HT) was estimated from its photo-CV onset to be about -0.77 V (vs Ag/AgCl). These values are very close. The conduction band edge of the steam-treated titania electrode (WE-S0) was about -0.81 V (vs Ag/AgCl) and more negative by about 40 mV than that of WE-HT. The factor causing this difference will be discussed later. The difference in the conduction band edge of the electrodes is due to the difference in their band gaps estimated by UV-Vis measurement as shown in Figure 4-2. The band gaps of WE-HT and WE-S0 were about 3.20 and 3.25 eV, respectively. The band

gap of WE-S0 was larger by about 50 meV than that of WE-HT. This value is very close to the difference in their conduction band edge levels.

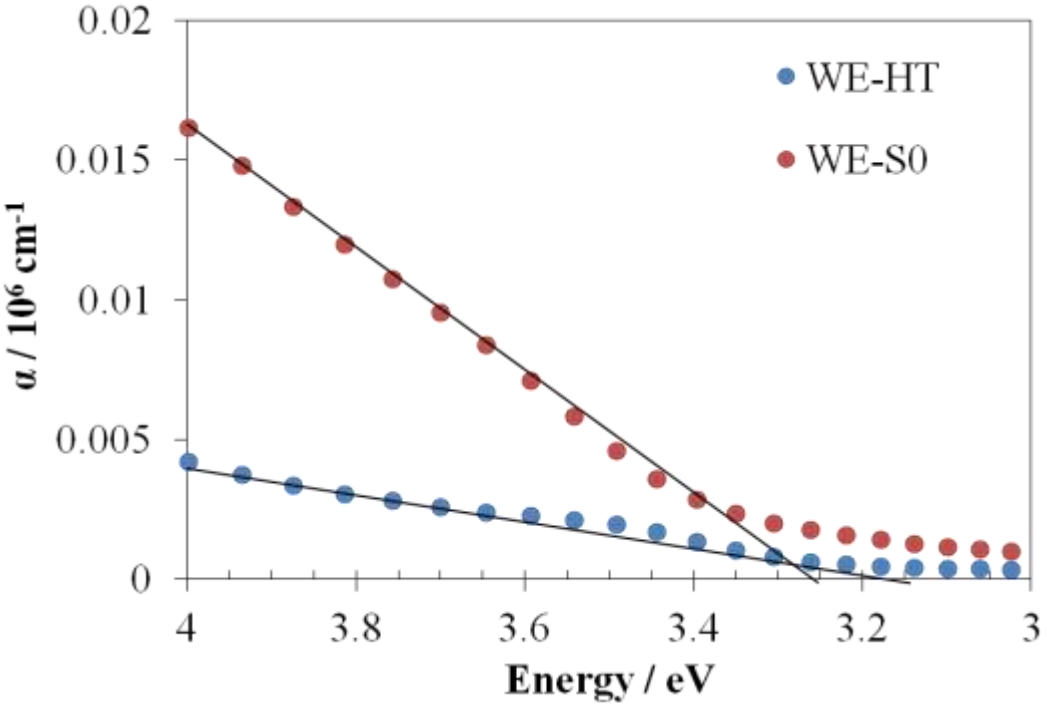

Figure 4–2 UV-vis absorption spectra and band gaps of the steam-treated (WE-S0) and heated (WE-HT) titania electrodes.

The onset potential values for the electrode with different dye contents are summarized in Table 4–1. The onset potential of the oxidation photocurrent was more negative in the electrode containing a greater amount of the dye, indicating that the conduction band edge of the titania shifted to a negative value with the dye content. The conduction band edge of WE-S3 was more negative by about 110 mV than that of WE-S0.

This result agreed with the prediction. It was reported that xanthene dye molecules formed a chelated complex with the titanium species on the titania surface in the dye-titania systems.[26–28] It was predicted that the negative surface electronic density of the titania would increase with an

increase in the amount of the dye–titania complex depending on the dye content in the electrode, which would result in a shift in the conduction band into a more negative direction. The previous study indicated that the steam treatment, which promoted the dye–titania complex formation, caused a negative shift in the conduction band edge of the titania.[6]

Table 4–1 The onset potential of the oxidation current of the titania electrode (WE-S0) and the dye-dispersing titania electrodes with different dye contents (WE-S1, WE-S2, and WE-S3).

Electrode	Onset Potential/ V vs Ag/AgCl
WE-S0	-0.811±0.013
WE-S1	-0.823±0.026
WE-S2	-0.880±0.033
WE-S3	-0.921±0.007
WE-HT	-0.771±0.022

A question is whether there is another factor shifting the conduction band edge of the titania other than the dye–titania complex formation. Actually, there can be many factors changing the conduction band edge of the titania. An adsorbent on the titania surface significantly changed the conduction band edge.[29,30] The particle size,[31] the surface protonation due to acid treatment,[32–34] and the dipole moment of the dye adsorbed on the titania[35,36] are also the factors which shift the conduction band edge of the titania. Therefore, further investigation is required in order to clarify this problem.

The XRD analysis and SEM observations of the electrodes were conducted in order to examine the influence of the dye content on the particle size. Figure 4–3 shows the XRD

patterns of the electrodes containing the different amounts of the dye. The average crystallite size of the crystalline particles of each electrode was estimated from their full width at half-maximum of the 25.3° peak using Sherrer's equation, $D=0.9\lambda/\beta\cdot\cos\theta$. The average crystallite size of the titania was about 5 nm for each electrode and was not significantly different between the electrodes.

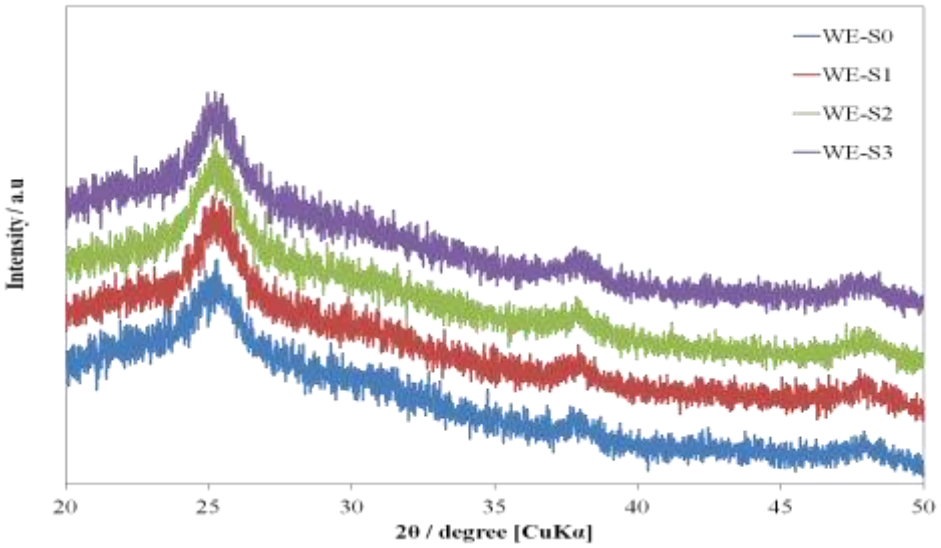

Figure 4–3 XRD patterns of the titania electrode (WE-S0) and the dye-dispersing titania electrodes (WE-S1, WE-S2, and WE-S3).

Figure 4–4 shows an SEM image of each electrode. The particle size in the electrode was about 10–20 nm and not significantly changed by the dye content. Based on this result, it was suggested that the possibility of the influence by a quantum size effect in this case is very low. Another factor, such as the surface protonation, cannot be the reason for such a change because no significant change in pH was observed even in the titania sol containing a higher amount of the dye.

Pandey et al. reported that the difference in the dipole moments between the dye and the titania induces a negative or positive shift in the surface potential. The positive dipoles, i.e., dipole

moments pointed toward the outer surface of the dyes adsorbed on the titania surface, were formed by most of the organic dyes at the titania/dye interface and shifted the titania conduction band edge in a positive direction.[3] The present result is opposite to that of Pandey et al., indicating that the hypothesis of Pandey et al. cannot explain the shift in the conduction band edge of the dye-dispersing titania. It presumed that the dipole moment factor of the dye in the dye-dispersing titania systems has a small effect. The dye molecules did not clearly exhibit an anisotropic property because the dye molecules were tightly encapsulated in the narrow spaces surrounded by the titania particles. However, further investigation is needed in order to discuss this problem in another study.

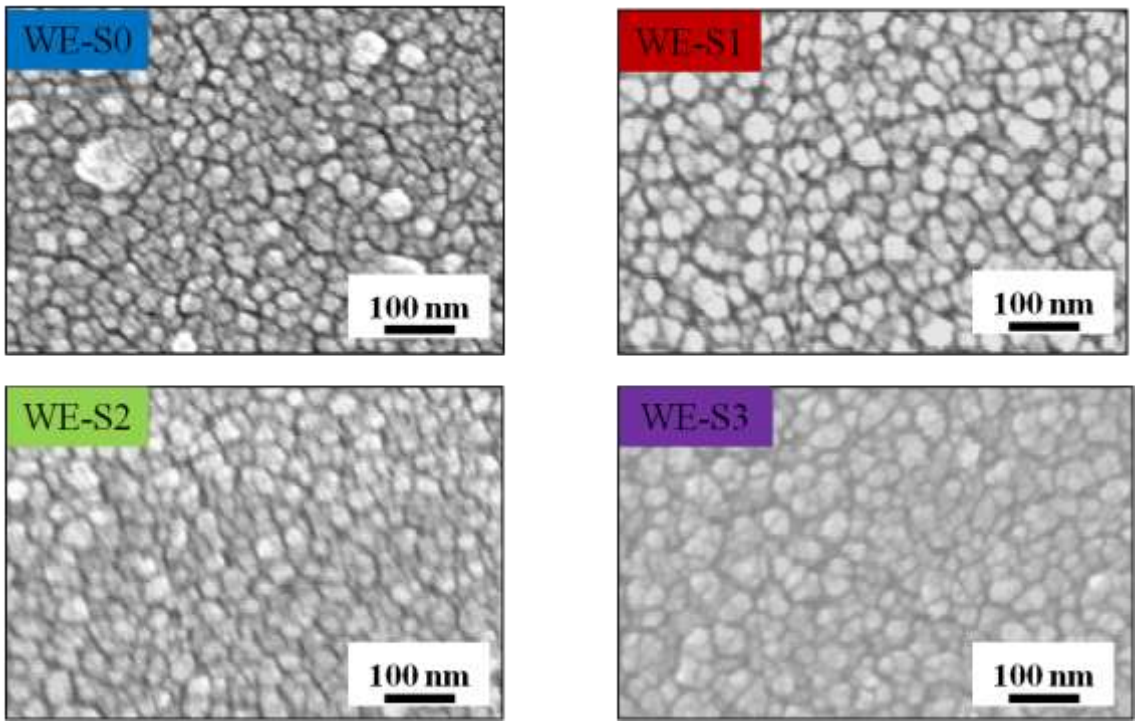

Figure 4–4 SEM images of the titania electrode (WE-S0) and the dye-dispersing titania electrodes (WE-S1, WE-S2, and WE-S3).

The most likely reason for the change in the conduction band edge vs. the dye content except

for the dye–titania complex formation is an adsorbent on the titania surface. The FTIR measurement was conducted in order to identify the species adsorbed on the titania surface of the electrodes. Figure 4–5 shows the FTIR spectrum of the dye-dispersing titania electrode as a function of the dye content. For comparison, the FTIR spectrum of fluorescein powder is also inserted in Figure 4–5.

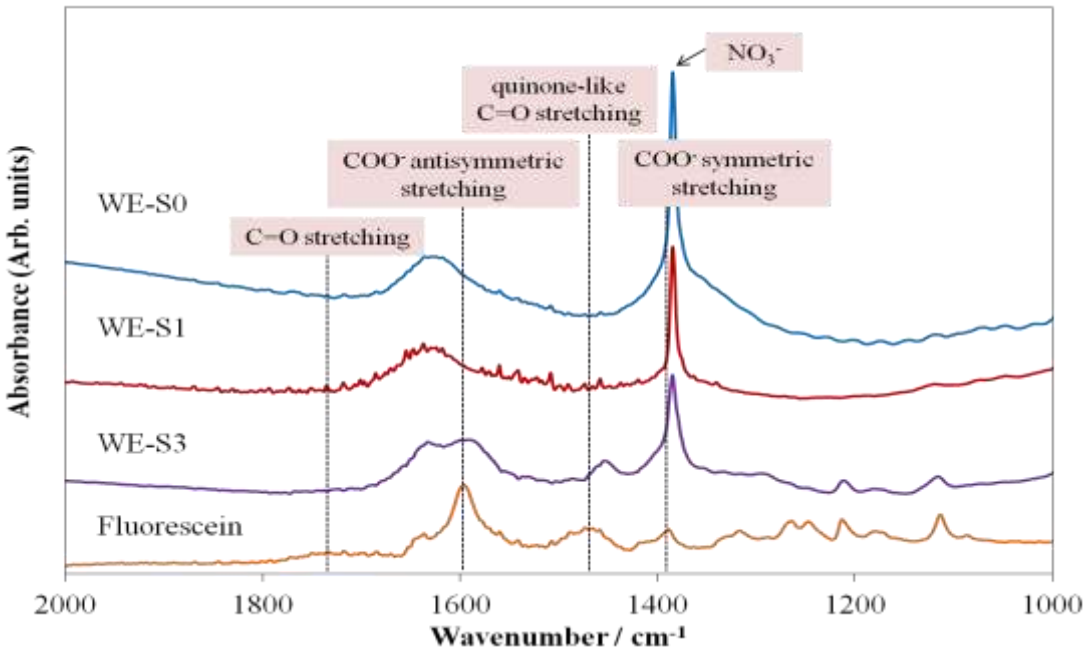

Figure 4–5 FTIR spectra of the titania electrode (WE-S0), the dye-dispersing titania electrodes (WE-S1 and WE-S3), and fluorescein powder.

The peaks of the carboxyl C=O stretching vibration and the carboxylate COO^- antisymmetric and symmetric stetching vibrations were observed at 1710, 1597, and 1391 cm^{-1} for the fluorescein powder, respectively. In addition, the band at 1490 cm^{-1} was assigned to the quinone-like C=O stretching vibration. In WE-S3, the peaks at 1620, 1585, 1470, and 1385 cm^{-1} were assigned to the absorbed water on the titania surface, the carboxylate COO^- antisymmetric stretching and the quinone-like C=O stretching vibrations of fluorescein, [6] and the adsorbed

NO_3^-[37], respectively. The carboxylate COO^- antisymmetric and quinone-like C=O stretching vibration peaks were shifted to a low wavenumber compared to those observed in the fluorescein powder due to the interaction between the functional groups and the titanium species of the titania. The carboxyl group of fluorescein was transformed to the carboxylate and formed a chelated complex with the titanium species.[6] The peaks at 1620 and 1385 cm^{-1} were also observed in WE-S0. The nitrate ion still remained on the electrodes even after the steam treatment.

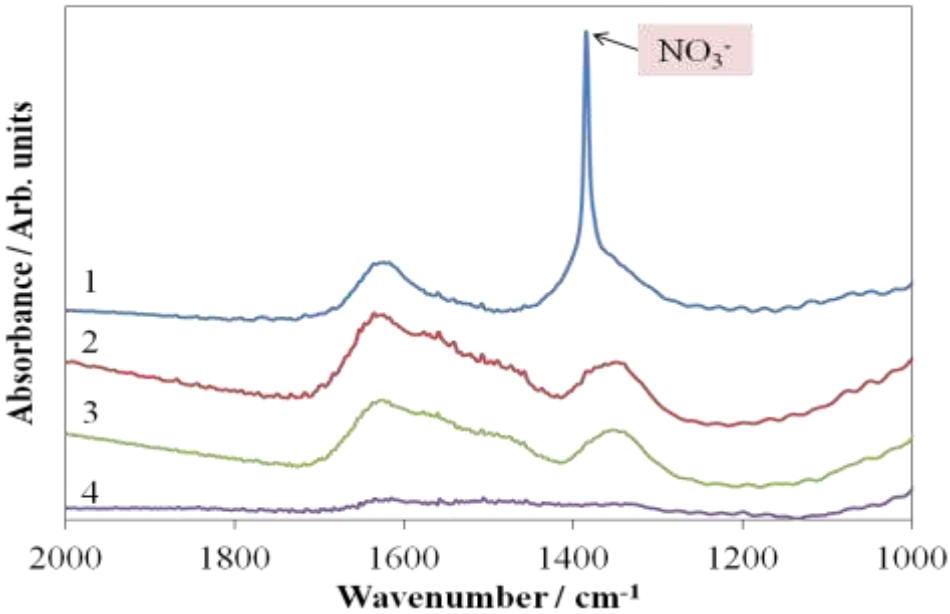

Figure 4–6 FTIR spectra of WE-S0 (1) before and after sodium hydroxide treatment for (2) 20 and (3) 40 min, and (4) WE-HT.

In order to clarify relationship between the amount of the adsorbed nitrate ions and the shift in the conduction band edge of the titania, the Photo-CV of the titania electrode was conducted before and after the sodium hydroxide solution treatment. Figure 4–6 shows the FT-IR spectra of each electrode measured before and after the sodium hydroxide treatment in order to confirm the nitrate ion remaining on the titania surface. In addition, the spectrum of WE-HT is also

shown in Figure 4-6. The intensity of the peak at 1385 cm^{-1}, assigned to nitrate ion, decreased with the sodium hydroxide treatment, and then the peak completely disappeared in the titania electrode after the 40-min steam treatment and after heating.

Figure 4–7 shows the Photo-CV curves of the titania electrodes before and after the sodium hydroxide treatment. The onset potentials of the oxidation photocurrents of each electrode are summarized in Table 4–2. The onset potential of the oxidation photocurrent of the electrode was shifted in a positive direction by about 20 and 60 mV after the 20- and 40-min sodium hydroxide treatments, respectively. This result indicated that the conduction band edge of the titania was shifted in a positive direction due to the decreasing amounts of nitrate ions adsorbed on the electrode. Based on these result, it is suggested that the main reason for the more positive level of the conduction band edge of WE-HT than that of WE-S0 as shown in Figure 4-1 was a smaller amount of nitrate ion in the WE-HT as shown in Figure 4-6.

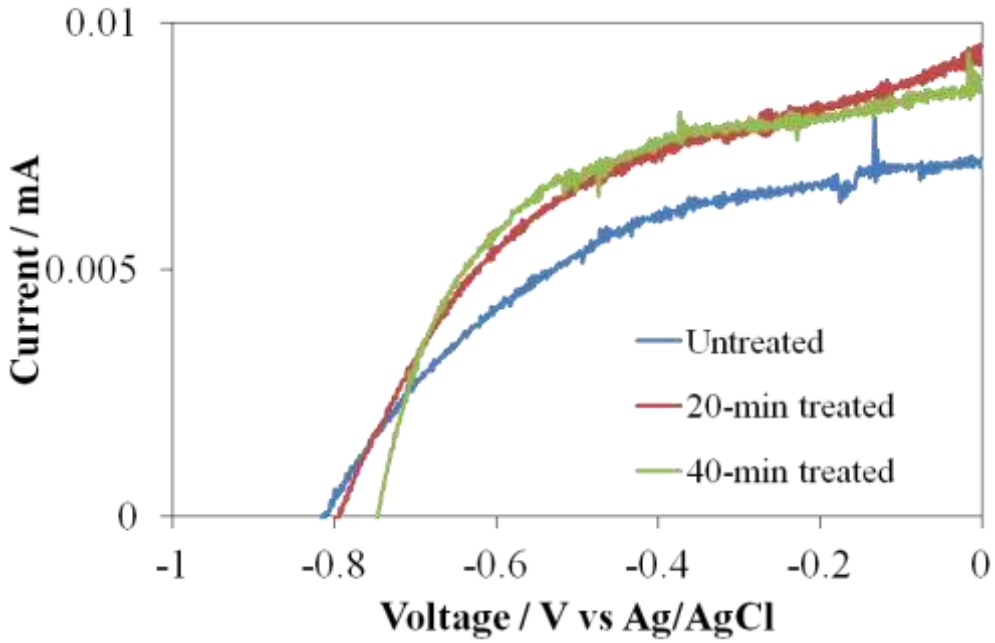

Figure 4–7 Oxidation current of the Photo-CV of the titania electrode before and after sodium hydroxide treatment for 20 and 40 min.

Table 4–2 The onset potential of the oxidation current of the titania electrode before and after the sodium hydroxide treatment for 20 and 40 min

Electrode	Onset Potential/ V vs. Ag/AgCl
Untreated	-0.81±0.013
20-min treated	-0.79±0.010
40-min treated	-0.75±0.003

It has not been concluded which factor, the dye–titania complex formation or nitrate ion adsorption, has a greater effect on the changes in the conduction band edge of the titania. The initial amount of nitrate ions in the dye-containing titania sol was 10-fold greater than that of the dye. The relative amounts of the dye molecules and nitrate ions adsorbed on the dye–titania gel electrode just after the preparation before steam treatment are assumed to be the same as those in the dye-containing titania sol. Based on this assumption, the approximate amounts of the dye molecules and nitrate ions in the dye-dispersing titania electrode WE-S3 were calculated before and after the steam treatment. The UV–vis and FTIR spectra were obtained in order to estimate the amounts of the dye molecules and nitrate ions, respectively.

Figure 4–8 shows the UV–vis and FTIR spectra of WE-S3 before and after the 120-min steam treatment. In the UV–vis spectra, the absorbance of the band at 470–480 nm assigned to the dye absorption decreased by 50% after the steam treatment. The absorbance at the peak assigned to the nitrate ion decreased by two-thirds as shown in the FTIR spectra. As the amounts of the dye molecules and nitrate ions were assumed to be 1 and 10, respectively, in the electrode before the steam treatment, they should be 0.5 and 3.3, respectively, after the steam treatment. Based on this approximate calculation, it was concluded that the amount of nitrate ions remaining on the electrode was 6.6 times greater than that of the dye although the negative shift in the conduction

band edge was 110 mV and 60 mV by the amount of the dye and nitrate ion, respectively. This result indicated that the effect of the dye–titania complex formation on the shift of the titania conduction band edge was greater than that of the nitrate ion adsorption due to strong interaction between the dye and titania through the carboxylate group of the dye.

(a)

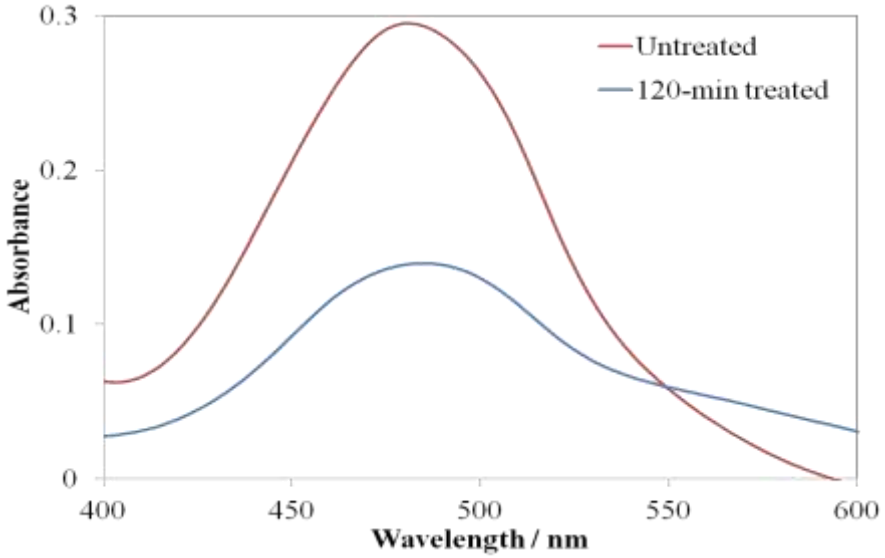

(b)

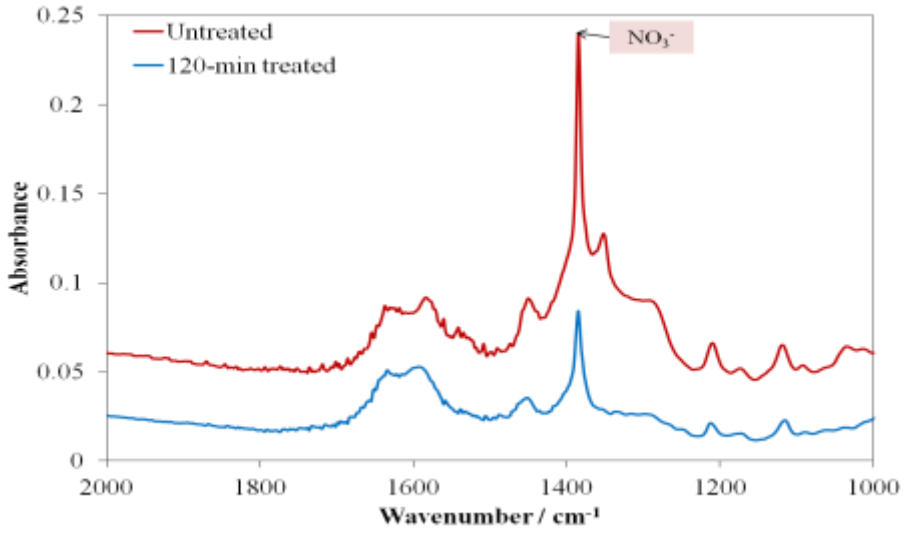

Figure 4–8 (a) UV–vis and (b) FTIR spectra of the dye-dispersing titania electrodes (WE-S3) before and after the 120-min steam treatment

4.3.2 Relationship between the dye and nitrate ions on the titania surface

In previous section, it was concluded that the dye–titania complex formation and nitrate ion adsorption shifted the conduction band edge of the titania in a negative direction. A schematic diagram of the relationship between the dye–titania complex formation and nitrate ion adsorption on the titania surface will be discussed in this section. An attention focused on the change in the dye–titania interaction found in the COO^- peak wavenumber and the change in the amount of the nitrate ion adsorbed on the titania surface vs. the dye content as shown in figure 4–5. The relative intensity of the peak at 1385 cm^{-1} assigned to NO_3^- decreased with an increase in the dye amount. On the other hand, the amount of the complex should increase with the dye content. Based on these results, it was suggested that the substitution of the dye molecules for the nitrate ions caused by the dye–titania complex formation as shown in Figure 4–9, which resulted in the greater negative shift in the titania conduction band edge with the higher dye content.

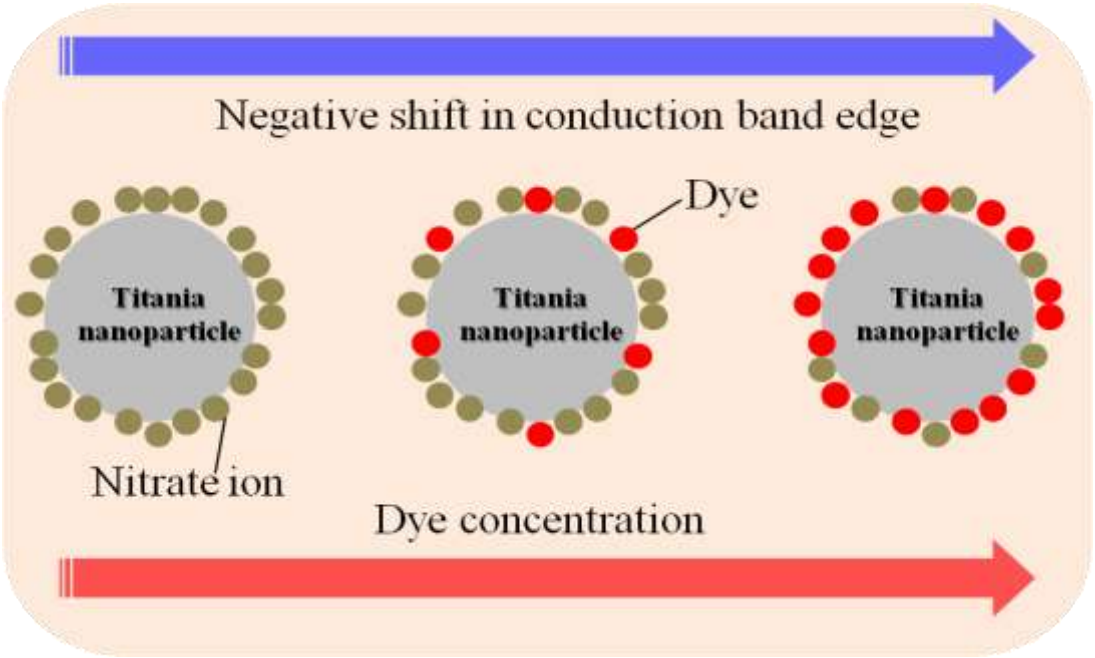

Figure 4–9 Schematic diagram of the substitution of the dye molecules for the nitrate ions on the titania surface.

4.3.3 Influence of the dye content on photoelectric conversion properties of the dye-dispersing titania electrode

The relationship between the shift in the conduction band edge and the change in V_{oc} with the dye content will now be described. Before this, the influence of the dye content on the absorption spectrum of each electrode was investigated. Figure 4–10 shows the absorption spectra of the dye-dispersing titania electrodes observed as a function of the dye content. All the electrodes exhibited broad absorption spectra ranging from 420 nm to 550 nm, and the absorption peaks are located around 480–490 nm, indicating that the dye–titania complex was formed on each electrode. The absorbance of the electrode increased with an increase in the dye content, and there is a slight difference in the absorption peaks of each electrode. This result indicated that the dye species in the dye–titania complex was not changed by the dye content. Based on the FTIR and UV–vis absorption spectra, the dye–titania complex species consisted of the anion (at around 470 nm) or the dianion species (at around 490 nm).[38,39]

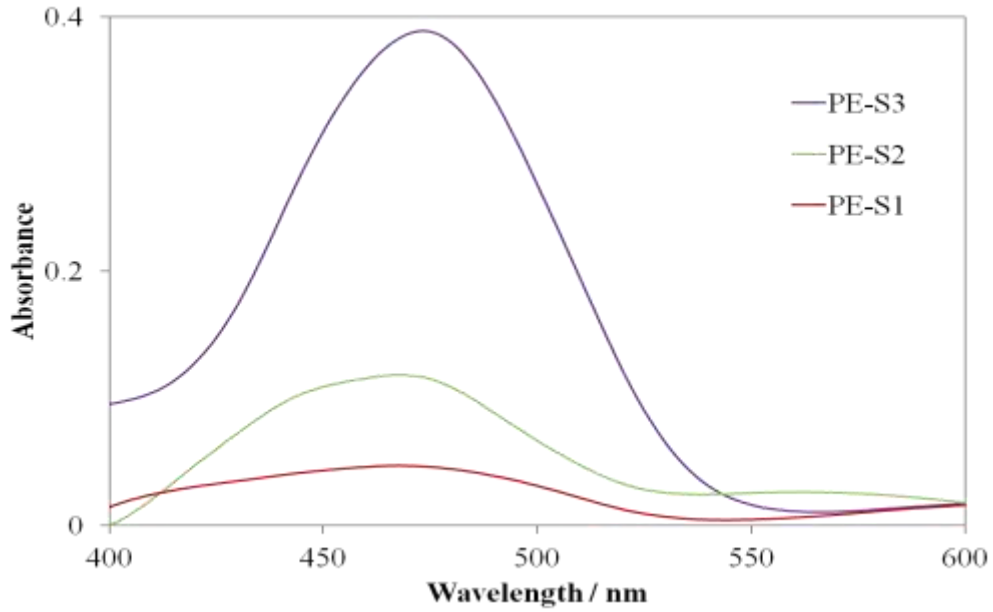

Figure 4–10 Absorption spectra of the dye-dispersing titania electrodes (PE-S1, PE-S2, and PE-S3).

The *I-V* curves of each electrode are shown in Figure 4–11, and their properties are summarized in Table 4–3. The V_{oc} of the dye-dispersing titania electrode increased with the dye content. The V_{oc} value of the PE-S3 electrode was higher by about 70 mV than that of the PE-S0 electrode. However, this value was lower by about 40 mV than that expected from the difference between their conduction band edges.

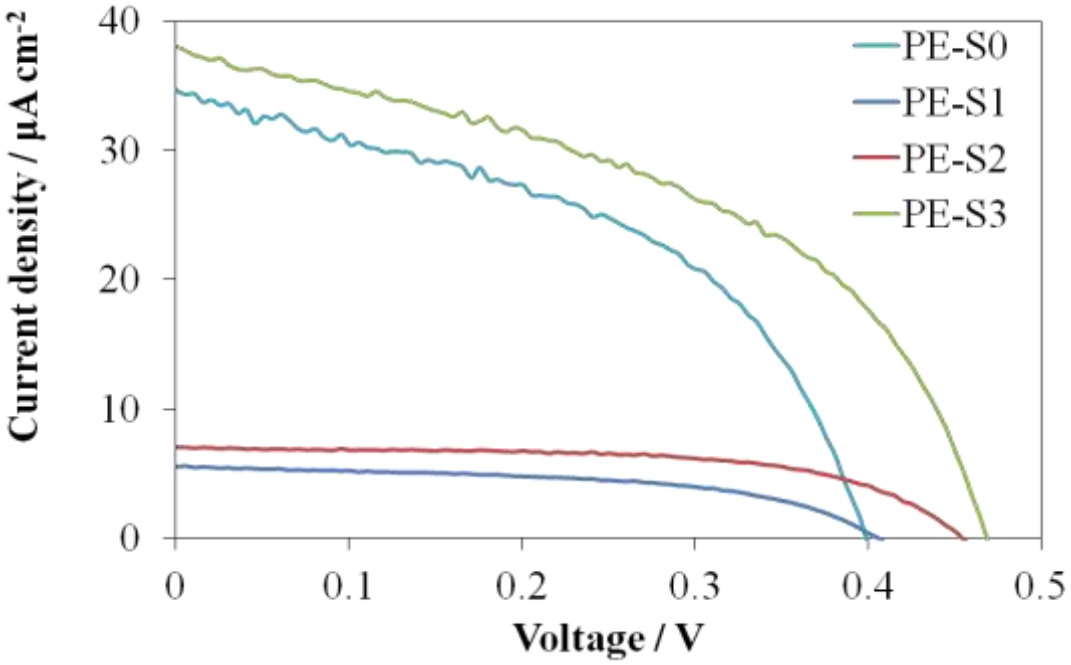

Figure 4–10 *I-V* curves of the titania electrode (PE-S0) and the dye-dispersing titania electrodes (PE-S1, PE-S2, and PE-S3).

V_{oc} is defined as the voltage difference between the electrolyte redox potential (E_{redox}/q) and the quasi-Fermi potential of electrons ($E_{F,n}/q$) in the titania. $E_{F,n}$ is determined by the potential of the conduction band edge and the electron density in the titania. V_{oc} is described as

$$V_{oc} = \frac{E_{CB}}{q} + \beta \frac{kT}{q} \ln\left(\frac{n}{N_{CB}}\right) - \frac{E_{redox}}{q} \qquad (1)^{40,41}$$

where E_{CB} is the energy level of the conduction band edge, N_{CB} is the total number of conduction band states in the semiconductor, n is the number of electrons in titania and q is the

elementary charge of the electron. β is the defect condition in the porous titania. For the ideal case, i.e., a defect-free semiconductor material, β=1. From equation (1), the level of the conduction band edge of the titania and the concentration of electrons in the titania are two important factors determining V_{oc} because E_{redox} is assumed to be constant. The electron density in the titania films is determined by the balance between the electron injection and back electron transport.[41,42]

Table 4–3 Photoelectric conversion properties of the titania electrode (PE-S0) and the dye-dispersing titania electrodes (PE-S1, PE-S2, and PE-S3)

Electrode	I_{sc} / μA cm^{-2}	V_{oc} / V	P_{max} / μW cm^{-2}	FF
PE-S0	34.6±0.99	0.40±0.01	6.4±1.71	0.46±0.11
PE-S1	5.56±0.73	0.41±0.01	1.2±0.03	0.53±0.05
PE-S2	7.00±3.38	0.45±0.03	1.9±0.87	0.61±0.08
PE-S3	38.07±9.41	0.47±0.01	7.6±0.92	0.41±0.15

Based on these results, the V_{oc} value mainly depends on the conduction band edge and electron density in the conduction band. It was suggested that the small change in the V_{oc} value for the dye-dispersing titania is due to a decrease in the electron density at the conduction band edge. As already described, the factors affecting the electron density are the electron injection and back electron transport. In a previous study, it was concluded that the dye–titania complex formation resulted in the fast electron transfer into the titania conduction band by transient absorption and time-resolved fluorescence spectroscopy.[7,9] The increase in the dye content in the electrode promoted the dye–titania complex formation, but the complex formation can also produce surface defects on the titania particle. Therefore, it is suggested that the decrease in the

electron density on the electrode with an increase in the dye content was mainly caused by the back electron transfer through the surface defects on the titania particle.

4.4 Conclusions

The titania and dye-dispersing titania electrodes were prepared by a nitric acid-catalyzed sol-gel process. The influence of the amounts of the dye and remaining nitrate ions in the dye-dispersing titania electrode on the change in the conduction band edge of the titania and the V_{oc} of the electrode was investigated.

The Photo-CV curves of the electrodes indicated that the conduction band edge of the titania was more negative in the electrode containing a higher amount of the dye. Compared to the dye-free electrode WE-S0, the conduction band edge of the dye-dispersing electrode WE-S3 was shifted by about 110 mV in the negative direction. The FTIR spectra of the steam-treated dye-dispersing titania electrode showed that the dye–titania complex was formed and nitrate ions remained on the electrode. The Photo-CV curves of the titania electrode before and after the sodium hydroxide treatment showed that the conduction band edge of the titania was shifted by about 60 mV in the positive direction due to desorption of the nitrate ions. This result indicated that the nitrate ions adsorbed on the titania electrode caused a negative shift in the conduction band edge due to their negative charge. The substitution of the dye molecules for the nitrate ions on the titania surface was caused by the dye–titania complex formation. Consequently, the conduction band edge was more negative in the electrode containing a higher amount of the dye. As predicted, the dye–titania complex formation also significantly affected the conduction band edge of the titania. This investigation also showed that the effect of the dye–titania complex formation on the shift in the titania conduction band edge (110 mV) was greater than that of the nitrate ion adsorption (60 mV) due to a strong interaction between the

dye and titania through the carboxylate group of the dye.

The shift in the titania conduction band edge corresponded to the change in the V_{oc} value (70 mV), but the change was lower than that expected from the shift in its conduction band edges. It was suggested that the small change in the V_{oc} value in the dye-dispersing titania was due to a decrease in the electron density at the conduction band caused by back electron transfer through the surface defect of the titania particle.

References

(1) D. P. Hagberg, T. Edvinsson, T. Marinado, G. Boschloo, A. Hagfeldt, L. Sun
Chemical Communications, 21 (2006), pp. 2245-2247

(2) J. Xia, S. Yanagida
Solar Energy, 85 (2011), pp. 3143-3159

(3) S. S. Pandey, S. Sakaguchi, Y. Yamaguchi, S. Hayase
Organic Electronics, 11 (2010), pp. 419-426

(4) Y. Chiba, A. Islam, Y. Watanabe, R. Komiya, N. Koide, L. Han
Japanese Journal of Applied Physics, 45 (2006), pp. L638-L640

(5) A. C. Khazraji, S. Hotchandani, S. Das, P. V. Kamat
Journal of Physical Chemistry B, 103 (1999), pp. 4693-4700

(6) H. Nishikiori, Y. Uesugi, S. Takami, R. A. Setiawan, T. Fujii, W. Qian, M. A. El-Sayed
Journal of Physical Chemistry C, 115 (2011), pp. 2880-2887

(7) H. Nishikiori, W. Qian, M. A. El-Sayed, N. Tanaka,; T. Fujii
Journal of Physical Chemistry Letters, 111 (2007), pp. 9008-9011

(8) H. Nishikiori, N. Tanaka, T. Kitsui, T. Fujii

Journal of Photochemistry and Photobiology A: Chemistry, 179 (2006), pp. 125-129

(9) R. A. Setiawan, H. Nishikiori, Y. Uesugi, K. Miyashita, M. A. El-Sayed, T. Fujii

Journal of Physical Chemistry C, 117 (2013), pp. 10308-10314

(10) H. Nishikiori, Y. Uesugi, N. Tanaka, T. Fujii

Journal of Photochemistry and Photobiology A: Chemistry, 207 (2009), pp. 204-208

(11) Z. S. Wang, Y. Cui, K. Hara, Y. Dan-oh, C. Kasada, A. Shinpo

Advanced Materials, 19 (2007), pp. 1138-1141

(12) K. Hara, Y. Dan-oh, C. Kasada, Y. Ohga, A. Shinpo, S. Suga, K. Sayama, H. Arakawa

Langmuir, 20 (2004), pp. 4205-4210

(13) Z. S. Wang, K. Hara, Y. Dan-oh, C. Kasada, Y. Ohga, A. Shinpo, S. Suga, H. Arakawa, H. Sugihara

Journal of Physical Chemistry B, 109 (2005), pp. 3907-3914

(14) H. Nishikiori, Y. Uesugi, R. A. Setiawan, T. Fujii, W. Qian, M. A. El-Sayed

Journal of Physical Chemistry C, 116 (2012), pp, 4848-4854

(15) M. J. Katz, M. J. D. Vermeer, O. K. Farha, M. J. Pellin, J. T. Hupp

Langmuir, 29 (2013), pp. 806-814

(16) S. N. Inamdar, P. P. Ingole, S. K. Haram

Chemphyschem, 9 (2008), pp. 2574-2579

(17) S. K. Haram, B. N. Quinn, A. J. Bard

Journal of the American Chemical Society, 123 (2001), pp. 8860-8861

(18) S. K. Haram, A. Kshirsagar, Y. G. Gurajathi, P. P. Ingole, O. A. Nene, G. B. Markad, S. P. Nanavati

Journal of Physical Chemistry C, 115 (2011), pp. 6243-6249

(19) J. M. Bolts, M. S. Wrighton

Journal of Physical Chemistry, 80 (1976), pp. 2641-2645

(20) M. Radecka, M. Rekas, A. Trenczek-Zajac, K. Zakrzewska

Journal of Power Sources, 181 (2008), , 46-55

(21) P. J. Cameron, L. M. Peter

Journal of Physical Chemistry B, 107 (2003), pp. 14394-14400

(22) A. O. T. Patrocinio, L. G. Paterno, N. Y. Murakami Iha

Journal of Photochemistry and Photobiology A: Chemistry, 205 (2009), pp. 23-27

(23) J. N. Hart, D. Menzies, Y. B. Cheng, G. P. Simon, L. Spiccia

Comptes Rendus Chimie, 9 (2006), pp. 622-626

(24) D. Reinhardt, S. Krieck, S. Meyer

Electrochimica acta, 52 (2006), pp. 825-830

(25) M. Gärtner, V. Dremov, P. Müller, H. Kisch

Chemical Physics and Physical Chemistry, 6 (2005), pp, 714-718

(26) M. Hilgendorff, V. Sundström

Journal of Physical Chemistry B, 102 (1998), pp. 10505-10514

(27) G. Ramakrishna, H. N. Ghosh

Journal of Physical Chemistry B, 105 (2001), pp. 7000-7008

(28) D. El Mekkawai, M. S. A. Abdel-Mottaleb

International Journal Photoenergy, 7 (2005), pp. 95-101

(29) L. Du, A. Furube, K. Hara, R. Katoh, M. Tachiya

Journal of Physical Chemistry C, 114 (2010), pp. 8135-8143

(30) X. Ren, Q. Feng, G. Zhou, C. H. Huang, Z. S. Wang

Journal of Physical Chemistry C, 114 (2010), pp. 7190-7195

(31) N. R. Neale, N. Kopidakis, J. V. de Lagemaat, M. Grätzel, A. J. Frank

Journal of Physical Chemistry B, 109 (2005), pp. 23183-23189

(32) Z. S. Wang, T. Yamaguchi, H. Sugihara, H. Arakawa

Langmuir, 21 (2005), pp. 4272-4276

(33) K. H. Park, E. M. Jin, H. B. Gu, S. E. Shim, C. K. Hong

Materials Letters, 63 (2009), pp. 2208-2211

(34) S. Hao, J. Wu, L. Fan, Y. Huang, J. Lin, Y. Wei

Solar Energy, 76 (2004), pp. 745-750

(35) B. Liu, X. Li, M. Liu, Z. Ning, Q. Zhang, C. Li, K. Mülen, W. Zhu

Dyes and Pigments, 94 (2012), pp. 23-27

(36) U. B. Cappel, S. Plogmaker, E. M. J. Johansson, A. Hagfeldt, G. Boschloo, H. Rensmo

Physical Chemistry Chemical Physics, 13 (2011), pp. 14767-14774

(37) S. Musić, M. Gotić, M. Ivanda, S. Popović, A. Turković, R. Trojko, A. Sekulić, K. Furić

Material Science and Engineering B, 47 (1997), pp. 33-40

(38) R. Sjöback, J. Nygren, M. Kubista

Spectrochimica Acta Part A: Molecular and Biomolecular Spectroscopy, 51 (1995), pp. L7-L21

(39) T. Fujii, A. Ishii, Y. Kurihara, M. Anpo

Research on Chemical Intermediate, 19 (1993), pp. 333-342

(40) T. Marinado, K. Nonomura, J. Nissfolk, M. K. Karlsson, D. P. Hagberg, L. Sun, S. Mori, A. Hagfeldt

Langmuir, 26 (2010), pp. 2592-2598

(41) Y. Liang, B. Peng, J. Chen

Journal of Physical Chemistry C, 114 (2010), pp. 10992-10998

(42) M. Miyashita, K. Sunahara, T. Nishikawa, Y. Uemura, N. Koumura, K. Hara, A. Mori, T.

Abe, E. Suzuki, S. Mori

Journal of the American Chemical Society, 130 (2008), pp. 17874-17881

Chapter 5

Photoelectric conversion properties of compositionally-graded dye–titania electrode

5.1 Introduction

The dye-sensitized solar cells (DSSCs) based on titania have attracted considerable interest as a new potential electric generator due to their low-cost production and simple fabrication process compared to conventional silicon-type solar cells.[1–4] The electron transfer dynamics in the titania electrode of DSSCs has been one of the subjects of active research for many years due to the importance of this factor regarding the improvement of the photoelectric conversion properties of such cells.

In a previous study, a new material called the dye-dispersing titania was introduced, which enhanced the efficiency of the light absorption and electron injection from the dye to the titania semiconductor.[5-10] It was reported that the steam treatment of the dye-dispersing titania films remarkably improved the photoelectric conversion efficiency due not only to the crystallization of the titania but also to the formation of the dye-titanium LMCT complex in the narrow pores of the titania.[9] In chapter 4, the dye–titania complex formation also significantly affected the change in the conduction band edge of the titania. The increase in the dye–titania complex formation resulted in a negative shift in the conduction band edge of the titania due to the strong interaction between the dye having the negative charge and titania.[5]

In this chapter, the conduction band potential of the titania was tried to be controlled by changing the amount of the dye–titania complex formed in the surface of the titania nanoparticle and prepare the multi-layered thin films of the compositionally-graded dye–titania. The

structure of the compositionally-graded dye–titania is schematically shown in Figure 5–1.

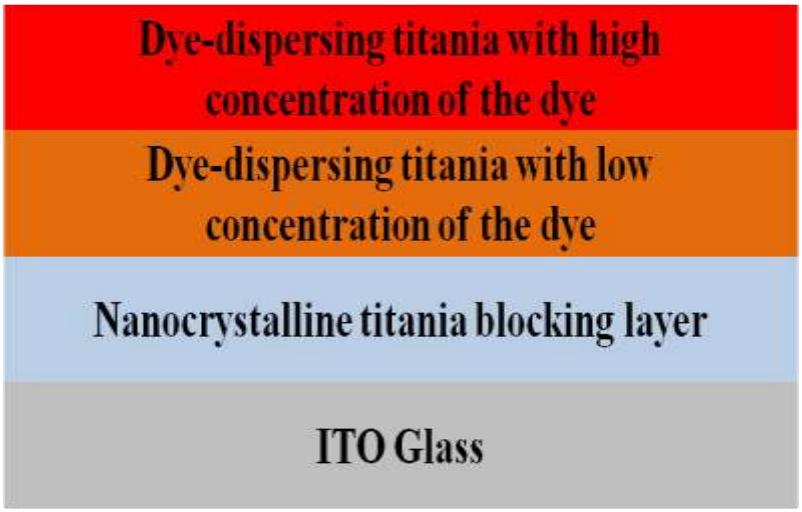

Figure 5–1 Structure of the compositionally-graded dye–titania

Three types of thin film layers were prepared on an ITO conducting glass. The nanocrystalline titania layer was prepared at the interface between the dye-dispersing titania layer and ITO conducting glass. This layer is also known as a blocking layer in DSSCs.[11–13] On the nanocrystalline layer, two types of the dye-dispersing titania layers with different concentrations of the dye were prepared. It is suggested that the conduction band edge of the titania in the dye-dispersing titania layer having a higher concentration of the dye is higher due to a higher amount of the dye–titania complex. It is expected that the formation of the step-like structure between the conduction band edges of the neighboring titania films can inhibit the back electron transfer and accelerate the electron transfer in the titania network of the dye-dispersing titania electrode.

In this chapter, the electron transfer efficiency in the compositionally-graded dye–titania working electrode was investigated by measuring the spectroscopic and photoelectric properties of such electrodes.

5.2 Experimental section

5.2.1 Materials

Titanium tetraisopropoxide, ethanol, fluorescein, hydrochloric acid, nitric acid, diethylene glycol, acetonitrile, tetrabutylammonium perchlorate, iodine, and lithium iodide (Wako, S or reagent grade) were used without further purification. Water was ion-exchanged and distilled. Glass plates coated with the transparent ITO electrode (AGC Fabritech) were soaked in hydrochloric acid (0.10 mol dm^{-3}) for 2h and then rinsed with water. The electrolyte for the photoelectric measurement consisted of a diethylene glycol solution of iodine (5.0×10^{-2} mol dm^{-3}) and lithium iodide (0.50 mol dm^{-3}).

5.2.2 Preparation of electrodes

The titania sols containing titanium alkoxide, nitric acid, pure water, ethanol, and fluorescein, in which the fluorescein concentrations were 0, 1.0×10^{-3}, and 1.0×10^{-2} mol dm^{-3}, were labeled S0, S1, and S2, respectively. The working electrode consisting of the multi-layered compositionally-graded dye–titania (WE-C) was prepared by the following steps: (1) The ITO electrode was dip-coated 3 times in S0 and then heated at 500°C for 30 min in order to form the crystalline titania; (2) this was dip-coated in S1 and then steam-treated for 2 h; (3) the resulting sample was dip-coated in S2 and then steam-treated for 2 h. The working electrode in which the S1 and S2 layers were in reverse order (WE-C') was also prepared. For comparison, the normal working electrode without the compositionally-graded dye–titania structure was also fabricated using S0 and S2 and labeled as WE-N. The film thickness of each working electrode is equal due to adjusting the number of layers of the thin films. The glass plates without the ITO were also coated with the dye-dispersing titania sols in order to obtain the XRD patterns of the titania.

5.2.3 Measurements

The crystalline phase of the film samples was determined using an X-ray diffractometer (Rigaku SmartLab). The UV–vis absorption spectra of the prepared electrode samples were observed using a UV–vis–near IR spectrophotometer (Shimadzu UV-3150).

The iodine-based electrolyte was allowed to soak into the space between the electrode sample and the counter Pt electrode. For the spectroscopic measurements, the electrode samples were irradiated by monochromatic light obtained from a fluorescence spectrophotometer (Shimadzu-RF-5300) with a 150 W Xe short arc lamp (Ushio UXL-155). During light irradiation, the short-circuit currents of the electrodes were measured by a digital multimeter (ADCMT 7461A). The *I-V* curves of the electrodes were measured by a potentiostat (Hokuto Denko HSV-100) during visible light (0.4 W cm^{-2}) irradiation at a wavelength longer than 400 nm emitted by the 150 W Xe short arc lamp using a sharp cutoff filter. The intensity at each wavelength of the light source was obtained using a power meter (Coherent Labmax top 0436C08R) in order to estimate the incident photon-to-current conversion efficiency (IPCE) and quantum efficiency for the photocurrent from the excited dye in the electrode samples. The light intensity was confirmed to correlate with the results of the potassium ferrioxalate actinometry. The visible absorbance of the present electrode samples was lower than 1.0, which was sufficient to measure the number of absorbed photons in order to calculate the quantum efficiency.

5.3 Results and Discussion

5.3.1 Absorption and photocurrent spectra

The absorption spectra of WE-C, WE-C’ and WE-N are shown in Figure 5–2. Each electrode exhibited a visible absorption ranging from 420 nm to 520 nm and the absorption peaks were

located around 480–490 nm. This result indicated that the main fluorescein species were the anion (at 450–480) and the dianion (at around 490 nm).[14,15] In spite of the film thickness of each electrode being equal, the absorbance of WE-C and WE-C' were lower than that of WE-N due to a lower amount of the dye incorporated in the titania films. As described in the section about the preparation procedure of the electrodes, WE-C and WE-C' were prepared using S1 and S2, whereas, WE-N was prepared using only S2. The concentration of the dye in the S1 layer is 10-fold lower than that of the S2 layer. Therefore, the amount of the dye contained in the WE-C and WE-C' are lower than that in WE-N.

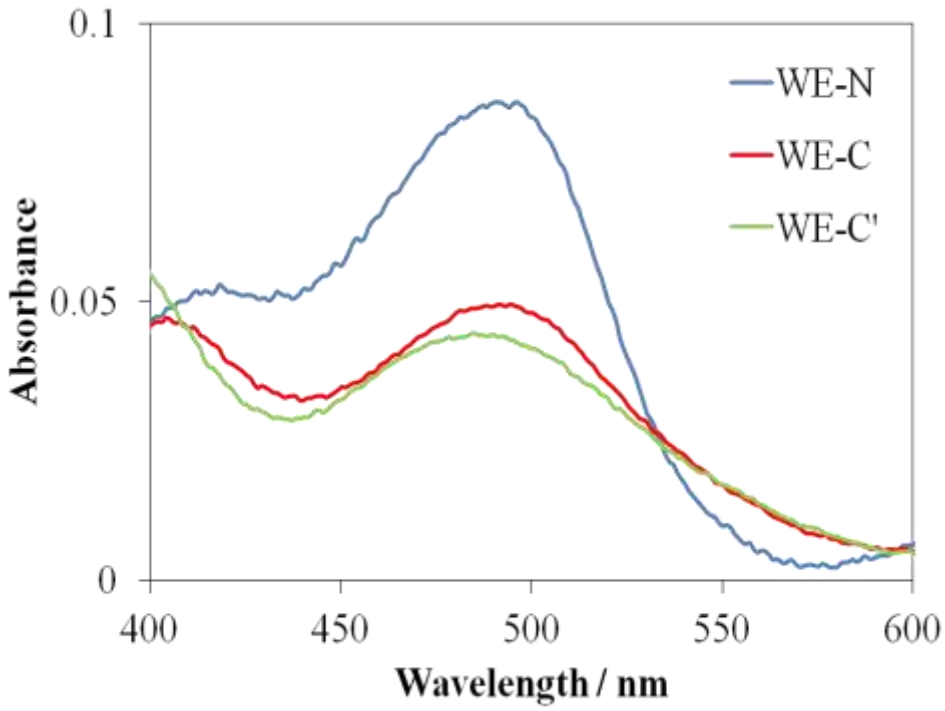

Figure 5–2 Absorption spectra of the compositionally-graded dye-titania (WE-C), irregularly-layered (WE-C'), and normal (WE-N) dye–titania electrodes

The IPCE spectra of each electrode are shown in Figure 5–3. The IPCE maximum of WE-C was greater than that of WE-C'. In spite of the lower absorbance, the IPCE maximum of WE-C

was also greater by 25 % than that of WE-N and was greater by more than 100% than that of WE-C'. The IPCE is determined by the important factors, i.e., (1) light harvesting efficiency, (2) electron injection efficiency at the dye-titania interfaces, and (3) electron transport efficiency in the titania.[16] Factors (1) and (2) for WE-N should be greater than that for WE-C because the amounts of the dye molecules and dye–titania complex in WE-N were greater than those in WE-C as shown in Figure 5–2. These results indicated that the increase in the IPCE value was due to factor (3), i.e., enhancement of the electron transport in WE-C. The rate of the back electron transfer of the injected electrons to the electrolyte in WE-C' and WE-N was faster than that in WE-C.

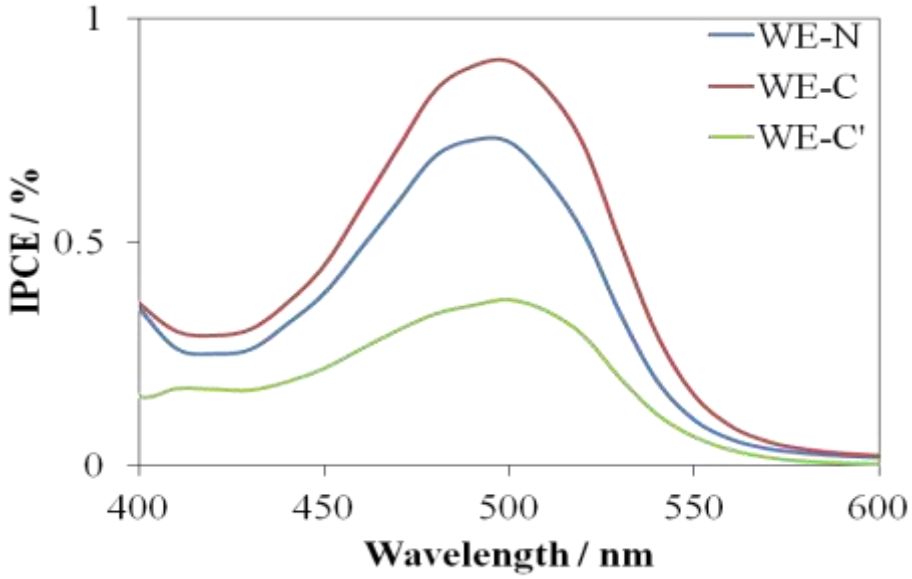

Figure 5–3 IPCE spectra of the compositionally-graded dye–titania (WE-C), irregularly-layered (WE-C') and normal (WE-N) dye–titania electrodes

5.3.2 Electron transport properties

The *I-V* curves of each electrode are shown in Figure 5–4 and their properties are summarized in Table 5–1. The open-circuit voltage (V_{oc}), fill factor, and quantum efficiency (QE) of WE-C

are higher by 13 %, 50%, and 85 %, respectively, than those of WE-N. They are also higher than those of WE-C'.

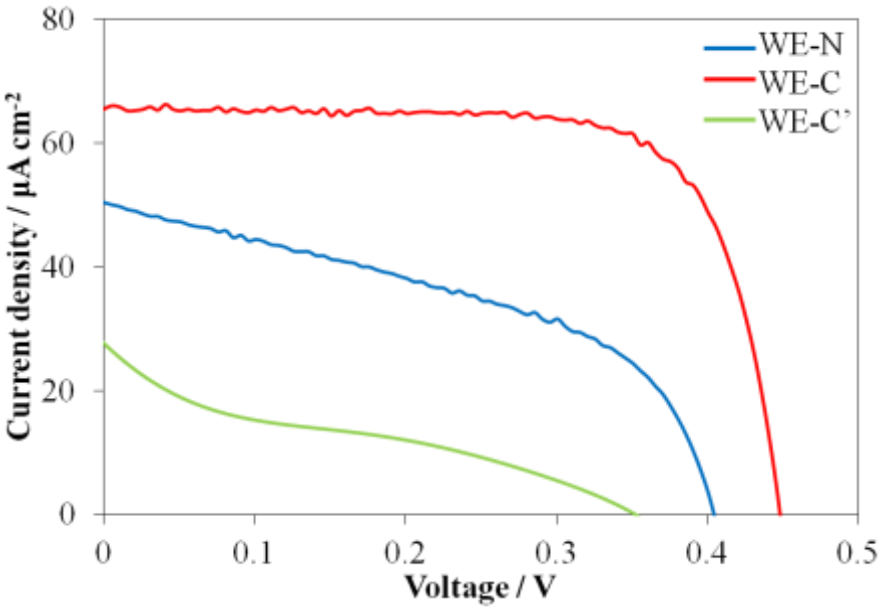

Figure 5–4 *I-V* curves of the compositionally-graded dye–titania (WE-C), irregularly-layered (WE-C'), and normal (WE-N) dye–titania electrodes

Table 5–1 Photoelectric conversion properties of the compositionally-graded dye–titania (WE-C), irregularly-layered (WE-C'), and normal (WE-N)

Electrode	J_{sc} / μA cm^{-2}	V_{oc} / V	P_{max} / μW cm^{-2}	FF	QE / %
WE-N	50.3 ±6.34	0.40±0.02	9.5 ±0.82	0.47 ±0.27	1.23± 0.31
WE-C	65.6 ±2.44	0.45±0.01	21.7 ±0.94	0.74 ±0.01	2.43±0.15
WE-C'	28.1 ±0.53	0.37±0.01	2.4 ±0.18	0.23 ±0.01	1.0±0.28

V_{oc} is defined as the voltage difference between the electrolyte redox potential (E_{redox}/q) and the quasi-Fermi potential of electrons ($E_{F,n}/q$) in the titania. $E_{F,n}$ is determined by the potential of the conduction band edge and the electron density in the titania. [17,18] The electron density in the

titania films is determined by the balance between the electron injection and back electron transport.[18,19]

It was suggested that suppressing the back electron transport was the main reason for the improvement in the V_{oc} because the electron injection in WE-N should be higher than that in the WE-C electrode. The fill factor is also strongly affected by the back electron transport.[16] The improvements in IPCE, V_{oc}, and FF in WE-C strongly indicated that the back electron transport as observed in WE-C was more effectively suppressed than that in WE-C' and WE-N .

The crystallinity of the titania nanoparticles is known as one of the factors affecting the back electron transfer.[20] The XRD pattern of each electrode is shown in Figure 5–5. The peaks at around 25.3°, 37.9°, 47.6° were observed indicating that anatase type crystals were produced in the film of each electrode. The crystallite size of each electrode was estimated from their full width at half-maximum of the 25.3°peak using Sherrer's equation, $D=0.9\lambda/\beta\cdot\cos\theta$. They were about 5 nm for both WE-C and WE-N. Based on these results, it was concluded that the crystallinity of each electrode was not significantly different and this factor cannot be a reason for the higher efficiency of the photoelectric conversion in WE-C.

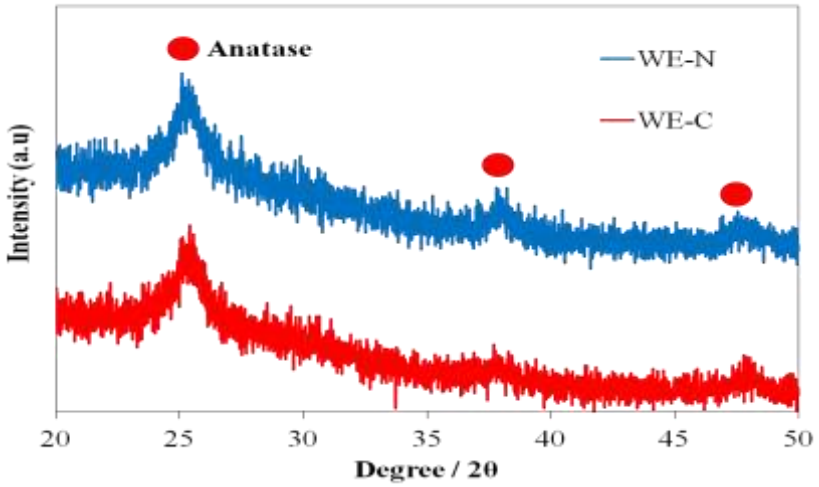

Figure 5–5 XRD patterns of the compositionally-graded dye–titania (WE-C) and normal (WE-N) electrodes

In chapter 4, the photocurrent onset of the dye-dispersing titania electrodes was determined by cyclic voltammetry during light irradiation for the band-gap excitation of the titania (Photo-CV) in order to estimate the shift in the conduction band edge of the titania with the dye content. The photo-CV curves of the electrodes indicated that the conduction band edge of the titania was more negative in the electrode containing a higher amount of the dye. Compared to the S1 layer, the conduction band edge of the S2 layer was shifted by about 100 mV in the negative direction. Based on these results, it was suggested that a step-like band structure formed by the conduction bands of the S1 and S2 layers in WE-C was the main factor causing enhancement of their photoelectric conversion properties. Based on these results, it was presumed that the step-like band structure in the WE-C provided the driving force of the electron transport and inhibited the back electron transfer as shown in Figure 5–6.

The effect of the step-like band structure on the photoelectric conversion properties of WE-C can be estimated from its electron injection efficiency. The efficiency values of the electron injection from the dye to the crystalline titania were estimated by dividing their QE values in visible range by those in UV range, which resulted from the dye and titania. The efficiency values for WE-C and WE-N were 33 % and 16 %, respectively. In the conventional DSSCs containing Ru complex dyes, the efficiency of the electron injection from the dye to titania is nearly equal to 100%. Based on a literature, the difference between the potentials of the LUMO of Ru complex dyes and the titania conduction band edge was about 0.20 eV.[21] It is suggested that the driving force of more than 0.20 eV was required for a highly efficient electron injection. Koops et al. reported the correlation between the shift in the titania conduction band edge and the electron injection efficiency. It was concluded that an increase in the driving force by 0.30 eV provided a 10-fold electron injection rate.[22] In WE-C, the differences between the conduction band edge levels of the S2 and S1 layers and the S1 and S0 layers were about 100

and 50 mV, i.e., the driving forces were about 0.10 and 0.05 eV, respectively. The electron injection efficiency for WE-C is expected to increase by about 3-fold and be close to 100% when the driving forces for the electron injection at the interfaces are about 0.30 and 0.25 eV, respectively.

The electron injection efficiency for WE-C with the double dye-dispersing titania layers was about 2-fold greater than that for WE-N with the single layer because the structure decreased the back electron transfer rate by 2-fold. The efficiency can be further improved by forming a greater number of the compositionally-graded dye-dispersing titania layers as well as increasing the driving force between the layers. The thickness of the dye-dispersing titania layer suppresses the back electron transfer although it causes the electron trapping due to a great amount of defects. The electron injection efficiency is expected to be close to 100% when 6 or 7 layers with the present driving force and thickness are formed on the crystalline titania layer.

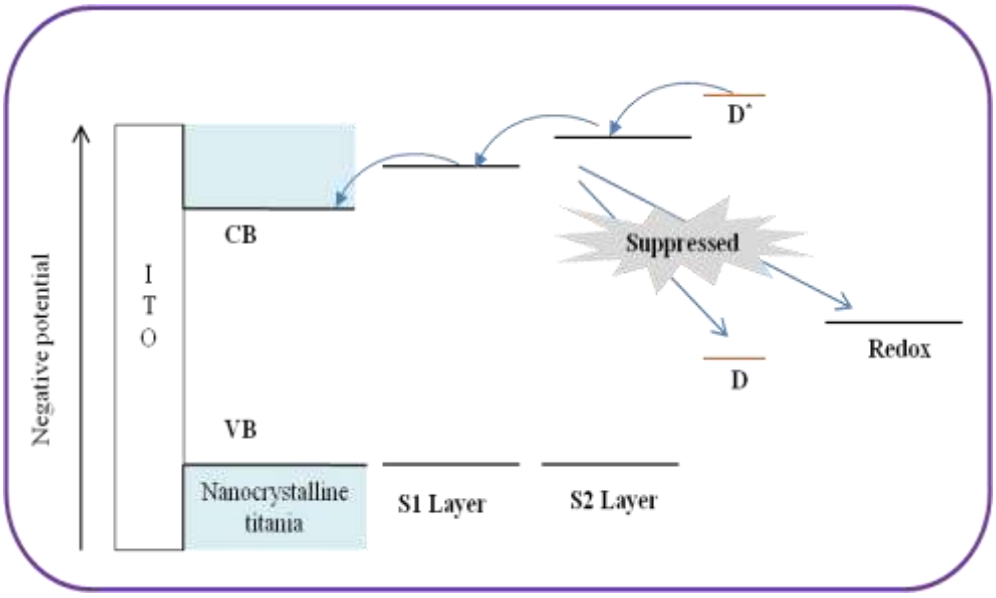

Figure 5–6 Electron transfer diagram in the compositionally-graded dye–titania (WE-C)

5.4 Conclusions

In conclusion, the photoelectric conversion of the compositionally-graded dye–titania electrode was higher than that of the normal electrode. It is suggested that the step-like structure in the conduction bands was formed by the combination of the S1 and S2 layers having different concentrations of dye in WE-C. The step-like structure in the conduction bands of the WE-C electrode provided the driving force of the electron transport and inhibited the back electron transfer.

References

(1) D. P. Hagberg, T. Edvinsson, T. Marinado, G. Boschloo, A. Hagfeldt, L. Sun
Chemical Communications, 21 (2006), pp, 2245-2247

(2) M. J. Katz, M. J. D. Vermeer, O. K. Farha, M. J. Pellin, J. T. Hupp
Langmuir, 29 (2013), pp. 806-814

(3) S. S. Pandey, S. Sakaguchi, Y. Yamaguchi, S. Hayase
Organic Electronics, 11 (2010), pp. 419-426

(4) Z. Iqbal,W. Q.Wu, D. B. Kuang, L. Wang, H. Meier, D. Cao
Dyes and Pigments, 96 (2013), pp, 722-731

(5) H. Nishikiori, Y. Uesugi, S. Takami, R. A. Setiawan, T. Fujii, W. Qian, M. A. El-Sayed
Journal of Physical Chemistry C, 115 (2011), pp. 2880-2887

(6) H. Nishikiori, W. Qian, M. A. El-Sayed, N. Tanaka,; T. Fujii
Journal of Physical Chemistry Letters, 111 (2007), pp. 9008-9011

(7) H. Nishikiori, N. Tanaka, T. Kitsui, T. Fujii
Journal of Photochemistry and Photobiology A: Chemistry, 179 (2006), pp. 125-129

(8) T. Kitsui, H. Nishikiori, N. Tanaka, T. Fujii

Journal of Photochemistry and Photobiology A: Chemistry, 192 (2007), pp, 220-225

(9) H. Nishikiori, Y. Uesugi, N. Tanaka, T. Fujii

Journal of Photochemistry and Photobiology A: Chemistry, 207 (2009), pp. 204-208

(10) R. A. Setiawan, H. Nishikiori, Y. Uesugi, K. Miyashita, M. A. El-Sayed, T. Fujii

Journal of Physical Chemistry C, 117 (2013), pp. 10308-10314

(11) P. J. Cameron, L. M. Peter

Journal of Physical Chemistry B, 107 (2003), pp. 14394-14400

(12) A. O. T. Patrocinio, L. G. Paterno, N. Y. Murakami Iha

Journal of Photochemistry and Photobiology A: Chemistry, 205 (2009), pp. 23-27

(13) J. N. Hart, D. Menzies, Y. B. Cheng, G. P. Simon, L. Spiccia

Comptes Rendus Chimie, 9 (2006), pp. 622-626

(14) R. Sjöback, J. Nygren, M. Kubista

Spectrochimica Acta Part A: Molecular and Biomolecular Spectroscopy, 51 (1995), pp. L7-L21

(15) T. Fujii, A. Ishii, Y. Kurihara, M. Anpo

Research on Chemical Intermediate, 19 (1993), pp. 333-342

(16) J. Xia, S. Yanagida

Solar Energy, 85 (2011), pp. 3143-3159

(17) T. Marinado, K. Nonomura, J. Nissfolk, M. K. Karlsson, D. P. Hagberg, L. Sun, S. Mori, A. Hagfeldt

Langmuir, 26 (2010), pp. 2592-2598

(18) Y. Liang, B. Peng, J. Chen

Journal of Physical Chemistry C, 114 (2010), pp. 10992-10998

(19) M. Miyashita, K. Sunahara, T. Nishikawa, Y. Uemura, N. Koumura, K. Hara, A. Mori, T.

Abe, E. Suzuki, S. Mori

Journal of American Chemical Society, 130 (2008), pp, 17874-17871

(20) G. Kantonisa, T. Stergiopoulosa, A.P. Katsoulidisb, P.J. Pomonisb, P. Falarasa

Journal of Photochemistry and Photobiology A: Chemistry, 217 (2011), pp, 236-241

(21) G. Ramakrishna, D. A. Jose, D. K. Kumar, A. Das, D. K. Palit, H. N. Ghosh

Journal of Physical Chemistry B, 109 (2005**)**, pp, 15445-15453

(22) S. E. Koops, B. C. O'Regan, P. R. F. Barnes, J. R. Durrant

Journal of American Chemical Society, 131 (2009), pp, 4808-4818

Chapter 6

General Conclusions

Influence of the dye–titania complex formation on the photoelectric conversion properties of the dye-dispersing titania was investigated in this dissertation. The UV–vis and FTIR spectra analyses were conducted in order to understand the mechanism of the complex formation in the dye-dispersing titania systems. Also, photocurrent onset and time-resolved fluorescence spectroscopy measurements were conducted in order to clarify the influence of the dye–titania complex formation on the shift in the conduction band edge and the electron transport efficiency from the sensitizer to titania, respectively. Furthermore, the photoelectric conversion properties of the electrodes using dye-dispersing titania was investigated by *I*-*V* curve and IPCE spectral measurements.

In chapter 2, it was concluded that the steam treatment enhanced the dye–titania interaction and promoted the dye–titania chelate complex formation on the titania pore surface. This is because active gaseous water promoted the hydrolysis of the titanium species and enhanced their reactivity. The titanium chelation of the dye molecule through its carboxylate and carbonyl of groups were promoted in the narrow spaces of the titania networks. The dye–titania complex formation significantly improved the photoelectric conversion efficiency of the dye-dispersing titania electrodes.

In chapter 3, based on the steady state and time-resolved fluorescence spectroscopy, a greater degree of fluorescence quenching was observed in the titania steam-treated for a longer time due to enhancement of the dye–titania interaction and the photoinduced electron injection from the dye into the titania. The fluorescence intensity just after excitation clearly decreased with the treatment time; i.e., the relative electron injection yield increased. Based on the results in

chapters 1 and 2, it was concluded that the dye–titania complex formation played an important role in the electron injection from the dye into the titania conduction band, which increased the photoelectric conversion efficiency of the electrode using dye-dispersing titania.

In chapter 4, it was shown that the dye–titania complex significantly affected the shift in the conduction band edge of titania. The photocurrent onset measurement indicated that the conduction band edge of the titania was more negative in the electrode containing a higher amount of the dye–titania complex. However, the FTIR spectra of the dye-dispersing titania electrodes showed that not only the dye–titania complex, but also the nitrate ions existed on the titania surface because they were prepared through a nitric acid-catalyzed sol–gel process. The nitrate ions adsorbed on the titania electrode also caused a negative shift in the conduction band edge due to their negative charge. Based on the degree of the shift, the effect of the dye–titania complex formation on the shift in the titania conduction band edge was greater than that of the nitrate ion adsorption due to the strong interaction between the dye and titania through the carboxylate group of the dye.

In chapter 5, the photoelectric conversion properties of compositionally-graded dye–titania electrode (WE-C) consisting of two types of the dye-dispersing titania layers with different concentration of the dye were investigated. The photoelectric conversion efficiency of WE-C was higher than the normal electrode (WE-N) because a step-like band structure was formed due to the difference in the conduction band level of WE-C. This structure is presumed to provide the driving force of the electron transport and inhibit the back electron transfer. The IPCE values, open-circuit voltage, fill factor, and quantum efficiency of WE-C were higher by 25 %, 13 %, 50%, and 85% than those of WE-N, respectively.

Finally, it was concluded that the dye–titania complex in the dye-dispersing titania significantly affected not only electron transfer from the sensitizer into the titania, but also the

conduction band edge of the titania. It was also confirmed that the conduction band edge of the titania can be controlled by adjusting the dye and titania compositions in the dye-dispersing titania systems. Furthermore, the step-like band structure was successful formed in a new material containing the dye-dispersing titania, “compositionally-graded dye–titania”. This material can improve the electron transport and photoelectric conversion efficiency of DSSCs.

List of Publications

Related to the doctoral dissertation

(1) Hiromasa Nishikiori, Yohei Uesugi, Shohei Takami, Rudi Agus Setiawan, Tsuneo Fujii, Wei Qian, and Mostafa A. El-Sayed

「Influence of Steam Treatment on Dye-Titania Complex Formation and Photoelectric Conversion Property of Dye-Doped Titania Gel」

Journal of Physical Chemistry C, 115 (2011), pp, 2880-2887

(2) Rudi Agus Setiawan, Hiromasa Nishikiori, Yohei Uesugi, Kyohei Miyashita, Mostafa A. El-Sayed, and Tsuneo Fujii

「Electron Transfer Process in Fluorescein-Dispersing Titania Gel Films Observed by Time-Resolved Fluorescence Spectroscopy」

Journal of Physical Chemistry C, 117 (2013), pp, 10308-10314

(3) Rudi Agus Setiawan, Hiromasa Nishikiori, Nobuaki Tanaka, and Tsuneo Fujii

「Photoelectric Conversion Properties of Compositionally-Graded Dye-Titania Electrod」

Chemistry Letters, 42 (2013), pp, 1391-1393

(4) Rudi Agus Setiawan, Hiromasa Nishikiori, Nobuaki Tanaka, and Tsuneo Fujii

「Influence of dye content on the conduction band edge of titania in the dye-dispersing titania electrodes」

Applied Catalyst B, Submitted

Unrelated to the doctoral dissertation

(1) Hiromasa Nishikiori, Yohei Uesugi, Rudi Agus Setiawan, Tsuneo Fujii, Wei Qian, and Mostafa A. El-Sayed

Journal of Physical Chemistry C, 116 (2012), pp, 4848-4854

(2) Hiromasa Nishikiori, Yohei Uesugi, Rudi Agus Setiawan and Katsuya Teshima

Journal of the Society of Inorganic Materials, Japan, 19 (2012), pp, 237-241

(3) Hiromasa Nishikiori, Rudi Agus Setiawan, Kento Miyamoto, Gagat Sukmono, Yohei Uesugi, Katsuya Teshima, and Tsuneo Fujii

RSC Advances, 2 (2012), pp, 4258–4267

(4) Hiromasa Nishikiori, Masaaki Ito, Rudi Agus Setiawan, Ayaka Kikuchi, Tomohiko Yamakami, and Tsuneo Fujii

Chemistry Letters, 41 (2012), pp, 725-727

(5) Hiromasa Nishikiori, Rudi Agus Setiawan, Kyohei Miyashita, Katsuya Teshima, and Tsuneo Fujii

Catalysis Science and Technology, 3 (2013), pp, 1512-1519

(6) Hiromasa Nishikiori, Kenta Todoroki, Daichi Natori, Rudi Agus Setiawan, Kyohei Miyashita, and Tsuneo Fujii

Chemistry Letters, 42 (2013), pp, 556-558

(7) Hiromasa Nishikiori, Rudi Agus Setiawan, Sayaka Kawamoto, Shinya Takagi, Katsuya Teshima, and Tsuneo Fujii

Catalysis Science and Technology, 3 (2013), pp, 2768-2792

(8) Hiromasa Nishikiori, Shun Hashiguchi, Masaaki Ito, Rudi Agus Setiawan, and Tsuneo Fujii

Applied Catalysis B: Environmental, 147 (2014), pp, 246-250

Acknowledgments

The author is extremely grateful to Prof. Hiromasa Nishikiori, Department of Environmental Science and Technology, Faculty Engineering, Shinshu University for his kind help, worthwhile advice, and continous encouragement throughout the course of this study.

The author sincerely thanks Prof. Nobuaki Tanaka, Department of Environmental Science and Technology, Faculty Engineering, Shinshu University for his helpful advice of this study and kind research guidance.

The author is greatly indebted to Prof. Tsuneo Fujii, Nagano Prefectural Institute of technology for his advice, guidance and kindness during this study.

The author would like to thank all the members of Nishikiori-Tanaka Laboratory for useful help and kindness.